DISSERTATION

submitted to the
Combined Faculties of the Natural Sciences and Mathematics
of the Ruperto Carola University of Heidelberg, Germany,
for the degree of
Doctor of Natural Sciences

Put forward by
MICHAEL DÜRR

Born in Lüneburg, Germany
Oral examination: 19 December 2013

Phenomenological Aspects of Theories for Baryon and Lepton Number Violation

Referees:
Prof. Dr. Manfred Lindner
and
Prof. Dr. Joerg Jaeckel

Abstract

The renormalizable couplings of the Standard Model are invariant under two accidental global symmetries, which correspond to conserved baryon and lepton numbers. In this thesis, we discuss possible roles of these symmetries in extension of the Standard Model. Two approaches are considered: explicit violation of lepton number by two units in the renormalizable couplings of the Lagrangian, and promotion of the global symmetries to local gauge symmetries that are spontaneously broken. The former approach directly leads to Majorana neutrino masses and neutrinoless double beta decay. We discuss the interplay of the contributions to this decay in a one-loop neutrino mass model, the colored seesaw mechanism. We find that, depending on the parameters of the model, both the light Majorana neutrino exchange and the contribution of the new colored particles may be dominant. Additionally, an experimental test is presented, which allows for a discrimination of neutrinoless double beta decay from unknown nuclear background using only one isotope. In the latter approach, fascinating implications originate from the attempt to write down an anomaly-free and spontaneously broken gauge theory for baryon and lepton numbers, such as an automatically stable dark matter candidate. When gauging the symmetries in a left–right symmetric setup, the same fields that allow for an anomaly-free theory generate neutrino masses via the type III seesaw mechanism.

Zusammenfassung

Die renormierbaren Kopplungen des Standard-Modells sind invariant unter zwei globalen Symmetrien mit den Erhaltungsgrößen Baryon- und Lepton-Zahl. In dieser Arbeit diskutieren wir die Rollen, die diese Symmetrien in Erweiterungen des Standard-Modells spielen können. Zwei Ansätze werden verfolgt: explizite Brechung der Lepton-Zahl um zwei Einheiten in den renormierbaren Kopplungen der Lagrangedichte, und Eichung der globalen Symmetrien mit anschließender spontaner Brechung. Der erste Ansatz führt direkt zu Majorana-Massen der Neutrinos und neutrinolosem Doppel-Betazerfall. Wir diskutieren die Beiträge zu diesem Zerfall im sogenannten *colored seesaw mechanism* und finden, dass sowohl der Austausch der leichten Majorana-Neutrinos als auch der Austausch der neuen Teilchen des Modells, die Farbladung tragen, dominant sein können. Zusätzlich präsentieren wir einen Test, der es erlaubt, unbekannte kernphysikalische Hintergründe vom Signal für neutrinolosen Doppel-Betazerfall in einem einzigen Isotop zu unterscheiden. Im zweiten Ansatz ergeben sich faszinierende Resultate aus dem Versuch, eine anomaliefreie und spontan gebrochene Eichtheorie für Baryon- und Lepton-Zahlen aufzuschreiben, z.B. finden wir einen Kandidaten für die dunkle Materie, der automatisch stabil ist. Bei Eichung der Symmetrien im links-rechts-symmetrischen Kontext erzeugen die gleichen Felder, die eine anomaliefreie Theorie garantieren, Neutrino-Massen über den *type III* Seesaw-Mechanismus.

Contents

Chapter 1

Intro: The Standard Model and beyond

> Our imagination is stretched to the utmost, not, as in fiction,
> to imagine things which are not really there,
> but just to comprehend those things which are there.
>
> *Richard P. Feynman*

During the 1960s, particle theorists stretched their imagination to the utmost, with the aim to "comprehend those things which are there" and to provide a description, at the level of elementary particles, of the processes happening in nature. Their efforts resulted in the so-called electroweak theory, which was put into its final form by Sheldon L. Glashow [1], Steven Weinberg [2], and Abdus Salam [3]. Together with quantum chromodynamics (QCD), the theory of the strong interaction, their electroweak theory forms the Standard Model of particle physics (SM), which has been extremely successful in its predictions ever since.

With the discovery of the top quark at the CDF [4] and DØ [5] experiments at the Tevatron at Fermilab in 1995, the existence of all SM fermions and gauge bosons was confirmed. However, the mechanism giving mass to all these particles remained elusive. Therefore, one of the aims of the Large Hadron Collider (LHC) at CERN in Switzerland was to prove or disprove the existence of the famous Higgs boson, the particle presumably responsible for the masses of the elementary particles via the Higgs mechanism. This mechanism was proposed independently by Peter W. Higgs [6], by François Englert and Robert Brout [7], as well as by Gerald S. Guralnik, Carl R. Hagen, and Tom W. B. Kibble [8] in 1964.

Eventually, in 2012, the discovery of this last missing piece of the Standard Model was reported by the ATLAS [9] and CMS [10] experiments. It remains to be conclusively shown that the discovered boson is indeed *the* SM Higgs boson, although all experimental results point in this direction. A second aim of the LHC was to discover some of the particles predicted by theories beyond the Standard Model. It seems, however, that the Standard Model is even more successful than many particle physicists had hoped: no persistent signs of new physics beyond it have shown up at the LHC so far.

Be that as it may, there are long-standing experimental and theoretical hints that the Standard Model is not the final particle physics theory, even leaving aside the fact that it is not a complete description of all forces in nature because it does not contain gravity. Particle theorists have continued to stretch their imagination with the aim to consistently extend the Standard Model, sometimes even imagining "things which are not really there." However, all these efforts by so many scientists have not been enough to solve the issues that remain.

I have also stretched my imagination during the past three years, and this thesis is my humble contribution in the endeavor to find a consistent extension of the Standard Model. To do so, we are guided by the concepts of baryon and lepton numbers, which could provide windows to the new physics necessary to solve the SM issues. Two different avenues are followed, and accordingly this thesis is divided into two parts: Part I (Chapters 2 and 3) contains a discussion of the special case of lepton number violation by two units, and Part II (Chapters 4 and 5) is dedicated to gauge theories of baryon and lepton numbers. Let us discuss the origin of the SM issues addressed in this thesis before we go *in medias res*.

Since the late 1990s, oscillation experiments with atmospheric [11], reactor [12], and solar [13] neutrinos have conclusively shown that neutrinos have a non-zero mass. Neutrino masses were not incorporated into the original version of the Standard Model, because neutrinos were thought to be massless at that time. However, the necessary modification of the Standard Model might be a trivial one: by adding right-handed neutrinos to the SM particle content, the Higgs mechanism can be used to generate Dirac neutrino masses in the same way it generates Dirac masses for the quarks and charged leptons. Due to the smallness of the neutrino masses, such a setup requires extremely tiny couplings of the right-handed neutrinos to the SM Higgs and lepton doublets. This solution is certainly not totally satisfactory from a theoretical point of view, and additional problems immediately arise. After introducing right-handed neutrinos, gauge invariance allows one to write down a lepton number violating Majorana mass term for these SM singlets. To truly make neutrinos Dirac particles, conservation of lepton number therefore has to be imposed in some form.

Giving up lepton number conservation and allowing for a Majorana mass term for the right-handed neutrinos offers the appealing possibility of using the seesaw mechanism [14–18] to explain the smallness of the neutrino masses, avoiding the aforementioned problem of tiny couplings.[1] Neutrinos are then Majorana particles, thereby violating lepton number by two units. The mass scale of the right-handed neutrinos cannot be related to the electroweak scale, the only energy scale present in

[1] This is the so-called type I seesaw. We discuss type II [19–23] and type III [24] seesaw later, which introduce scalar and fermionic triplets of $SU(2)_L$, respectively.

the Standard Model, because they are SM singlets. Therefore, the Majorana masses of the introduced singlets can expected to be very large. This might just be the way nature chose neutrino masses to be generated, but will probably never allow to test their origin in experiments. Most certainly nature does not care too much about our ability to test fundamental processes experimentally, thus such arguments do not provide evidence for or against a particular mechanism. Nevertheless, it is interesting to explore alternative mechanisms for neutrino masses that allow for an experimental test, possibly even at current experiments. We come back to all these issues in Chapter 2 and discuss neutrino masses in more detail.

It is an open question whether the total lepton number L is conserved in nature. In neutrino oscillations, only the individual lepton flavor numbers are broken (L_e, L_μ, and L_τ). Violation of total lepton number could be observed in various experiments, but at the moment the most promising experimental test (if lepton number is violated by two units) is the search for neutrinoless double beta decay ($0\nu\beta\beta$). Recently, experiments using different isotopes reported improved lower bounds on the half-life of the decay: EXO-200 [25] and KamLAND-Zen [26] using the isotope ^{136}Xe, and GERDA [27] using the isotope ^{76}Ge. Limits for both isotopes are of the order 10^{25} y, thus showing that $0\nu\beta\beta$, if existent at all, is an extremely rare decay.

It is often stated that an observation of $0\nu\beta\beta$ would provide us with the absolute neutrino mass scale, but that is true only if the decay is mediated exclusively by light Majorana neutrinos. Then, the so-called effective Majorana mass $m_{0\nu\beta\beta}$ could be extracted from the measured half-life, with some uncertainty coming from the imperfectly known nuclear matrix elements.

However, any other lepton number violating theory might also contribute to $0\nu\beta\beta$. This opens a window to test new physics beyond the Standard Model that may or may not be connected to neutrino masses directly. We discuss $0\nu\beta\beta$ in some detail in Chapter 3. Especially, we present two original results: in Section 3.2, we discuss the $0\nu\beta\beta$ phenomenology of the colored seesaw mechanism, a one-loop neutrino mass model that is introduced in Chapter 2. In Section 3.3, we discuss how to cross check a possible observation of $0\nu\beta\beta$ by considering the decays to the first excited 0^+ states in addition to the ground state transition.

Another long-standing mystery is the phenomenon of dark matter (DM). It was already noticed by Fritz Zwicky in the 1930s [28] that there must be a non-luminous (and therefore dubbed "dark") matter component in galaxy clusters. Today, we have evidence on vastly different scales for a non-baryonic form of matter that interacts at least gravitationally with visible matter and makes up about 26% of the energy density of the Universe. We do not really have a clue about the origin and nature of this form of matter. Many theoretical ideas exist to describe the DM sector, which could be as complex as the visible sector. Among the very popular particle candidates for

cold DM are weakly interacting massive particles (WIMPs) and axions; see Ref. [29] for an overview of particle candidates. Due to the lack of a definite observation of DM particles in experiments, the particle nature of dark matter is far from settled and alternative explanations such as a modification of gravity are also pursued [30].

To not immediately be ruled out, a DM candidate must be stable on cosmological time scales and may not carry electromagnetic charge. It is of course appealing not to introduce such a particle by hand but to try to connect the solution of the DM puzzle to the solution of some other problem remaining in the Standard Model. The textbook examples for this approach are supersymmetric theories (SUSY). These theories were originally proposed to solve the hierarchy problem and it turned out that a symmetry called R-parity had to be introduced to forbid proton decay. This symmetry makes the lightest SUSY particle stable and thus, if neutral, a DM candidate [31].

This thesis is concerned with non-SUSY theories only, and we cannot go into as much details on dark matter as on the other topics discussed before. Nevertheless, we will see that a DM candidate can arise in the models we introduce for the solution of one or the other SM issue. See Section 2.4.1 for a neutrino mass model with a DM candidate, and Section 4.4.6 for a fermionic DM candidate originating from a gauge theory for baryon and lepton numbers. The stability of the latter DM candidate is a consequence of the breaking of the gauge symmetry and does not have to be demanded by hand. Another interesting feature of the latter DM candidate is that it carries baryon number. Calling dark matter non-baryonic merely refers to the fact that it must be different from ordinary matter that is made of quarks (and leptons). In the context of the Standard Model, quarks are the only particles that carry baryon number, and they form protons and neutrons, the building blocks of atomic nuclei.

The phenomena of neutrino masses and dark matter are experimental hints for the necessity of an extension of the Standard Model, and we have seen that the concepts of baryon and lepton numbers may play an important role in formulating a consistent description. However, there also is an issue with baryon and lepton numbers in the Standard Model from a more theoretical perspective: when writing down the full SM Lagrangian, i.e., all Lorentz-invariant and renormalizable terms that are invariant under the SM gauge group, one realizes that all these terms accidentally conserve baryon and lepton numbers. Contrary to this fact, we have hints that both may be broken in nature. Having mentioned before that neutrino masses may point towards a violation of lepton number, we also know that baryon number must be broken in order to explain the matter–antimatter asymmetry in the Universe.

Taking into account non-renormalizable interactions, higher-dimensional operators such as

$$\mathcal{O}_5 = \frac{c_5}{\Lambda_L} LLHH \quad \text{and} \quad \mathcal{O}_6 = \frac{c_6}{\Lambda_B^2} QQQL \tag{1.1}$$

can always be added to the Standard Model [32, 33]. The notation is a symbolic one: L is a lepton doublet, H is the SM Higgs field, and Q is a quark doublet. c_5 and c_6 are coupling constants, which can be calculated if we know the underlying fundamental theory at a higher scale. The so-called Weinberg operator $\mathcal{O}_5$ violates lepton number L by two units and generates Majorana neutrino masses after electroweak symmetry breaking. The operator $\mathcal{O}_6$ breaks both lepton number L and baryon number B by one unit, but conserves $B - L$. It is responsible for proton decay, and the corresponding experimental bounds are strong, for more details see the discussion in Section 2.2. Thus, we have to postulate the existence of a great desert between the weak scale where the Standard Model lives and a scale $\Lambda_B > 10^{14-16}\,\text{GeV}$ where we can understand the origin of the baryon number violating interactions.

The problem of proton decay is immanent in Grand Unified Theories (GUTs) that unify the strong with the electroweak interaction, because they also unify baryons and leptons in the same multiplets such that baryon and lepton numbers necessarily are broken. By computing the operators mediating proton decay in these theories and then using the running of gauge couplings, it is at least possible to understand at which scale the GUT gauge group is spontaneously broken to the SM gauge group, and hence why the scale Λ_B is so large. Due to the presence of baryons and leptons in the same multiplets, baryon and lepton numbers cannot be treated as independent symmetries in these theories.

In this thesis, we are concerned with the origin of baryon and lepton numbers as global symmetries and we want to treat them individually. Therefore, we pursue a different approach, namely the promotion of baryon and lepton numbers to independent local gauge symmetries. Similar attempts exist in the literature [34–37]. Despite the spontaneous breaking of these symmetries at a low scale, the charges of the fields are such that baryon number violating processes are very suppressed even in the presence of non-renormalizable interactions. Such models provide a way to understand the suppression of baryon and lepton number violating interactions without the necessity of a large desert. Unfortunately, all the proposed solutions [34–37] are in disagreement either with the recent constraints from the LHC experiments or with cosmological data. We dedicate Chapters 4 and 5 to the search of viable models realizing this idea.

The last issue of the Standard Model that we discuss in this thesis is the violation of parity, i.e., the $V - A$ structure of the weak interaction. It is appealing to consider this observation as a low-energy phenomenon, and assume that left–right symmetry is restored at higher energies. This is the basis of so-called left–right symmetric theories [14, 15, 23, 38–41]. Starting from a left–right symmetric gauge group, parity is broken spontaneously in these models by the vacuum expectation values (VEVs) of some scalar fields. An especially interesting feature of these models is the presence of right-handed neutrinos in the right-handed lepton doublets. This allows for a direct

implementation of neutrino masses. Additionally, also the seesaw mechanism (a hybrid version of type I and type II) arises quite naturally in these models, such that the spontaneous breakdown of parity can be connected to the smallness of the neutrino masses. An implementation of type III seesaw is also possible. In Chapter 5 we gauge $U(1)_B$ and $U(1)_L$ in a left–right symmetric framework, and will thus be able to connect the spontaneous breakdown of parity with the spontaneous breaking of baryon and lepton numbers.

Finally, we conclude and give some outlook in Chapter 6.

A remark on publications

Most of the results presented in this thesis were already published before, exist as an e-print on the arXiv, or are work in progress, and all of them were done together with collaborators: Section 3.2 is based on a project together with Sandhya Choubey, Manimala Mitra, and Werner Rodejohann [42]; Section 3.3 is based on a collaboration with Manfred Lindner and Kai Zuber [43]; Chapter 4 is based on a paper together with Pavel Fileviez Pérez and Mark B. Wise [44], and the full exploration of the model currently is work in progress; finally, Chapter 5 is based on a collaboration with Pavel Fileviez Pérez and Manfred Lindner [45]. Also see my conference proceedings discussing the interplay between neutrinoless double beta decay, lepton number violating new physics, and Majorana neutrino masses [46, 47].

Some projects done during my PhD time were too far from the main focus of this thesis, such that the results cannot be presented here due to limitations of space. Such was the fate of a collaboration with Damien P. George and Kristian L. McDonald [48] on the phenomenological aspects of a neutrino mass model in a warped extra-dimensional setup. A project together with Mayumi Aoki, Jisuke Kubo, and Hiroshi Takano [49] on multi-component DM systems also had to be left out, as well as an exploration of the DM phenomenology of a simplified version of the model presented in Chapter 4, which was done together with Pavel Fileviez Pérez [50]. A paper published together with Manfred Lindner and Alexander Merle [51] essentially contains the (extended) results of my diploma thesis, which will not be repeated here. I will nevertheless point the reader to these results in a suitable place and comment on the relation to the results presented in this thesis.

Part I

Lepton number violation by two units

Chapter 2

Neutrino masses

As mentioned in the introduction in Chapter 1, one of the solid evidences for the necessity to modify the SM of particle physics is the observation of neutrino oscillations in atmospheric, reactor, and solar neutrino experiments [11–13]. The results of these experiments prove that neutrinos have a non-vanishing mass; this chapter presents the corresponding basics. To lay the ground for the rest of this thesis, we start with some details of the Standard Model of particle physics in Section 2.1. After that, in Section 2.2, we discuss higher-dimensional operators that violate baryon and lepton numbers. These operators will guide us in the search for viable extensions of the SM in the rest of this thesis. We present the famous seesaw mechanisms for the generation of Majorana neutrino masses in Section 2.3, and discuss a different pathway to small neutrino masses, namely radiative generation, in Section 2.4. Finally, we summarize this chapter in Section 2.5.

2.1 The Standard Model of particle physics

The Standard Model of particle physics is a gauge theory based on the gauge group

$$G_{\text{SM}} = SU(3)_C \otimes SU(2)_L \otimes U(1)_Y, \tag{2.1}$$

which consists of the gauge group of quantum chromodynamics, $SU(3)_C$, with C for "color," and of the electroweak gauge group $G_{\text{EW}} = SU(2)_L \otimes U(1)_Y$. Here, the index L refers to the fact that only left-handed fields take part in weak interactions, and Y is the weak hypercharge.

The Standard Model fields and their corresponding transformation properties under the gauge group G_{SM} are listed in Tab. 2.1. For later use, we also give the baryon number B and the lepton number L of the quarks and leptons. These quantum numbers are the charges of the fields under the global symmetries $U(1)_B$ and $U(1)_L$, which are accidentally conserved by the renormalizable couplings of the Standard Model Lagrangian. We discuss the origin of these accidental global symmetries in Part II of

Table 2.1: Field content of the Standard Model of particle physics and corresponding transformation properties under the Standard Model gauge group $G_{\rm SM}$. Additionally, we list the baryon and lepton numbers of the fermionic fields. The SM quarks and leptons come in three families, $\alpha = 1, 2, 3$, but we will often suppress the family index α in the remainder of this thesis. The electric charge is defined as $Q = Y + T_3$, where T_3 is weak isospin.

Type	Spin	Field	$SU(3)_C$	$SU(2)_L$	$U(1)_Y$	$U(1)_B$	$U(1)_L$
Quarks	$\frac{1}{2}$	$Q_L^\alpha = \begin{pmatrix} u_L^\alpha \\ d_L^\alpha \end{pmatrix}$	**3**	**2**	$\frac{1}{6}$	$\frac{1}{3}$	0
		u_R^α	**3**	**1**	$\frac{2}{3}$	$\frac{1}{3}$	0
		d_R^α	**3**	**1**	$-\frac{1}{3}$	$\frac{1}{3}$	0
Leptons	$\frac{1}{2}$	$\ell_L^\alpha = \begin{pmatrix} \nu_L^\alpha \\ e_L^\alpha \end{pmatrix}$	**1**	**2**	$-\frac{1}{2}$	0	1
		e_R^α	**1**	**1**	-1	0	1
Higgs boson	0	$H = \begin{pmatrix} H^+ \\ H^0 \end{pmatrix}$	**1**	**2**	$\frac{1}{2}$	0	0
Gauge bosons	1	G^a, $a = 1, \ldots, 8$	**8**	**1**	0	0	0
		W^b, $b = 1, 2, 3$	**1**	**3**	0	0	0
		B^0	**1**	**1**	0	0	0

this thesis, where we promote them to local gauge symmetries. Fantastic implications originate from the attempt to write down anomaly-free theories for gauged baryon and lepton numbers. The fields that have to be introduced in addition the SM fields in Tab. 2.1 allow, e.g., for an implementation of neutrino masses or provide us with a DM candidate.[1]

The fermionic fields (particles with half-integer spin) of the SM are the so-called quarks and leptons. They come in three families with identical quantum numbers, with the only difference between the families being their masses. The Higgs boson

[1] Note that the "L" in $SU(2)_L$ refers the left-handedness of the weak interaction, whereas the "L" in $U(1)_L$ refers to lepton number. Although it is not considered good practice to use the same letter for different meanings, we think that it will be clear from the context to which "L" we refer.

is a scalar particle, i.e., it has spin zero. The gauge bosons with spin one mediate the different forces of the SM: the gluons G^a ($a = 1, \ldots, 8$) mediate the strong interaction, and the W-bosons W^b ($b = 1, 2, 3$) and the B^0 boson mediate the electroweak interaction. Note that there are no right-handed neutrinos in the SM particle spectrum, because the neutrinos were considered to be massless when creating the SM.

The principle of gauge invariance strongly restricts the possible interactions of the theory, and renders all SM fields massless before the spontaneous breaking of G_{EW} to $U(1)_{\mathrm{EM}}$, the electromagnetic gauge group with the massless photon as gauge boson. The electroweak symmetry breaking is achieved by the neutral component of the Higgs field obtaining a VEV

$$\langle H^0 \rangle = \frac{1}{\sqrt{2}} v, \tag{2.2}$$

where $v = 246\,\mathrm{GeV}$.[2] This mechanism, the famous Higgs mechanism, gives all SM particles a mass proportional to v. Let us demonstrate the Higgs mechanism for the SM charged leptons as an example. Taking into account the quantum numbers of the fields given in Tab. 2.1, we can write down the gauge invariant term

$$-\mathcal{L}_Y \supset Y^{\ell}_{\alpha\beta} \overline{\ell^{\alpha}_L} H e^{\beta}_R + \mathrm{h.c.}, \tag{2.3}$$

where Y^{ℓ} is a Yukawa coupling matrix, and α and β are family indices. Repeated indices are summed over in all cases, i.e., the Einstein summation convention is used. After electroweak symmetry breaking, we obtain Dirac mass terms for the charged leptons,

$$-\mathcal{L}_Y \supset M^{e}_{\alpha\beta} \overline{e^{\alpha}_L} e^{\beta}_R + \mathrm{h.c.}, \tag{2.4}$$

where the Dirac mass matrix is given by

$$M^{e}_{\alpha\beta} = \frac{v}{\sqrt{2}} Y^{\ell}_{\alpha\beta}. \tag{2.5}$$

The electroweak gauge bosons also obtain a mass after electroweak symmetry breaking, but we do not want to go into more detail here.

Neutrino masses cannot be generated in the same way, because right-handed neutrinos are not contained in the SM, see Tab. 2.1, and therefore a Yukawa term similar to Eq. (2.3) cannot be written down for the neutrinos. As already mentioned in the introduction in Chapter 1, we would not obtain a completely satisfying explanation for neutrino masses even if we introduced right-handed neutrinos (and imposed lepton number conservation to forbid Majorana mass terms for them).

[2] The Higgs VEV v can be determined from the Fermi coupling constant G_F via $v = (\sqrt{2} G_F)^{-1/2}$. The value of G_F can be measured precisely in muon decay experiments. The most current value provided by the MuLan collaboration is $G_F = 1.1663788(7) \times 10^{-5}\,\mathrm{GeV}$ [52].

Neutrino masses are many orders of magnitude smaller than the masses of the charged leptons: a lower limit on the neutrino mass scale can be obtained from the larger of the two measured mass-squared differences,[3] the atmospheric mass-squared difference [53]

$$\Delta m^2_{\text{atm}} \approx 2.4 \times 10^{-3}\,\text{eV}^2 \tag{2.6}$$

leading to

$$m_\nu^{\text{osc}} \gtrsim 0.05\,\text{eV}. \tag{2.7}$$

Upper limits on the neutrino masses can be obtained in different experiments. The kinematical mass

$$m_\beta = \sqrt{\sum_i |U_{ei}|^2\, m_i^2} \tag{2.8}$$

can be deduced from the endpoint spectrum of single beta decay experiments. Here, U_{ei} are the elements of the first line of the neutrino mixing matrix that is introduced in Section 2.3.1 to diagonalize the mass matrix of the light neutrino species; m_i ($i = 1, 2, 3$) are the eigenvalues of the neutrino mass eigenstates. The current bound is [54]

$$m_\beta \leq 2.3\,\text{eV} \tag{2.9}$$

The upcoming KATRIN experiment [55] is expected to reach a sensitivity of $m_\beta \leq 0.2\,\text{eV}$. In cosmology, the sum of the light neutrino masses

$$\Sigma = \sum_i m_i \tag{2.10}$$

can be extracted from observations. The current limit is [56]

$$\Sigma \leq 0.23\,\text{eV}. \tag{2.11}$$

Thus neutrino Yukawa couplings of the order 10^{-12} are necessary to generate neutrino masses of the desired order. We take this issue as a motivation to search for alternative approaches to neutrino masses, and discuss different possibilities in the rest of this chapter.

2.2 Higher-dimensional operators in the Standard Model

All renormalizable couplings of mass dimension four or smaller that we can write down with the SM particle content in Tab. 2.1 conserve baryon and lepton numbers.

[3] Note that neutrino oscillation experiments can determine the two mass-squared differences between the three light neutrino mass eigenstates. It is therefore possible that the lightest neutrino mass eigenstate has a zero mass.

Going to higher-dimensional operators, we can easily find operators that violate baryon and/or lepton number, a fact first noticed by Weinberg [32], see also the discussion by Wilczek and Zee [33].

A possible operator breaking lepton number arises at dimension five,

$$\mathcal{O}_5 = \frac{c_5}{\Lambda_L}\left(\ell_L^T C i\sigma_2 H\right)\left(H^T i\sigma_2 \ell_L\right). \tag{2.12}$$

Here, Λ_L is the scale where lepton number is broken and c_5 is a dimensionless coupling; C is the charge conjugation matrix. Family indices have been suppressed for simplicity. After electroweak symmetry breaking, when the SM Higgs has obtained its VEV, a neutrino mass term is generated. Assuming a coupling c_5 of order one, we find that the scale Λ_L has to be large to generate neutrino masses at the eV level, i.e.,

$$\Lambda_L \lesssim 10^{14}\,\text{GeV}. \tag{2.13}$$

This operator guides us in the search for viable neutrino mass models in the rest of this thesis. All the models we present contain heavy particles that realize the dimension five Weinberg operator at tree or one-loop level.

Baryon number violating operators that induce proton decay arise at dimension six. With the SM particle content in Tab. 2.1, we can write down the operators

$$\mathcal{O}_6^1 = \frac{c_6^1}{\Lambda_B^2}\left(Q_L^T C i\sigma_2 Q_L\right)\left(Q_L^T C i\sigma_2 \ell_L\right), \tag{2.14}$$

$$\mathcal{O}_6^2 = \frac{c_6^2}{\Lambda_B^2}\left(Q_L^T C \tau^a i\sigma_2 Q_L\right)\left(Q_L^T C \tau_a i\sigma_2 \ell_L\right), \tag{2.15}$$

$$\mathcal{O}_6^3 = \frac{c_6^3}{\Lambda_B^2}\left(Q_L^T C i\sigma_2 Q_L\right)\left(u_R^T C e_R\right), \tag{2.16}$$

$$\mathcal{O}_6^4 = \frac{c_6^4}{\Lambda_B^2}\left(Q_L^T C i\sigma_2 \ell_L\right)\left(u_R^T C d_R\right), \tag{2.17}$$

$$\mathcal{O}_6^5 = \frac{c_6^5}{\Lambda_B^2}\left(u_R^T C u_R\right)\left(d_R^T C e_R\right), \tag{2.18}$$

$$\mathcal{O}_6^6 = \frac{c_6^6}{\Lambda_B^2}\left(u_R^T C d_R\right)\left(u_R^T C e_R\right). \tag{2.19}$$

$SU(3)_C$ and family indices have been suppressed here for simplicity. All these operators violate B and L, but conserve $B-L$. Proton decay has not been observed experimentally, and the bounds on the lifetime of the decay are severe. The lower limits on the mean lifetime are of the order

$$\tau_p > 10^{31-33}\,\text{y}, \tag{2.20}$$

depending on the decay mode [57]. The decay mode with the largest lower limit on the mean lifetime is the channel

$$p \to e^+ \pi^0 \tag{2.21}$$

with a lower limit on the lifetime of

$$\tau_p > 8.2 \times 10^{33}\,\mathrm{y} \tag{2.22}$$

at 90% CL [58].

From $\mathcal{O}_6$, we can make a naive estimation of the proton decay rate

$$\Gamma_p = \frac{c_6^2}{\Lambda_B^4} m_p^5, \tag{2.23}$$

where m_p is the mass of the proton. Using the bounds on the proton decay lifetime given above and a not too small or too large coupling c_6, we find that the scale of baryon number violation must be very high,

$$\Lambda_B > 10^{14-16}\,\mathrm{GeV}. \tag{2.24}$$

Therefore, we have to postulate the existence of a great desert between the electroweak scale where the Standard model lives and the large scale Λ_B, where we can understand the origin of the baryon number violating interactions.

We provide a solution to this issue in Part II of this thesis, where we gauge baryon and lepton numbers individually. We will be concerned with viable theories that can be broken at the low scale without the need to rely on the existence of the aforementioned desert. When breaking baryon number, we have to make sure to break it in a way that does not introduce the dangerous proton decay operators given above. The charges of the fields introduced in the models we discuss in Chapters 4 and 5 are such that baryon number violating processes are suppressed even in the presence of higher-dimensional operators.

2.3 The seesaw mechanism

Let us discuss the neutrino masses generated by the Weinberg operator in Eq. (2.12) in some more detail. At tree-level, there are only three realizations of this operator [59]: the famous seesaw mechanisms of type I, type II, and type III. All three types introduce exactly one new representation of the SM gauge group. Of course, there may be hybrid scenarios between two or more of the three types.

All three mechanisms can be naturally realized in left–right symmetric theories, where the seesaw scale can be related to the scale where the discrete left–right parity is broken spontaneously. We discuss such theories in more detail in Chapter 5.

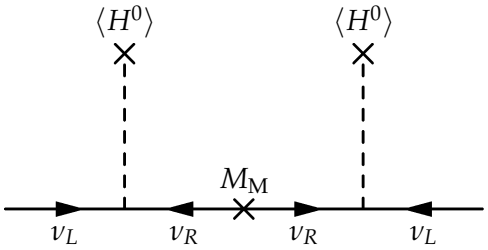

Figure 2.1: Feynman diagram of the Majorana neutrino mass term in the type I seesaw mechanism, which introduces right-handed neutrinos $\nu_R \sim (\mathbf{1}, \mathbf{1}, 0)$ with a Majorana mass M_{M}.

2.3.1 Type I seesaw

In type I seesaw [14–18], one adds fermionic singlets to the SM particle content, i.e.,

$$\nu_R^\alpha \sim (\mathbf{1}, \mathbf{1}, 0)\,. \tag{2.25}$$

In principle, an arbitrary number n of these can be introduced, $\alpha = 1, \ldots, n$. To explain the two mass-squared differences observed in neutrino oscillation experiments, at least two singlets are required. The relevant couplings are a Yukawa coupling to the SM Higgs and a Majorana mass term for the right-handed singlets,

$$-\mathcal{L}_{\text{Type I}} \supset Y^\nu \overline{\ell_L} \tilde{H} \nu_R + \frac{1}{2} M_{\mathrm{M}} \overline{(\nu_R)^c} \nu_R + \text{h.c.}, \tag{2.26}$$

where $\tilde{H} = i\sigma_2 H^*$. The Yukawa term generates a Dirac mass term for the neutrinos after electroweak symmetry breaking, in complete analogy to the Yukawa terms for the charged leptons in Eq. (2.3). Thus, the full neutrino mass term we obtain after electroweak symmetry breaking is

$$-\mathcal{L}_{\text{Type I}} \supset \frac{1}{2} \overline{(\nu_L \; (\nu_R)^c)} \begin{pmatrix} 0 & M_{\mathrm{D}} \\ M_{\mathrm{D}}^T & M_{\mathrm{M}} \end{pmatrix} \begin{pmatrix} (\nu_L)^c \\ \nu_R \end{pmatrix} + \text{h.c.} \tag{2.27}$$

with

$$M_{\mathrm{D}} = Y^\nu \frac{v}{\sqrt{2}}. \tag{2.28}$$

See Fig. 2.1 for the Feynman diagram of type I seesaw.

Note that the Dirac mass term connects the left-handed neutrino components of the lepton doublets with the right-handed singlet neutrinos, whereas the Majorana mass term connects the right-handed neutrinos with their charge-conjugates,

$$(\nu_R)^c = C\overline{\nu_R}^T, \tag{2.29}$$

and violates lepton number by two units (when assigning lepton number to the right-handed neutrinos).

Assuming that $M_{\mathrm{M}} \gg M_{\mathrm{D}}$,[4] one obtains the light neutrino mass matrix

$$\mathcal{M}_\nu = M_{\mathrm{D}} M_{\mathrm{M}}^{-1} M_{\mathrm{D}}^T \tag{2.30}$$

after block diagonalization of the neutrino mass matrix in Eq. (2.27). This neutrino mass matrix (and all the following that we obtain in the different realizations of the Weinberg operator) can be diagonalized by the Pontecorvo–Maki–Nakagawa–Sakata (PMNS) [60–62] neutrino mixing matrix U_{PMNS}, such that

$$U_{\mathrm{PMNS}}^\dagger \mathcal{M}_\nu U_{\mathrm{PMNS}}^* = \mathcal{M}_\nu^{\mathrm{diag}} = \mathrm{diag}\,(m_1, m_2, m_3)\,, \tag{2.31}$$

with m_i being the light neutrino mass eigenvalues. The mixing matrix U_{PMNS} is the neutrino equivalent to the Cabibbo–Kobayashi–Maskawa (CKM) mixing matrix in the quark sector [63, 64].

For the canonical type I seesaw, the Yukawa couplings are taken to be of order one which results in a value of M_{D} of about the electroweak scale. Thus the new singlets should have a mass

$$M_{\mathrm{M}} \lesssim 10^{14}\,\mathrm{GeV} \tag{2.32}$$

for sub-eV light neutrinos. It will therefore practically be impossible to probe this neutrino mass mechanism directly, because this energy is out of reach of current (and most certainly any future) experiments. Of course, the Yukawa couplings could be much smaller. Taking $M_{\mathrm{D}} \approx m_e$, one should have

$$M_{\mathrm{M}} \lesssim 1\,\mathrm{TeV}. \tag{2.33}$$

This mass scale is in the reach of the LHC. However, one has to remember that these neutrinos are SM singlets, so they only participate in any electroweak process through their mixing with the light neutrinos. Therefore, any such physical process is suppressed by the heavy–light mixing

$$|V_{\nu_L \nu_R}|^2 = \frac{M_{\mathrm{D}}^2}{M_{\mathrm{M}}^2} = \frac{\mathcal{M}_\nu}{M_{\mathrm{M}}}, \tag{2.34}$$

and thus unobservably small.

The only hope could be that the type I seesaw actually is embedded into a gauge extension of the SM, such as $G_{\mathrm{SM}} \otimes U(1)_{B-L}$. This is possible because the addition of

[4] This and all following estimations of mass scales refer to the size of the eigenvalues of the corresponding matrices.

three right-handed neutrinos makes this gauge group anomaly-free.[5] The corresponding new gauge boson Z_{B-L} may be produced at the LHC through its gauge interactions with the quarks, and could subsequently decay to a pair of Majorana neutrinos, such that no small mixing is involved. Quite distinctive features such as dileptons plus jets, or displaced vertices due to the decays of the heavy Majorana neutrinos could arise in such a model. A discussion of the corresponding collider phenomenology is beyond the scope of this thesis, see, e.g., Ref. [65] for a detailed analysis of such models at the LHC.

2.3.2 Type II seesaw

Type II seesaw is the extension of the SM, where one extra scalar triplet,

$$\Delta = \begin{pmatrix} \delta^+/\sqrt{2} & \delta^{++} \\ \delta^0 & -\delta^+/\sqrt{2} \end{pmatrix} \sim (\mathbf{1}, \mathbf{3}, 1) \tag{2.35}$$

is introduced [19–23]. The relevant terms of the Lagrangian are

$$\mathcal{L}_{\text{Type II}} \supset -Y_\Delta \overline{(\ell_L)^c} i\sigma_2 \Delta \ell_L + \text{h.c.} - V(H, \Delta), \tag{2.36}$$

where

$$V(H,\Delta) = -M_H^2 H^\dagger H + M_\Delta^2 \text{Tr}\left(\Delta^\dagger \Delta\right) + \left(\mu H^T i\sigma_2 \Delta^\dagger H + \text{h.c.}\right) + \text{quartic terms.} \tag{2.37}$$

Lepton number is explicitly broken by two units, because the simultaneous presence of the Yukawa term Y_Δ and the μ-term in $V(H,\Delta)$ does not allow for a consistent assignment of lepton numbers to the fields. After spontaneous symmetry breaking, when the Higgs fields have obtained the VEVs

$$\langle H \rangle = \begin{pmatrix} 0 \\ v/\sqrt{2} \end{pmatrix} \text{ and } \langle \Delta \rangle = \begin{pmatrix} 0 & 0 \\ v_\Delta/\sqrt{2} & 0 \end{pmatrix}, \tag{2.38}$$

a neutrino mass matrix

$$\mathcal{M}_\nu = \sqrt{2} Y_\Delta v_\Delta \tag{2.39}$$

is generated. Minimizing the potential (assuming a heavy Higgs triplet such that the quartic terms can be neglected), we find that the VEV of the triplet is actually induced by the VEV of the Higgs doublet, i.e.,

$$v_\Delta \approx \frac{\mu v^2}{\sqrt{2} M_\Delta^2}. \tag{2.40}$$

[5] We discuss the gauging of global symmetries and the corresponding anomalies in more detail in Chapter 4.

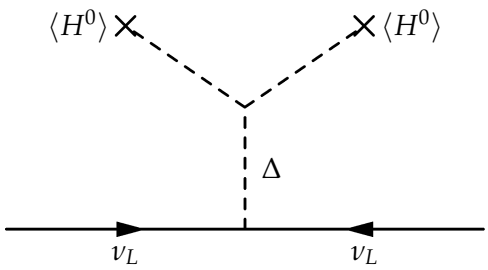

Figure 2.2: Feynman diagram of the Majorana neutrino mass term in the type II seesaw mechanism, which introduces a scalar triplet $\Delta \sim (\mathbf{1}, \mathbf{3}, 1)$. The VEV of the scalar triplet is induced by the VEVs of the neutral component of the SM Higgs.

See Fig. 2.2 for the corresponding Feynman diagram. Taking $Y_\Delta \approx 1$ and assuming $\mu \approx M_\Delta$, we would thus need $M_\Delta \approx 10^{14}\,\text{GeV}$ for a neutrino mass of the order eV.

The type II seesaw mechanism can be naturally embedded into a class of left–right symmetric theories. It always is a hybrid scenario between type I and type II seesaw in that case, due to the presence of right-handed neutrinos in the right–handed doublets. See Chapter 5 for more details.

The triplet VEV v_Δ can constrained to be small. The VEVs have to fulfill the relation

$$v^2 + 2v_\Delta^2 = (246\,\text{GeV})^2\,, \tag{2.41}$$

because the W mass is found to be

$$m_W = \frac{g^2(v^2 + 2v_\Delta^2)}{4}. \tag{2.42}$$

The Z mass is

$$m_Z = \frac{g^2(v^2 + 4v_\Delta^2)}{4\cos^2\theta_W}, \tag{2.43}$$

where θ_W is the Weinberg angle. This leads to a change in the tree-level ρ parameter

$$\rho \equiv \frac{m_W^2}{m_Z^2\cos^2\theta_W} = \frac{1 - \frac{2v_\Delta^2}{v^2}}{1 - \frac{4v_\Delta^2}{v^2}}. \tag{2.44}$$

The current experimental limit constrains the ρ parameter to be close to one [57],

$$\rho = 1.0004^{+0.0003}_{-0.0004}, \tag{2.45}$$

such that

$$v_\Delta < \mathcal{O}(\text{GeV}) \ll v. \tag{2.46}$$

Of course, the type II seesaw can be tested directly if the mass scale of the triplet is within reach of the LHC. The most spectacular signature would be the lepton number violating decay of the doubly charged Higgs to same-sign leptons,

$$\delta^{\pm\pm} \to e_i^{\pm} e_j^{\pm}, \tag{2.47}$$

which is the dominant decay channel if $v_\Delta < 10^{-4}\,\text{GeV}$ [66]. For that final state, limits from current LHC searches constrain [67]

$$m_{\delta^{++}} > 409\,\text{GeV}. \tag{2.48}$$

For $v_\Delta > 10^{-4}\,\text{GeV}$, the dominant decay channel is

$$\delta^{\pm\pm} \to W^{\pm} W^{\pm}, \tag{2.49}$$

and the limits on the mass of $\delta^{\pm\pm}$ are weaker. Prospects of LHC searches strongly depend on the size of v_Δ and also on the triplet mass splittings. A more detailed discussion is provided in Refs. [66, 68].

2.3.3 Type III seesaw

The third option to realize the Weinberg operator at tree level is the type III seesaw mechanism, where at least two extra fermionic triplets with zero weak hypercharge,

$$\rho_\alpha \sim (\mathbf{1}, \mathbf{3}, 0), \tag{2.50}$$

are added [24]. The relevant term in the Lagrangian is

$$-\mathcal{L}_{\text{Type III}} \supset Y_\rho \ell_L^T C i\sigma_2 \rho H + \frac{1}{2} M_\rho \text{Tr}(\rho^T C \rho) + \text{h.c.} \tag{2.51}$$

The structure of the neutrino mass matrix is very similar to type I seesaw. After integrating out the heavy triplets, the mass matrix for the light neutrinos is given by

$$\mathcal{M}_\nu = Y_\rho M_\rho^{-1} Y_\rho^T v^2. \tag{2.52}$$

Just as before, for order one Yukawa couplings, a huge mass $M_\rho \lesssim 10^{14}\,\text{GeV}$ is necessary for light neutrino masses of the order 1 eV or below. See Fig. 2.3 for the corresponding Feynman diagram.

The cleanest channel to search for these new fermionic triplets at the LHC is the trilepton final state. Current LHC results constrain the masses of the fermionic triplets to be of 100 GeV or higher [69].

The type III seesaw mechanism can be easily incorporated into left–right symmetric theories [70]. We do so in Chapter 5, where it will turn out that the minimal left–right symmetric model that allows for gauging baryon and lepton numbers separately contains exactly the fields that can generate neutrino masses via type III seesaw.

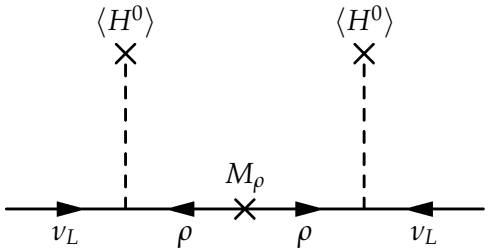

Figure 2.3: Feynman diagram of the Majorana neutrino mass term in the type III seesaw mechanism, which introduces fermionic triplets $\rho \sim (\mathbf{1}, \mathbf{3}, 0)$ with a Majorana mass term M_ρ.

2.4 Radiative neutrino masses

Neutrino masses do not have to be generated at tree level. Their smallness might point to a generation at loop level, using the suppression coming from the loop factors to make their masses tiny compared to the other fermion masses in the SM. A benefit of loop-induced neutrino masses is the possible lightness of the required new particles, with their masses potentially being around the TeV scale and therefore being testable at the LHC. We saw in the last section that the new particles in tree-level realizations have to be heavy to suppress the neutrino masses (assuming no unnaturally small couplings). This renders these new particles practically unobservable in experiments.

We present two one-loop examples in this subsection: the Ma model [71] and the colored seesaw mechanism [72, 73]. Another one-loop model is the Zee model, in which an $SU(2)_L$ singlet scalar that is electrically charged and an additional $SU(2)_L$ doublet scalar [74] are introduced. Often, a simplified version of this model is studied, where a discrete symmetry is imposed to only allow for one of the scalar doublets to couple to the leptons, the so-called Zee–Wolfenstein model [74, 75]. The Zee–Wolfenstein model is ruled out by neutrino data but the original Zee model can satisfy the experimental constraints, see, e.g., Ref. [76]. Of course, it is also possible to generate neutrino masses at more than one loop: an example is the Zee–Babu model at two loops [77, 78].

2.4.1 The Ma model

By introducing fermionic singlets (right-handed neutrinos) and an additional Higgs doublet,

$$N_i \sim (\mathbf{1}, \mathbf{1}, 0) \quad \text{and} \quad \eta = \begin{pmatrix} \eta^+ \\ \eta^0 \end{pmatrix} \sim \left(\mathbf{1}, \mathbf{2}, \frac{1}{2}\right), \tag{2.53}$$

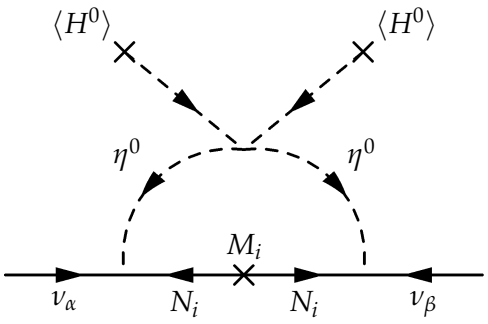

Figure 2.4: One-loop neutrino mass in the Ma model [71].

and imposing an exact $\mathcal{Z}_2$ symmetry under which all SM fields are even and the new fields are odd, tree-level neutrino masses can be forbidden. This is the so-called Ma model [71]. Additionally, the exact $\mathcal{Z}_2$ symmetry forbids a VEV for η. The part of the Lagrangian involving the couplings of the new singlet neutrinos is

$$-\mathcal{L}_N = h_{\alpha j}\overline{\ell_{L\alpha}}\tilde{\eta}N_j + \frac{1}{2}M_i\overline{N_i^c}N_i + \text{h.c.}, \tag{2.54}$$

with $\tilde{\eta} = i\sigma_2\eta^*$, and the scalar potential is given by

$$\begin{aligned} V(H,\eta) = {} & m_1^2 H^\dagger H + m_2^2 \eta^\dagger\eta + \frac{1}{2}\lambda_1\left(H^\dagger H\right)^2 + \frac{1}{2}\lambda_2\left(\eta^\dagger\eta\right)^2 \\ & + \lambda_3\left(H^\dagger H\right)\left(\eta^\dagger\eta\right) + \lambda_4\left(H^\dagger\eta\right)\left(\eta^\dagger H\right) + \frac{1}{2}\lambda_5\left[\left(H^\dagger\eta\right)^2 + \text{h.c.}\right]. \end{aligned} \tag{2.55}$$

Thus, the generation of a neutrino mass at the one-loop level is possible, see Fig. 2.4. The neutrino mass matrix can be calculated to be

$$\mathcal{M}_{\alpha\beta} = \sum_k \frac{h_{\alpha k}h_{\beta k}M_k}{16\pi^2}\left(\frac{m_R^2}{m_R^2 - M_k^2}\ln\frac{m_R^2}{M_k^2} - \frac{m_I^2}{m_I^2 - M_k^2}\ln\frac{m_I^2}{M_k^2}\right), \tag{2.56}$$

where m_R and m_I are the masses of the real part η_R^0 and the imaginary part η_I^0 of η^0, respectively. This neutrino mass is thus induced by a difference between m_R and m_I, which can be calculated to be

$$m_R^2 - m_I^2 = 2\lambda_5 v^2, \tag{2.57}$$

and thus the seesaw scale can be reduced by a factor of $\lambda_5/(16\pi^2)$.

This model has two candidates for the dark matter of the Universe. Due to the imposed $\mathcal{Z}_2$ symmetry either the lightest fermionic singlet N_1 or the lightest of the scalar mass eigenstates η_R^0 or η_I^0 is stable.

It is possible to extend the Ma model by additional fields and an additional $\mathcal{Z}_2'$ symmetry, to realize a multi-component dark matter model. Such a model was proposed in collaboration with Mayumi Aoki, Jisuke Kubo, and Hiroshi Takano in Ref. [49], where we additionally introduced a Majorana fermion χ and a real scalar boson ϕ (both SM singlets) to obtain a three-component DM system, together with the real component of the doublet η introduced before. Usually, each unbroken symmetry guarantees the stability of one DM particle. By choosing

$$m_{\eta_R^0} > m_\chi > m_\phi \text{ and } m_{\eta_R^0} < m_\chi + m_\phi, \tag{2.58}$$

the decay of η_R^0 is kinematically forbidden and three stable DM particles exist. In such a setup, DM conversions and DM semi-annihilations are possible in addition to the standard DM annihilations that usually control the relic density. It was shown that the DM relic density can be very sensitive to these non-standard processes. The solution of the coupled Boltzmann equations in the presence of more than one DM particle is somewhat out of the main focus of this thesis and will not be included here, see Ref. [49] for more details.

2.4.2 The colored seesaw mechanism

Another radiative possibility is the so-called colored seesaw mechanism [72, 73]. Neutrino masses in agreement with the experimental data can be generated by adding fields in the adjoint of $SU(3)_C$ to the particle content of the SM, namely a scalar color octet

$$\Phi = \begin{pmatrix} \Phi^+ \\ \Phi^0 \end{pmatrix} = \begin{pmatrix} \Phi^+ \\ \frac{1}{\sqrt{2}}\left(\Phi_{\mathrm{r}}^0 + \Phi_{\mathrm{i}}^0\right) \end{pmatrix} \sim \left(\mathbf{8}, \mathbf{2}, \frac{1}{2}\right) \tag{2.59}$$

and two or more color octet fermions

$$\Psi_i \sim (\mathbf{8}, \mathbf{1}, 0)\,. \tag{2.60}$$

Sticking to real representations of $SU(3)_C$ avoids new anomalies, where the lowest-dimensional real representation is the adjoint.

The Lagrangian of the new sector is

$$-\mathcal{L}_\nu \supset Y_\nu^{\alpha i}\overline{\ell_{L\alpha}}\, i\sigma_2\, \mathrm{Tr}\left(\Phi^\dagger \Psi_i\right) + \frac{1}{2} M_{\Psi_i} \mathrm{Tr}\left(\overline{\Psi_i^c}\Psi_i\right) + \lambda_{\Phi H} \mathrm{Tr}\left(\Phi^\dagger H\right)^2 + \text{h.c.}, \tag{2.61}$$

where the traces are over color matrices. The mass matrix of the color octet fermions can be taken to be diagonal, without loss of generality. Greek indices correspond to

flavor states, and roman indices correspond to mass eigenstates. $\lambda_{\Phi H}$ and M_{Ψ_i} are taken to be real for simplicity.

The color octet scalar also couples to the quarks via

$$-\mathcal{L}_Q \supset \overline{d_R}\kappa_D \Phi^\dagger Q_L + \overline{u_R}\kappa_U Q_L \Phi + \text{h.c.} \tag{2.62}$$

Baryon number is conserved in these interactions, such that this model does not need an additional mechanism to suppress baryon number violating interactions. The new colored fields can decay to SM quark–antiquark pairs via the coupling in Eq. (2.62), so that there is no problem with cosmological constraints. Rotating the quark fields into the physical basis, the Lagrangian reads

$$\begin{aligned}
\mathcal{L}_Q = {} & \bar{d}\left[P_L\left(D_R^\dagger \kappa_D U_L\right) - P_R\left(D_L^\dagger \kappa_U^\dagger U_R\right)\right]\Phi^- u \\
& + \bar{u}\left[P_R\left(U_L^\dagger \kappa_D^\dagger D_R\right) - P_L\left(U_R^\dagger \kappa_U D_L\right)\right]\Phi^+ d \\
& + \frac{\Phi_\mathrm{r}^0}{\sqrt{2}}\bar{d}\left[P_L\left(D_R^\dagger \kappa_D D_L\right) + P_R\left(D_L^\dagger \kappa_D^\dagger D_R\right)\right] d \\
& + \frac{\Phi_\mathrm{r}^0}{\sqrt{2}}\bar{u}\left[P_L\left(U_R^\dagger \kappa_U U_L\right) + P_R\left(U_L^\dagger \kappa_U^\dagger U_R\right)\right] u \\
& - i\frac{\Phi_\mathrm{i}^0}{\sqrt{2}}\bar{d}\left[P_L\left(D_R^\dagger \kappa_D D_L\right) - P_R\left(D_L^\dagger \kappa_D^\dagger D_R\right)\right] d \\
& + i\frac{\Phi_\mathrm{i}^0}{\sqrt{2}}\bar{u}\left[P_L\left(U_R^\dagger \kappa_U U_L\right) - P_R\left(U_L^\dagger \kappa_U^\dagger U_R\right)\right] u.
\end{aligned} \tag{2.63}$$

Here, $U_{L,R}$ and $D_{L,R}$ are the rotation matrices for up- and down-type quarks u and d.

If one assumes minimal flavor violation (MFV),[6]

$$\kappa_U = c_U Y_U \quad \text{and} \quad \kappa_D = c_D Y_D \tag{2.64}$$

with some constants c_U and c_D, the physical interactions can be rewritten using the quark masses m_U, m_D, and the Cabibbo–Kobayashi–Maskawa (CKM) quark mixing matrix V_CKM [63, 64] as

$$\begin{aligned}
\mathcal{L}_Q^\mathrm{MFV} = {} & \frac{\sqrt{2}}{v}\bar{d}\left(P_L c_D m_D V_\mathrm{CKM}^\dagger - P_R c_U V_\mathrm{CKM}^\dagger m_U\right)\Phi^- u \\
& + \frac{\sqrt{2}}{v}\bar{u}\left(P_R c_D V_\mathrm{CKM} m_D - P_L c_U m_U V_\mathrm{CKM}\right)\Phi^+ d \\
& + c_D\frac{m_D}{v}\Phi_\mathrm{r}^0 \bar{d}d + c_U\frac{m_U}{v}\Phi_\mathrm{r}^0 \bar{u}u + ic_D\frac{m_D}{v}\Phi_\mathrm{i}^0 \bar{d}\gamma_5 d - ic_U\frac{m_U}{v}\Phi_\mathrm{i}^0 \bar{u}\gamma_5 u.
\end{aligned} \tag{2.65}$$

[6] The framework of MFV requires that all flavor-violating interactions are linked to the structure of the ordinary Yukawa couplings, which is exactly what the condition in Eq. (2.64) demands in our case. MFV can be defined more rigorously, see, e.g., Ref. [79].

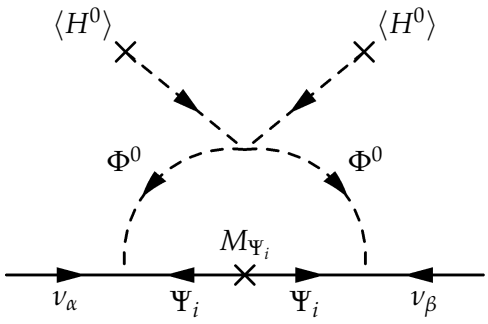

Figure 2.5: One-loop neutrino mass generated by the color octet particles in the colored seesaw mechanism [72, 73].

$\mathrm{SU}(3)_C$ remains unbroken. Therefore, the new scalar does not obtain a VEV and the neutrinos remain massless at tree level. No additional symmetry has to be imposed in this model to achieve this, as opposed to the Ma model where a $\mathcal{Z}_2$ symmetry forbids neutrino masses at tree level. As displayed in Fig. 2.5, a neutrino mass is generated at the one-loop level, given by [72, 73]

$$M_\nu^{\alpha\beta} = \sum_i v^2 \frac{\lambda_{\Phi H}}{16\pi^2} Y_\nu^{\alpha i} Y_\nu^{\beta i} \mathcal{I}\left(M_\Phi, M_{\Psi_i}\right). \tag{2.66}$$

Here, v is the SM Higgs VEV as before, M_Φ the mass of the new scalar, and $\mathcal{I}(M_\Phi, M_{\Psi_i})$ is a loop function of the octet particle masses given by

$$\mathcal{I}_i \equiv \mathcal{I}\left(M_\Phi, M_{\Psi_i}\right) = M_{\Psi_i} \frac{M_\Phi^2 - M_{\Psi_i}^2 + M_{\Psi_i}^2 \ln\left(\frac{M_{\Psi_i}^2}{M_\Phi^2}\right)}{\left(M_\Phi^2 - M_{\Psi_i}^2\right)^2}. \tag{2.67}$$

For $M_\Phi \gg M_{\Psi_i}$, the neutrino mass matrix can be approximated as

$$M_\nu^{\alpha\beta} \approx \sum_i v^2 \frac{\lambda_{\Phi H}}{16\pi^2} Y_\nu^{\alpha i} Y_\nu^{\beta i} \frac{M_{\Psi_i}}{M_\Phi^2}. \tag{2.68}$$

The color octet fermions have the same quantum numbers as gluinos in supersymmetric theories. The Particle Data Group gives $M_\Psi > 8 \times 10^2\,\mathrm{GeV}$ as their best limit [57]. For the octet scalars, current bounds are about 2 TeV [80, 81]. Usually, these bounds are derived assuming negligible couplings to the quarks, i.e., production only in the gluon fusion channel. The color octet scalar has interactions with the quarks in the colored seesaw scenario, therefore these bounds may be weakened. Using these values and $v = 246\,\mathrm{GeV}$, one needs

$$Y_\nu^2 \lambda_{\Phi H} \approx 10^{-8} \tag{2.69}$$

in order to obtain neutrinos with mass around eV. Thus, it is perfectly viable to have an explanation for the light neutrino masses that is in reach of the LHC. Using neutrino Yukawa couplings of order one, this amounts to a value

$$\lambda_{\Phi H} \approx 10^{-8}. \tag{2.70}$$

We study such values in our survey of $0\nu\beta\beta$ in the colored seesaw scenario in Section 3.2. Note that, for such values, there is a strong hierarchy between $\lambda_{\Phi H}$ and the Yukawa coupling of the quarks. Radiative corrections might spoil this hierarchy, for example in diagrams in which the quartic $\Phi^\dagger\Phi^\dagger HH$ coupling is mediated by quark loops. However, in the limit where only the coupling of Φ to the up and down quark is non-zero, which is sufficient for our $0\nu\beta\beta$ analysis, this diagram is suppressed heavily by $(m_{u,d}/v)^2$ and causes no problem.

The structure of the neutrino mass matrix is similar to the seesaw mechanism. Just as with heavy singlets or triplets in type I or type III seesaw, respectively, one heavy fermionic field corresponds to one massive light neutrino. The two mass-squared differences observed in neutrino oscillation experiments [53] thus require at least two additional heavy fermions, as mentioned before. Therefore, with $i = 1, 2$, one of the light neutrinos will be massless. We focus on the case $i = 1, 2, 3$ in our analysis in Section 3.2, but we also mention the results for the case $i = 1, 2$.

In some sense, neutrino masses and lepton number violation can be decoupled in this model. In Eqs. (2.61) and (2.62), two independent sources of lepton number violation exist. The first term of Eq. (2.61) may be used to assign lepton number to the color octet particles. If one assigns lepton number to Ψ_i, the colored fermion mass term is lepton number violating. If one assigns lepton number to Φ, then both the $\lambda_{\Phi H}$ term in Eq. (2.61) and the quark couplings to Φ in Eq. (2.62) are lepton number violating. Thus, even if $\lambda_{\Phi H} = 0$ and the one-loop neutrino masses in Eq. (2.66) vanish, there is a source of lepton number violation in the theory. Specifically, there are be non-vanishing contributions to $0\nu\beta\beta$, which we discuss in more detail in Section 3.2. Since lepton number is not conserved, higher order diagrams will of course lead to very small neutrino masses also in this case. In addition, lepton flavor conservation is violated even for vanishing $\lambda_{\Phi H}$ from the term proportional to Y_ν. We take the bounds from lepton flavor violating decays into account in our analysis in Section 3.2.

Colored fields offer the great advantage of being easy to produce at the LHC (if their masses are around the TeV scale), so that there is the possibility that this mechanism for neutrino masses may be probed independently. Production and decay mechanisms of the colored octet scalars were first studied in detail in Refs. [82, 83]. If the neutral component of the octet scalar is the lightest new particle, it will decay to quark–antiquark pairs via the coupling in Eq. (2.62). Another option is the decay at one loop via terms in the scalar potential to gluons [84]. Due to a mass splitting between

the octet scalars introduced by the SM Higgs VEV [84], decays such as $\Phi^{\pm} \to \Phi^0 W^{\pm}$ might be allowed. Alternatively, the probably dominant decay mode is $\Phi^{\pm} \to t\bar{b}$, also via the coupling in Eq. (2.62).

Production and decay of the colored fermions was discussed in detail in Ref. [73]. The octet fermions will be produced in pairs via the strong interaction,

$$pp \to \Psi_i \Psi_i, \tag{2.71}$$

either in gluon–gluon fusion or in quark–antiquark annihilation. The dominant decay modes will depend on the masses of the octet particles. In Section 3.2 we consider the case that the scalar is heavier than the fermion, such that for $M_\Phi > M_{\Psi_i} > m_t$ the most dominant decay channel is via an off-shell charged scalar octet into a charged lepton and a quark pair [73]

$$\Psi_i \to \ell_k^+ \bar{t} b \;\text{ or }\; \Psi_i \to \ell_k^- t \bar{b}, \tag{2.72}$$

or for $M_\Phi > M_{\Psi_i} > 2m_t$[7] via an off-shell neutral scalar octet into neutrinos and a top quark pair

$$\Psi_i \to \nu_k \bar{t} t \;\text{ or }\; \Psi_i \to \bar{\nu}_k t \bar{t}. \tag{2.73}$$

It was found that, for fermionic octets up to a few TeV in mass, events with same-sign dileptons plus multiple jets in the final state could be detectable over SM background as an indication of lepton number violation in the decay of the fermionic octets [73].

2.5 Summary

This section provided an introduction to the concepts used throughout the rest of this thesis. We started with the SM of particle physics as a gauge theory and presented the particle content with the corresponding transformation properties under the gauge group G_{SM} given in Eq. (2.1). Any particle physics model intended to solve any of the issues remaining in the SM extends G_{SM} by additional gauge factors and/or extends the SM particle content given in Tab. 2.1. We discussed approaches to neutrino masses introducing extra particles in this chapter, and we will extend both the gauge group and the particle content of the SM in Part II, where we discuss gauge theories for baryon and lepton numbers.

Then, we turned to extensions of the SM to incorporate neutrino masses. We focussed on the implementation of Majorana neutrino masses. The generic tree-level realizations of the Weinberg operator were discussed in some detail: the famous seesaw mechanisms of type I, type II, and type III. Although being minimal extensions of the

[7] Assuming no mass splitting for the color octet scalars, i.e., them being much heavier than the electroweak scale.

SM in the sense that they only introduce one new representation to the particle content, and no new gauge groups are necessary, this solution is somewhat unsatisfactory. If one wants to avoid unnaturally small couplings (as was the original aim when going from Dirac neutrino masses via the Higgs mechanism to Majorana neutrino masses via the seesaw mechanism), the new particles have to live at a scale

$$\Lambda_{\text{seesaw}} \lesssim 10^{14}\,\text{GeV}, \tag{2.74}$$

which makes it impossible to test this neutrino mass mechanism experimentally.

The radiative neutrino mass models we discussed (we presented the Ma model and the colored seesaw mechanism in some detail) do not suffer from the problem of large scales, because the additional loop factors can be used to suppress the neutrino masses. The additionally introduced particles can then live at the TeV scale and therefore be tested, e.g., at the LHC.

One does not have to rely on loops or large masses of mediators to suppress the neutrino masses compared to the other fermion masses in the SM. A more exotic option is to allow the right-handed neutrinos, which are SM singlets, to be part of some hidden sector, and to use features of this sector to understand the origin of the light neutrino masses. Going to extra-dimensional setups, a realization of this idea is the so-called mini-seesaw mechanism in warped space [85], which combines naturally suppressed Dirac and Majorana masses leading to light SM neutrinos via a low-scale seesaw. This is achieved by allowing the right-handed neutrinos to be bulk fields in a warped extra dimension. The suppression of the Dirac mass scale is then achieved by a small wave function overlap between the bulk neutrinos and the SM fields, which are confined to the UV brane. The suppression of the Majorana masses is generated by warping. Thus, no small couplings or large scales have to be involved for tiny neutrino masses. As a key feature of this model, a tower of Kaluza–Klein modes of sterile neutrinos exists and mixes with the SM. A detailed phenomenological analysis for these (of the order GeV) sterile neutrinos was done in [48] in collaboration with Kristian L. McDonald and Damien P. George, and it was shown that viable parameter space exists in which light neutrino masses can be generated without relying on supra-TeV scales. Lepton flavor violation in $\mu \to e\gamma$, neutrinoless double beta decay, and invisible Z decays were discussed, and key observables lie just below current experimental sensitivities. For example, the most recent MEG limit for $\mu \to e\gamma$ already cuts into the parameter space. Thus, there is hope that in such a setup the origin of neutrino mass may be probed directly. Introducing extra-dimensional theories is beyond the scope of this thesis, so we refer the interested reader to the original publications [48, 85] for more details.

Chapter 3

Neutrinoless double beta decay

At least theoretically, it is an interesting possibility that not only the individual lepton flavor numbers L_e, L_μ, and L_τ are not conserved in nature, but also the total lepton number $L = L_e + L_\mu + L_\tau$ is broken. Currently, the most promising experimental test for lepton number violation is neutrinoless double beta decay ($0\nu\beta\beta$), which we discuss in this chapter. We start with a general introduction to $0\nu\beta\beta$ in Section 3.1. In Section 3.2, we discuss the phenomenology of $0\nu\beta\beta$ in detail for one of the models from the neutrino mass model zoo that we introduced in Section 2.4.2 of the last chapter: the colored seesaw mechanism. After that, in Section 3.3, we tackle a more experimental question and discuss the possibility of discriminating $0\nu\beta\beta$ from unknown nuclear background lines in only one isotope by considering the decay to excited states in addition to the ground state transition. We give a summary of this chapter in Section 3.4.

3.1 Basics of neutrinoless double beta decay

Thirty-five even/even nuclei (even number N of neutrons and even number Z of protons) can undergo the second-order process double beta decay, because the first-order process single beta decay is energetically forbidden or at least strongly suppressed. This observation can be made from the semi-empirical Bethe–Weizsäcker mass formula [86, 87], which describes the binding energy of a nucleus and contains a term for the tendency of protons and neutrons to form pairs. The pairing energy is positive for even/even atomic nuclei, thus increasing the binding energy and therefore decreasing the mass of the nucleus, and negative for odd/odd ones, thus decreasing the binding energy and increasing the mass. The pairing energy vanishes for even/odd or odd/even nuclei. As a result, the mass parabolae of even/even and odd/odd nuclei split, as shown in Fig. 3.1. In that case, single beta decay is forbidden if the (potential) daughter nucleus has a larger mass than the decaying one. In some cases, single beta decay is energetically allowed because the neighboring odd/odd nucleus is lower in mass, but the spin difference between the states of parent and daughter nucleus strongly suppresses the decay. This is the case in, e.g., ^{96}Zr.

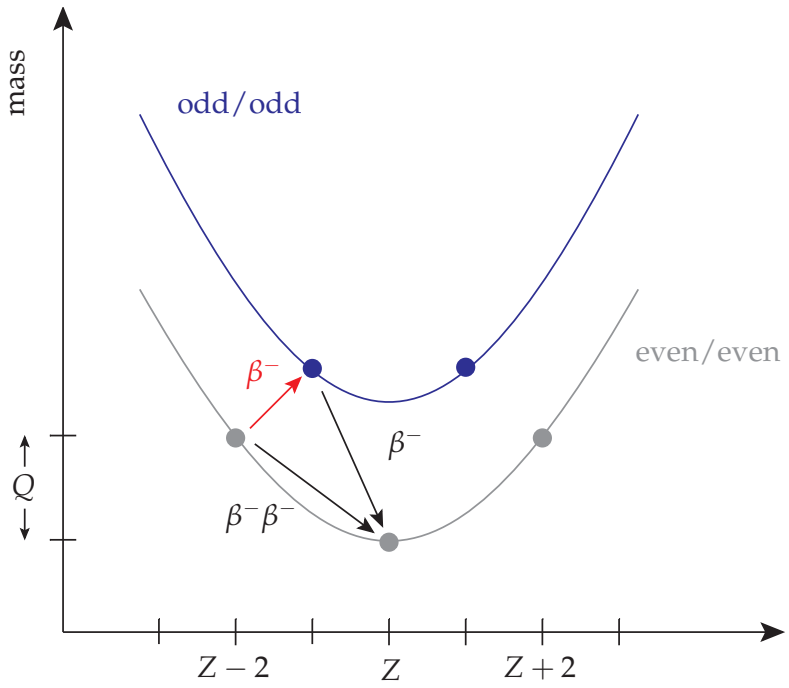

Figure 3.1: Mass parabolae of even/even (gray) and odd/odd (blue) nuclei. For some even/even nuclei the first-order process single beta decay (denoted by β^- in the figure) is energetically forbidden, see the red arrow, because the (potential) daughter nucleus has a larger mass. In that case, the second-order process double beta decay (denoted by $\beta^-\beta^-$) can occur. The Q-value of double beta decay is the mass difference between the decaying nucleus and its daughter nucleus.

In the SM, double beta decay of a nucleus with mass number $A = N + Z$ may occur in the two-neutrino mode,

$$(Z, A) \rightarrow (Z + 2, A) + 2e^- + 2\bar{\nu}_e \quad (2\nu\beta\beta), \tag{3.1}$$

where two electrons and two antineutrinos are emitted. Thus, $2\nu\beta\beta$ decay conserves lepton number. It has been observed experimentally in several isotopes with half-lives in the range 10^{18-24} y [88].

If lepton number is broken in nature (by two units), the neutrinoless mode,

$$(Z, A) \rightarrow (Z + 2, A) + 2e^- \quad (0\nu\beta\beta), \tag{3.2}$$

is also allowed, where only two electrons are emitted. This decay mode has not yet been observed experimentally and the best half-life limits are of the order 10^{25} y. The best

Table 3.1: Best experimental lower limits on the half-lives of $0\nu\beta\beta$ for the isotopes ^{76}Ge and ^{136}Xe (at 90% CL).

Isotope	$T^{0\nu}_{1/2}$ [years]	Experiment
^{76}Ge	$\geq 1.9 \times 10^{25}$	Heidelberg–Moscow (HdM) [92]
^{76}Ge	$\geq 1.57 \times 10^{25}$	IGEX [93, 94]
^{76}Ge	$\geq 2.1 \times 10^{25}$	GERDA [27]
^{76}Ge	$\geq 3.0 \times 10^{25}$	combination HdM, IGEX, GERDA [27]
^{136}Xe	$\geq 1.6 \times 10^{25}$	EXO-200 [25]
^{136}Xe	$\geq 1.9 \times 10^{25}$	KamLAND-Zen [26]
^{136}Xe	$\geq 3.4 \times 10^{25}$	combination EXO-200, KamLAND-Zen [26]

lower limits for ^{76}Ge and ^{136}Xe from the current round of experiments are provided in Tab. 3.1. Note that a subgroup of the Heidelberg–Moscow collaboration, which used ^{76}Ge as double beta isotope, claims to have a positive signal and gives the half-life [89]

$$T^{0\nu}_{1/2} = 1.19^{+0.37}_{-0.23} \times 10^{25}\,\text{y}. \tag{3.3}$$

A later analysis results in [90]

$$T^{0\nu}_{1/2} = 2.23^{+0.44}_{-0.31} \times 10^{25}\,\text{y}, \tag{3.4}$$

although it has some known inconsistencies [91]. The results from GERDA phase I [27] now strongly disfavor the claim. Earlier results from KamLAND-Zen and EXO-200 were also incompatible with it (for all but one nuclear matrix element calculation) [25, 26]. In any case, the Heidelberg–Moscow collaboration provided (in a different analysis) the most stringent limit on $0\nu\beta\beta$ in ^{76}Ge before GERDA; see Tab. 3.1.

The two modes of double beta decay can be distinguished experimentally by the energy spectrum of the emitted electrons. For $0\nu\beta\beta$, the energies of the two electrons add up to the total released energy of the nuclear transition, the so-called Q-value. For $2\nu\beta\beta$, the spectrum of the total kinetic energy of the two electrons is continuous because the emitted neutrinos may take away an arbitrary amount of energy. For a comparison of the spectra, see Fig. 3.2.

Other lepton number violating processes depending on the same particle physics parameters as $0\nu\beta\beta$ are neutrinoless double positron decay ($0\nu\beta^+\beta^+$),

$$(A, Z) \rightarrow (A, Z-2) + 2e^+, \tag{3.5}$$

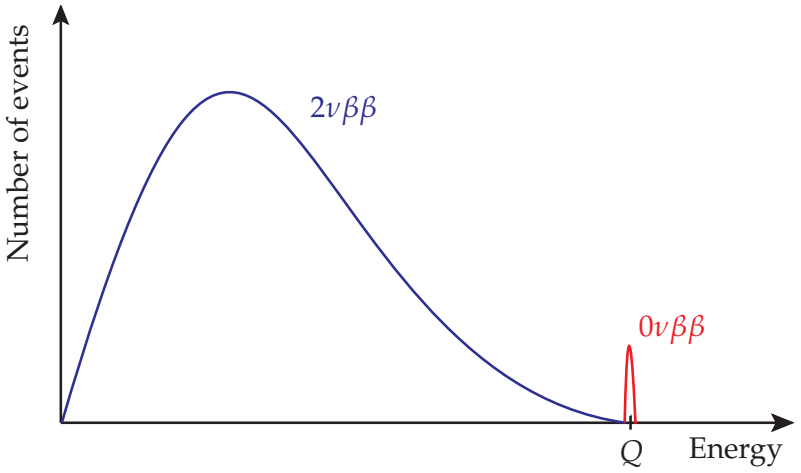

Figure 3.2: Schematic plot of the spectrum of the total energy of the emitted electrons for the two modes of double beta decay. The spectrum for $2\nu\beta\beta$ is continuous, because the emitted neutrinos may take away an arbitrary amount of energy. The spectrum for $0\nu\beta\beta$ is a single peak at the Q-value of the nuclear transition.

positron emitting electron capture $(0\nu\beta^+\text{EC})$,

$$e_b^- + (A, Z) \rightarrow (A, Z-2) + e^+, \tag{3.6}$$

and double electron capture $(0\nu\text{ECEC})$,

$$2e_b^- + (A, Z) \rightarrow (A, Z-2)^*, \tag{3.7}$$

where the latter two include bound state electrons e_b^-. In 0νECEC, the final nucleus is in an excited state and will de-excite via emission of photons. All of these processes are somewhat suppressed in comparison to $0\nu\beta\beta$. In this thesis, we therefore focus on $0\nu\beta\beta$, which we discuss in more detail in the following subsections.

3.1.1 The standard mechanism: light Majorana neutrino exchange

Shortly after Majorana published his symmetric theory for particles and antiparticles [95], it was realized that the so-called Racah sequence [96] is possible if the neutrino is its own antiparticle (a so-called Majorana particle) and if it has a non-vanishing rest mass to account for the helicity matching,

$$(Z, A) \rightarrow (Z+1, A) + e^- + \overline{\nu}_e \tag{3.8}$$

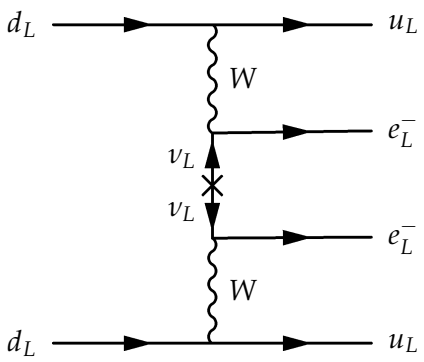

Figure 3.3: The standard mechanism of neutrinoless double beta decay: light Majorana neutrino exchange.

$$(Z+1, A) + \nu_e \to (Z+2, A) + e^-. \tag{3.9}$$

With virtual neutrinos, this is a realization of neutrinoless double beta decay. This decay was first discussed by Furry as early as 1939 [97].

The particle physics amplitude of $0\nu\beta\beta$ mediated by light Majorana neutrinos (see the corresponding Feynman diagram in Fig. 3.3) is given by

$$\mathcal{A}_\nu = G_F^2 \sum_{i=1}^{3} \frac{U_{ei}^2 m_i}{p^2 - m_i^2}, \tag{3.10}$$

where U_{ei} are the elements of the first line of the PMNS neutrino mixing matrix that we introduced in Eq. (2.31), m_i $(i = 1, 2, 3)$ are the light neutrino mass eigenvalues, and p is the momentum exchange of the process. G_F is the Fermi coupling constant. For this nuclear process, the typical momentum scale $\langle p^2 \rangle$ is set by the size of the nucleus. A typical distance between two nucleons is $r \approx 10^{-13}$ cm, such that we arrive at

$$\langle p^2 \rangle \approx \frac{1}{r^2} \approx (100\,\mathrm{MeV})^2. \tag{3.11}$$

For light Majorana neutrinos, $m_i^2 \ll \langle p^2 \rangle$, we can thus approximate

$$\mathcal{A}_\nu \simeq G_F^2 \sum_{i=1}^{3} \frac{U_{ei}^2 m_i}{\langle p^2 \rangle}, \tag{3.12}$$

From the amplitude, the half-life $T_{1/2}^{0\nu}$ of neutrinoless double beta decay can be calculated to be

$$\frac{1}{T_{1/2}^{0\nu}} = \frac{m_{0\nu\beta\beta}^2}{m_e^2} \left| \mathcal{M}^{0\nu} \right|^2 G^{0\nu}(Q, Z). \tag{3.13}$$

See the seminal survey of neutrinoless double beta decay by Doi *et al.* [98] for details of the corresponding calculation.

The nuclear matrix element $\mathcal{M}^{0\nu}$ and the phase space integral $G^{0\nu}(Q, Z)$ depend on the nucleus under consideration. The electron mass m_e is only introduced in order to make the "coupling constant" $m_{0\nu\beta\beta}/m_e$ dimensionless. In a different convention, this factor is absorbed into the phase space factor. Assuming the standard mechanism for $0\nu\beta\beta$, it is thus possible to measure the so-called effective Majorana mass of the electron neutrino, $m_{0\nu\beta\beta}$. Below, we discuss the three building blocks of the half-life formula in Eq. (3.13).

The effective mass

The effective mass used in Eq. (3.13) is given by

$$m_{0\nu\beta\beta} = \left| \sum_{i=1}^{3} U_{ei}^2 m_i \right| . \tag{3.14}$$

A widely parameterization of the PMNS matrix U, which is unitary in a framework with three light neutrino species, is [22]

$$\mathcal{U} = \begin{pmatrix} c_{12}c_{13} & s_{12}c_{13} & s_{13}e^{-i\delta} \\ -s_{12}c_{23} - c_{12}s_{23}s_{13}e^{i\delta} & c_{12}c_{23} - s_{12}s_{23}s_{13}e^{i\delta} & s_{23}c_{13} \\ s_{12}s_{23} - c_{12}c_{23}s_{13}e^{i\delta} & -c_{12}s_{23} - s_{12}c_{23}s_{13}e^{i\delta} & c_{23}c_{13} \end{pmatrix} S, \tag{3.15}$$

where $c_{ij} = \cos\theta_{ij}$, $s_{ij} = \sin\theta_{ij}$, and δ is the Dirac CP phase. This parameterization is now adopted as standard by the Particle Data Group [57]. θ_{ij} are the mixing angles measured in neutrino oscillation experiments [53], see Appendix A for current values. In case of Dirac neutrinos, S is the unit matrix; for Majorana neutrinos,

$$S = \mathrm{diag}\left(1, e^{i\frac{\alpha}{2}}, e^{i\frac{\beta}{2}+i\delta}\right), \tag{3.16}$$

where α and β are the two Majorana CP phases.

Using this parameterization for the PMNS mixing matrix U, the effective mass can be expressed as

$$m_{0\nu\beta\beta} = \left| c_{13}^2 \left(m_1 c_{12}^2 + e^{i\alpha} m_2 s_{12}^2 \right) + e^{i\beta} m_3 s_{13}^2 \right| . \tag{3.17}$$

In neutrino oscillation experiments, the sign of the mass-squared difference $\Delta m_{31}^2 \equiv m_3^2 - m_1^2$ cannot be determined. Therefore, two hierarchies of the neutrino masses are possible:

$$m_1 < m_2 \ll m_3 \ \text{(normal hierarchy)}, \tag{3.18}$$

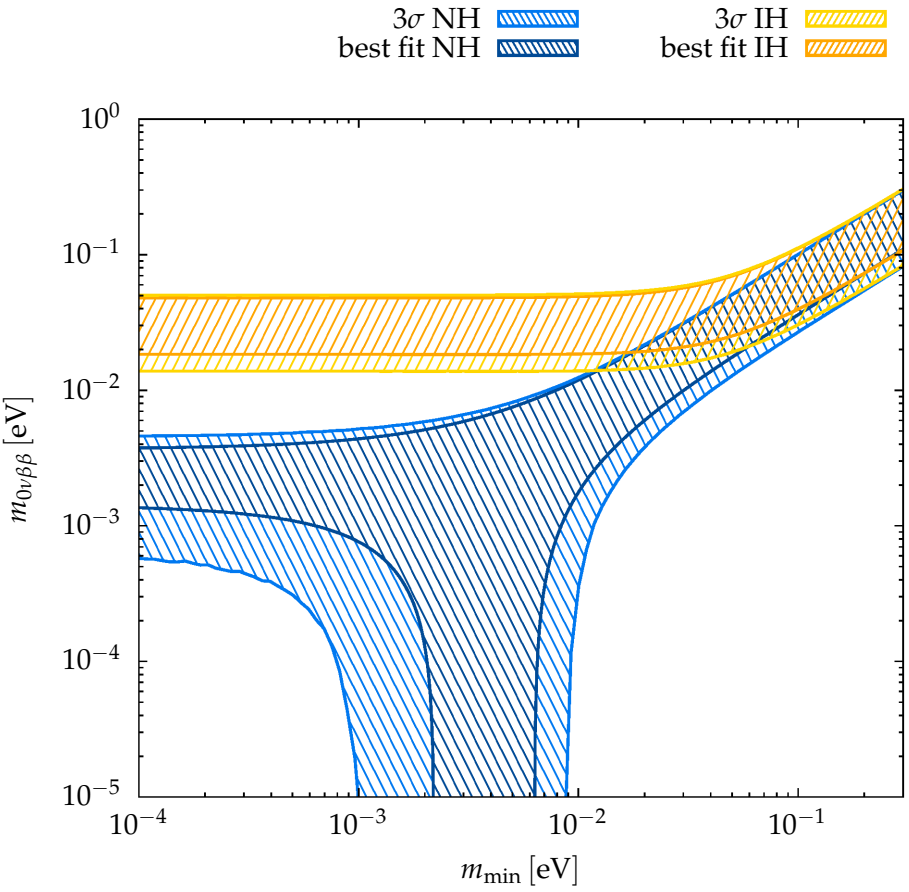

Figure 3.4: The effective Majorana mass $m_{0\nu\beta\beta}$ as a function of the lightest neutrino mass eigenvalue $m_{\text{min}} = m_1$ for normal (blue/light blue) and $m_{\text{min}} = m_3$ for inverted (orange/yellow) mass hierarchy. In the quasi degenerate regime, where m_{min} is much larger than the mass-squared differences measured in oscillation experiments, the two bands overlap. Bold colors denote the best fit values range (varying the unknown CP phases only), light colors give the ranges where all oscillation parameters are varied inside their 3σ values ranges.

$$m_3 \ll m_1 < m_2 \text{ (inverted hierarchy).} \tag{3.19}$$

For both hierarchies, we denote the smallest neutrino mass eigenvalue by m_{min} (m_1 for normal hierarchy, m_3 for inverted hierarchy). If

$$m_{\text{min}} \gg \sqrt{|\Delta m^2_{31}|}, \tag{3.20}$$

both orderings overlap in the so-called degenerate regime. For a more detailed discussion of the results of neutrino oscillation experiments, see Ref. [53].

We can use the oscillation parameters given in Appendix A and calculate the effective mass as a function of the lightest neutrino mass eigenvalue. Even for the best-fit values, there is some uncertainty in the value due to the variation of the unknown Majorana phases. The result is plotted in Fig. 3.4. Note that for inverted hierarchy a lower limit on $m_{0\nu\beta\beta}$ exists, whereas for normal hierarchy, for a certain range of m_1, the double beta contribution of the light neutrinos may vanish due to cancellations in the expression for the effective mass $m_{0\nu\beta\beta}$.

Due to uncertainties in the nuclear matrix element calculations, see below for a more detailed discussion, there is some uncertainty in the upper limits on $m_{0\nu\beta\beta}$ that can be inferred from experiment. The most recent result for ^{76}Ge comes from the GERDA [27] experiment, which provides a range

$$m_{0\nu\beta\beta} \leq (0.2 - 0.4)\,\text{eV}. \tag{3.21}$$

A combination of the results of EXO-200 and KamLAND-Zen on $0\nu\beta\beta$ in ^{136}Xe provides a range [26]

$$m_{0\nu\beta\beta} \leq (0.12 - 0.25)\,\text{eV}. \tag{3.22}$$

Compare the other limits for neutrino masses given before; see Eqs. (2.9) and (2.11).

Phase space factors

Due to the phase space factor $G^{0\nu}(Q, Z)$, the total decay rates and hence the inverse half-lives of $0\nu\beta\beta$ depend strongly on the available Q-value: $G^{0\nu}(Q, Z)$ scales with Q^5. Therefore, isotopes with a high Q-value (above about 2 MeV) are usually considered for experiments on double beta decay. This restricts the candidates to 11 promising isotopes, which are given in Tab. 3.2 together with the corresponding Q-values, matrix elements $\mathcal{M}^{0\nu}$, and phase space factors $G^{0\nu}(Q, Z)$, all for the decay to the ground state of the daughter nucleus.

The original calculations of the phase space factors for $0\nu\beta\beta$ [98–102] are only approximate, because the electron wave functions are approximated at the nuclear radius and electron screening is not included. The newer approaches take exact Dirac wave

Table 3.2: List of all double beta isotopes with a Q-value larger than 2 MeV. The corresponding Q-values, nuclear matrix elements $\mathcal{M}^{0\nu}$, and phase space factors $G^{0\nu}$ are given, for the decay to the ground state of the daughter nucleus. All Q-values with an error larger than 1 keV are taken from Ref. [105]. All other Q-values were recently remeasured using Penning traps [106–114]. The matrix elements are IBM-2 calculations [115]. The phase space factor for $^{124}_{50}$Sn is from Ref. [103], all other phase space factors are from the more recent calculation in Ref. [104]. g_A is the axial coupling.

Decay	Q [keV]	$\mathcal{M}^{0\nu}$ [115]	$G^{0\nu}$ $[g_A^4 \mathrm{y}^{-1}]$ [103, 104]
$^{48}_{20}\mathrm{Ca}\rightarrow^{48}_{22}\mathrm{Ti}$	4267.98±0.32 [106]	1.98 ± 0.59	2.49×10^{-14}
$^{76}_{32}\mathrm{Ge}\rightarrow^{76}_{34}\mathrm{Se}$	2039.061±0.007 [107]	5.42 ± 1.03	2.34×10^{-15}
$^{82}_{34}\mathrm{Se}\rightarrow^{82}_{36}\mathrm{Kr}$	2997.9±0.3 [108]	4.37 ± 0.83	1.01×10^{-14}
$^{96}_{40}\mathrm{Zr}\rightarrow^{96}_{42}\mathrm{Mo}$	3347.7±2.2 [105]	2.53 ± 0.40	2.03×10^{-14}
$^{100}_{42}\mathrm{Mo}\rightarrow^{100}_{44}\mathrm{Ru}$	3034.40±0.17 [109]	3.73 ± 0.60	1.57×10^{-14}
$^{110}_{46}\mathrm{Pd}\rightarrow^{110}_{48}\mathrm{Cd}$	2017.85±0.64 [110]	3.62 ± 0.58	4.79×10^{-15}
$^{116}_{48}\mathrm{Cd}\rightarrow^{116}_{50}\mathrm{Sn}$	2813.50±0.13 [111]	2.78 ± 0.44	1.66×10^{-14}
$^{124}_{50}\mathrm{Sn}\rightarrow^{124}_{52}\mathrm{Te}$	2287.8±1.5 [105]	3.50 ± 0.67	9.04×10^{-15}
$^{130}_{52}\mathrm{Te}\rightarrow^{130}_{54}\mathrm{Xe}$	2526.97±0.23 [111]	4.03 ± 0.77	1.41×10^{-14}
$^{136}_{54}\mathrm{Xe}\rightarrow^{136}_{56}\mathrm{Ba}$	2457.83±0.37 [112, 113]	3.33 ± 0.63	1.46×10^{-14}
$^{150}_{60}\mathrm{Nd}\rightarrow^{150}_{62}\mathrm{Sm}$	3371.38±0.20 [114]	2.32 ± 0.37	6.20×10^{-14}

functions with finite nuclear size and electron screening into account [103]. The calculations can be additionally improved by using a Coulomb potential derived from a realistic proton density distribution in the daughter nucleus [104]. The values of the phase space factors for the transition to the ground state of the daughter nucleus as well as for the transition to the first excited 0^+ state are calculated in the literature [103, 104]. For the ground state, values of the different calculations agree on the percent level. We have combined both data sets in Tab. 3.2, which gives the values for the ground state transition. Later, when we discuss double beta decay to excited states in Section 3.3, we give the values for the transition to the first excited 0^+ state in Tab. 3.3.

Nuclear matrix elements

The nuclear matrix elements $\mathcal{M}^{0\nu}$ cannot be measured and have to be calculated numerically. Throughout this thesis we use the most current values of the nuclear matrix elements for $0\nu\beta\beta$ calculated in the microscopic interacting boson model (IBM-2) [115, 116], providing values for the transition to the ground state and the first excited state of the daughter nucleus.

Many different models for the calculation of the nuclear matrix elements are on the market, using different approximations. The various approaches give a spread in matrix elements by about a factor of two. An overview of the current situation, and a comparison of alternative approaches to the IBM-2 nuclear matrix elements can be found in Ref. [115].

3.1.2 Other lepton number violating mechanisms

Light Majorana neutrino exchange (see Fig. 3.3) is usually assumed to be the dominant contribution to $0\nu\beta\beta$. It is, however, important to point out that neutrinoless double beta decay is a black box:[1] we do not observe the virtually exchanged particles directly, so any $\Delta L = 2$ lepton number violation process in models for physics beyond the Standard Model may trigger the decay.[2]

One model-independent approach to $0\nu\beta\beta$ is the separation into long-range and short-range contributions [119, 120]. In the long-range contributions, a light neutrino is exchanged, whereas in the short-range contributions, some heavy new physics mediator is exchanged.

Considering the short-range contributions, $0\nu\beta\beta$ becomes an effective vertex diagram as shown in Fig. 3.5, as the heavy new physics can be integrated out. The most general Lorentz-invariant Lagrangian for $0\nu\beta\beta$ is given by [120]

$$\mathcal{L} = \frac{G_F^2}{2} m_p^{-1} \left(\epsilon_1 JJj + \epsilon_2 J^{\mu\nu} J_{\mu\nu} j + \epsilon_3 J^\mu J_\mu j + \epsilon_4 J^\mu J_{\mu\nu} j^\nu + \epsilon_5 J^\mu J j_\mu \right), \tag{3.23}$$

where the hadronic currents are

$$J = \overline{u} \left(1 \pm \gamma_5\right) d, \; J^\mu = \overline{u} \gamma^\mu \left(1 \pm \gamma_5\right) d, \; J^{\mu\nu} = \overline{u} \frac{i}{2} \left[\gamma^\mu, \gamma^\nu\right] \left(1 \pm \gamma_5\right) d, \tag{3.24}$$

and the leptonic currents are

$$j = \overline{e} \left(1 \pm \gamma_5\right) e^c, \; j^\mu = \overline{e} \gamma^\mu \left(1 \pm \gamma_5\right) e^c. \tag{3.25}$$

[1] We discuss the so-called "black box" or Schechter–Valle theorem [117] in the next subsection.

[2] It should be clear that $\Delta L = 2$ lepton number violating new physics will induce Majorana neutrino masses at some loop level. A model where this happens only at four-loop level, so that the neutrinos are pseudo-Dirac particles, but a sizable contribution to $0\nu\beta\beta$ may arise from new particles is given in Ref. [118].

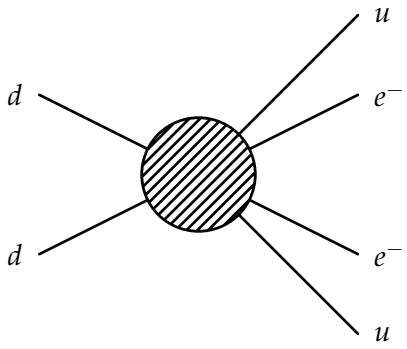

Figure 3.5: Effective dimension-nine operator for neutrinoless double beta decay.

From the experimental non-observation of neutrinoless double beta decay, limits on the coupling constants ϵ_i can be deduced (on-axis evaluation), see [120] and also [121] for current values.

The scaling with G_F and m_P chosen in Eq. (3.23) is motivated by comparison with light neutrino exchange. The effective operator for $0\nu\beta\beta$ is of dimension nine, such that the ϵ_i scale as

$$\epsilon_i \propto \Lambda_{0\nu\beta\beta}^{-5}. \tag{3.26}$$

The resulting amplitude can be compared with the amplitude of $0\nu\beta\beta$ in the light neutrino picture,

$$\mathcal{A}_{\text{light}} \simeq G_F^2 \left| \sum_i \frac{U_{ei}^2 m_i}{\langle p^2 \rangle - m_i^2} \right| \simeq (2.7\,\text{TeV})^{-5}, \tag{3.27}$$

with typical values of

$$m_{0\nu\beta\beta} = \left| \sum U_{ei}^2 m_i \right| \simeq 0.5\,\text{eV} \tag{3.28}$$

for the effective mass and

$$\langle p^2 \rangle \simeq 0.01\,\text{GeV}^2 \gg m_i^2 \tag{3.29}$$

for the exchanged momentum. Thus, a model with a heavy physics scale of

$$\Lambda_{0\nu\beta\beta} \simeq \mathcal{O}(\text{TeV}) \tag{3.30}$$

can give contributions to $0\nu\beta\beta$ of a similar size as those from light neutrino exchange.

The dimension nine operator in Fig. 3.5 can be decomposed in terms of the quantum numbers of the internal mediators, see Ref. [121] for an exhaustive list. At tree-level, two different topologies are possible, see Fig. 3.6. This decomposition of course includes the short-range as well as the long-range contributions.

There is a plethora of lepton number violating new physics models that contain a $0\nu\beta\beta$ mechanism on the market, the usual suspects being seesaw models with the

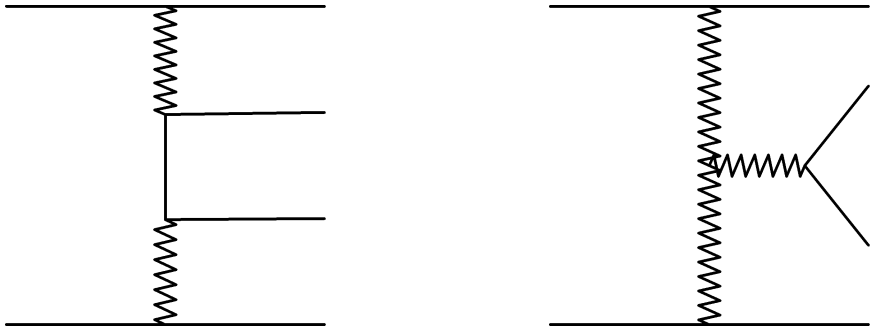

Figure 3.6: The two tree-level topologies of neutrinoless double beta decay diagrams [121]. The plain lines are fermions, the zigzag lines can be scalar or vector particles.

exchange of heavy Majorana neutrinos (type I) [122] or Higgs triplets (type II) [123],[3] left–right symmetric models [23, 124], and R-parity violating SUSY [125, 126]. A full discussion of possible diagrams is beyond the scope of this thesis and can be found in a current review focussing on particle physics models for $0\nu\beta\beta$ [127]. Let us give the diagrams for left–right symmetric models as an example below, because neutrino masses are generated through a combined seesaw type I and type II in these setups, such that the corresponding diagrams are also present. In Section 3.2, we perform a detailed analysis of $0\nu\beta\beta$ in another new physics model: the colored seesaw mechanism [72, 73].

Example: left–right symmetric theories

Left–right symmetric theories will be discussed in more detail in Section 5, where we connect the spontaneous breakdown of parity in these models to the breaking of baryon and lepton numbers. An interesting feature of these theories is the large number of diagrams for $0\nu\beta\beta$ and their possible interplay. Neutrinos usually acquire a Majorana mass in these models through the seesaw mechanism, and the standard diagram will therefore be present, see Fig. 3.3. However, lepton number violation is possible in various vertices in left–right symmetric theories, such that many other diagrams can contribute, see Fig. 3.7. Compare to the diagrams to the two general topologies in Fig. 3.6: both topologies are present in the left–right symmetric model. A quite detailed survey of the different possible diagrams in the parameter space of left–right symmetric theories was performed recently [128]. Depending on the scale of new physics, the different diagrams can have different magnitude. An unambiguous

[3] In type III seesaw, the neutral component of the fermionic triplets can play a similar role in $0\nu\beta\beta$ as the heavy neutrino in type I seesaw.

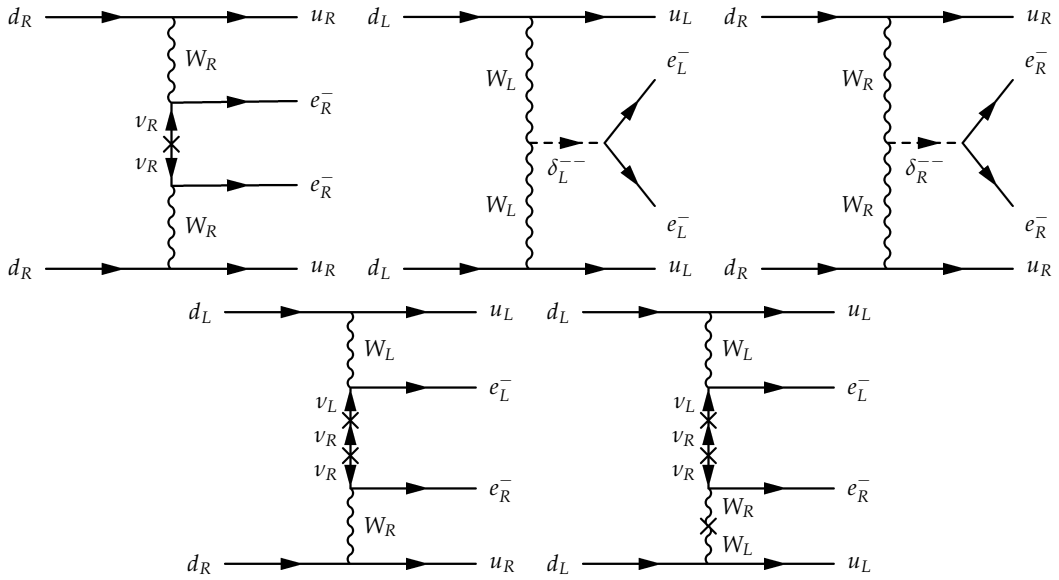

Figure 3.7: Additional diagrams for $0\nu\beta\beta$ decay in the left–right symmetric model, besides light Majorana neutrino exchange. The lower line displays the so-called λ-diagram (left) and the so-called η-diagram (right).

analysis is impossible. There are regions in parameter space where the often neglected so-called λ- and η-diagrams (see lower line of Fig. 3.7) give sizable contributions to $0\nu\beta\beta$. Currently, with the LHC up and running, the connection between $0\nu\beta\beta$ and the LHC for left–right symmetric theories are also discussed [129].

3.1.3 The Schechter–Valle theorem

As we have seen before, a Majorana mass term for the neutrinos can give a sizable rate for $0\nu\beta\beta$. However, as we also have seen, light Majorana neutrino exchange is not the only possible realization of $0\nu\beta\beta$ at the particle physics level. If $0\nu\beta\beta$ is mediated by a diagram not containing virtual Majorana neutrinos, the connection between the Majorana nature of the neutrinos and $0\nu\beta\beta$ is not direct anymore. In that case, the so-called Schechter–Valle or black box theorem saves the connection between $0\nu\beta\beta$ and a Majorana mass for the neutrino, independent of the mechanism underlying the decay: if $0\nu\beta\beta$ is observed with a non-zero rate, it is possible to draw the diagram in Fig. 3.8, which is a Majorana mass term for the electron neutrino [117]. The theorem can be extended by showing that there cannot be any symmetry protecting a zero Majorana mass for the neutrino if $0\nu\beta\beta$ is observed [130, 131]. It can also be extended to arbitrary lepton number and lepton flavor violating processes by taking into account mixing

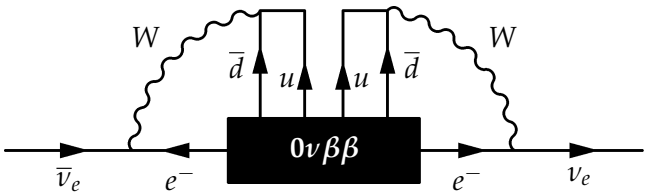

Figure 3.8: Black box (or Schechter–Valle) diagram: four-loop neutrino Majorana mass term generated by a non-vanishing neutrinoless double beta decay operator [117].

between the neutrino generations [132].

However, the diagram is four-loop (see Fig. 3.8) and therefore strongly suppressed. A quantitative analysis for point-like operators (heavy new physics contributions)—compare the most general Lagrangian for the decay in Eq. (3.23)—was performed together with Manfred Lindner and Alexander Merle in [51] and showed that the result is many orders of magnitude smaller than the neutrino masses one expects to have from the observed mass splittings in oscillation experiments. Thus the assertion of the theorem is merely academic. Lepton number violating new physics, which is not necessarily related to neutrino masses at tree level, may induce black box operators that explain a (possibly) observed rate of neutrinoless double beta decay. The smallness of the black box contributions to neutrino mass, however, shows that other neutrino mass terms must exist. Those could be of Majorana type as well as of Dirac type. If the neutrinos are mainly Majorana particles, the mass mechanism will be the dominant part of the black box operator. If the neutrinos are mainly Dirac, then other lepton number violating new physics dominates $0\nu\beta\beta$. Translating an observed rate of $0\nu\beta\beta$ into neutrino mass would then be completely misleading.

3.2 Neutrinoless double beta decay mediated by color octets

In this section we discuss the neutrinoless double beta decay phenomenology of the colored seesaw mechanism [72, 73], which we introduced as a possible neutrino mass mechanism in Section 2.4.2. Two contributions to $0\nu\beta\beta$ arise in this model, and we compare them in what follows. The direct contribution is the virtual exchange of the newly introduced color octet particles, see Fig. 3.9, whereas the indirect one is the usual light Majorana neutrino exchange, see Fig. 3.3. The latter is an indirect contribution, because the light Majorana neutrino mass is generated radiatively by the colored fields, see Fig. 2.5 and the corresponding discussion in Section 2.4.2 for more details. In

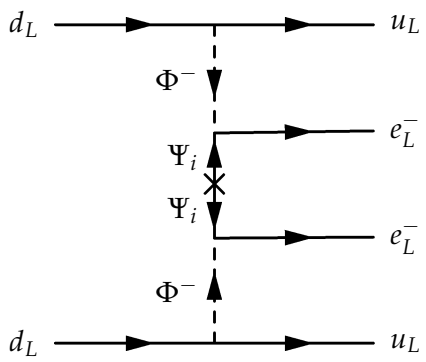

Figure 3.9: Direct contribution to neutrinoless double beta decay by the color octet particles of the colored seesaw mechanism [72, 73]. The indirect contribution from neutrino masses, the standard mechanism shown in Fig. 3.3, is also present. We discuss the interplay between the two contributions in detail in this section.

general, depending on the parameters of the model, the color octet contribution can dominate over the Majorana neutrino exchange. We take the constraints from lepton flavor violating processes such as $\mu \to e\gamma$ into account when performing the analysis.

The main results presented in this section were published together with Sandhya Choubey, Manimala Mitra, and Werner Rodejohann [42]. The discussion was updated to incorporate the most current neutrino oscillation data obtained from global fits [53] (provided in Appendix A for convenience). The most current MEG limit for $\mu \to e\gamma$ [133] was also taken into account.

3.2.1 Direct and indirect contributions to the decay

The relevant part of the Lagrangian responsible for neutrinoless double beta decay mediated by the colored octets is

$$\mathcal{L}_{0\nu\beta\beta} \supset \bar{u}\left[P_R\left(U_L^\dagger \kappa_D^\dagger D_R\right)_{11} - P_L\left(U_R^\dagger \kappa_U D_L\right)_{11}\right]\Phi^+ d + Y_\nu^{ei}\overline{e_L}(\Phi^+)^*\Psi_i, \tag{3.31}$$

compare the full Lagrangian of the model in Section 2.4.2.

The effective operator responsible for neutrinoless double beta decay thus is

$$\left\langle uuee \left| \mathcal{L}_{\text{eff}}^{\Delta L_e=2}(x) \right| dd \right\rangle,$$

with

$$\mathcal{L}_{\text{eff}}^{\Delta L_e=2}(x) = \sum_i (Y_\nu^{ei})^2 \frac{1}{M_\Phi^4 M_{\Psi_i}}\left[\bar{u}\left(P_R(U_L^\dagger \kappa_D^\dagger D_R)_{11} - P_L(U_R^\dagger \kappa_U D_L)_{11}\right) d\right]$$

$$\times \left[\bar{u}\left(P_R(U_L^\dagger \kappa_D^\dagger D_R)_{11} - P_L(U_R^\dagger \kappa_U D_L)_{11}\right) d\right] (\overline{e_L} e_L^c). \quad (3.32)$$

Let us assume $\kappa_U \ll \kappa_D$ and concentrate on the right-chiral part only for illustration. We can then define the coupling of the color octet to the quarks as

$$y_{11} = (U_L^\dagger \kappa_D^\dagger D_R)_{11} \quad (3.33)$$

and find the particle physics amplitudes of the two contributions to be

$$\mathcal{A}_{\text{light}} \simeq G_F^2 \frac{m_{0\nu\beta\beta}}{\langle p^2 \rangle} \text{ and } \mathcal{A}_{\text{color}} \simeq \frac{y_{11}^2}{M_\Phi^4} \sum_i \frac{(Y_\nu^{ei})^2}{M_{\Psi_i}}. \quad (3.34)$$

Here $\mathcal{A}_{\text{color}}$ is the amplitude for the direct contribution (color octet exchange) and $\mathcal{A}_{\text{light}}$ the indirect contribution due to the light Majorana neutrino exchange. As before, $\langle p^2 \rangle \approx (100\,\text{MeV})^2$. In a general setup, both contributions depend differently on the model parameters.

The neutrino Yukawa couplings Y_ν can be expressed in terms of light neutrino masses, mixings, color octet masses and a Casas–Ibarra [134] matrix $\mathcal{R}$ as

$$Y_\nu = \sqrt{\frac{16\pi^2}{\lambda_{\Phi H}}} \frac{1}{v} U_{\text{PMNS}} \sqrt{M_\nu^{\text{diag}}}\, \mathcal{R} \sqrt{(\mathcal{I}^{\text{diag}})^{-1}}, \quad (3.35)$$

where

$$\mathcal{I}^{\text{diag}} = \text{diag}(\mathcal{I}_1, \mathcal{I}_2, \mathcal{I}_3) \quad (3.36)$$

and U_{PMNS} is the neutrino mixing matrix. A general parameterization of the complex orthogonal[4] Casas–Ibarra matrix $\mathcal{R}$ [134] is given by

$$\mathcal{R} = \begin{pmatrix} \hat{c}_2\hat{c}_3 & \hat{c}_2\hat{s}_3 & \hat{s}_2 \\ -\hat{c}_1\hat{s}_3 - \hat{s}_1\hat{s}_2\hat{c}_3 & \hat{c}_1\hat{c}_3 - \hat{s}_1\hat{s}_2\hat{s}_3 & \hat{s}_1\hat{c}_2 \\ \hat{s}_1\hat{s}_3 - \hat{c}_1\hat{s}_2\hat{c}_3 & -\hat{s}_1\hat{c}_3 - \hat{c}_1\hat{s}_2\hat{s}_3 & \hat{c}_1\hat{c}_2 \end{pmatrix}, \quad (3.37)$$

with $\hat{s}_i = \sin\hat{\theta}_i$, $\hat{c}_i = \cos\hat{\theta}_i$ $(i = 1, 2, 3)$. $\hat{\theta}_1$, $\hat{\theta}_2$, and $\hat{\theta}_3$ are arbitrary complex angles.

In that case, one can re-write the color octet amplitude in terms of the PMNS matrix elements U_{ei}:

$$\mathcal{A}_{\text{color}} \simeq \frac{16\pi^2}{\lambda_{\Phi H} v^2} \frac{y_{11}^2}{M_\Phi^4} \left(\sum_i m_i U_{ei}^2 \sum_j \frac{\mathcal{R}_{ij}^2}{M_{\Psi_j} \mathcal{I}_j^d} + 2 \sum_{j<i} \sqrt{m_i m_j}\, U_{ei} U_{ej} \sum_k \frac{\mathcal{R}_{ik}\mathcal{R}_{jk}}{M_{\Psi_k} \mathcal{I}_k^d} \right). \quad (3.38)$$

[4] That is, it satisfies the orthogonality condition $\mathcal{R}^T\mathcal{R} = \mathbb{1}$.

Thus, in case the new octet fermions are degenerate in mass, i.e., for $M_{\Psi_k} = M_\Psi$, both contributions are be proportional to the effective Majorana mass of the light neutrinos, $m_{0\nu\beta\beta} = \sum m_i U_{ei}^2$, because the elements of $\mathcal{R}$ drop out of this expression. Therefore, if the light neutrino contribution vanishes due to some cancelation, the color octet contribution also vanishes identically. In the general case, however, the neutrino exchange mechanism can be dominating or sub-leading, depending on the masses of the octets and the quartic coupling governing the interaction between the color octet scalar and the Standard Model Higgs boson.

The existence of our direct contribution to $0\nu\beta\beta$ by the new colored fields was noted in the literature before, but not studied in detail [72]. In the phenomenological survey of the model [73], MFV was assumed to avoid large flavor changing neutral current effects. Strong constraints on these processes exist, and the scalar octet can contribute to, e.g., K^0–$\bar{K}^0$ mixing or to $b \to s\gamma$ [84]. In the MFV setup, the coupling of the charged member of the weak doublet scalar octet to a quark q is proportional to m_q/v, see Eq. (2.65). Thus, the amplitude of the direct contribution to $0\nu\beta\beta$ is suppressed by $m_{u,d}^2/v^2$ and completely negligible. When departing from the MFV framework, a sizable rate can be obtained, as we show in what follows. Note that the octet contribution to neutrinoless double decay that we consider in this thesis only depends on the coupling of the scalar octet Φ to an up and a down quark. In all possible flavor changing neutral current diagrams this coupling never appears on its own. For instance, in K^0–$\bar{K}^0$ mixing diagrams or in $b \to s\gamma$ it appears together with couplings involving 2nd and 3rd generation quarks. While this is not a completely satisfying situation, we nevertheless note that in the limit of only the coupling to up and down quarks being non-zero, we face no phenomenological problem. In addition, neutrinoless double decay is the only place in which this coupling appears on its own and hence it is the only place where it can be constrained directly.

3.2.2 Lepton flavor violation

Lepton flavor violation in the charged lepton sector is also possible in this model [135], see Fig. 3.10, and the branching ratio (BR) is given by

$$\mathrm{BR}(l_\alpha \to l_\beta \gamma) = \frac{3\alpha_{\mathrm{em}}}{4\pi G_F^2 M_\Phi^4} \left| \sum_i Y_\nu^{\beta i} (Y_\nu^{\alpha i})^* \mathcal{F}(x_i) \right|^2 , \tag{3.39}$$

with

$$\mathcal{F}(x_i) = \frac{1 - 6x_i + 3x_i^2 + 2x_i^3 - 6x_i^2 \ln(x_i)}{12(x_i - 1)^4} \tag{3.40}$$

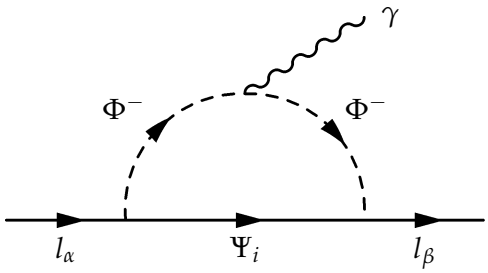

Figure 3.10: Lepton flavor violation in the colored seesaw scenario [72, 73].

and

$$x_i = \frac{M_{\Psi_i}^2}{M_\Phi^2}. \tag{3.41}$$

Here, $\alpha_{\rm em}$ is the fine structure constant.

Let us rewrite the branching ratio of $\mu \to e\gamma$ in terms of the neutrino parameters and the matrix $\mathcal{R}$ as

$$\mathrm{BR}(\mu \to e\gamma) = \frac{3\alpha_{\rm em}}{4\pi G_F^2 M_\Phi^4} \frac{(16\pi^2)^2}{\lambda_{\Phi H}^2 v^4} \left| \sum_k \frac{\mathcal{F}(x_k)}{\mathcal{I}_k} \sum_{i,j} U_{ei} U_{\mu j}^* \mathcal{R}_{ik} \mathcal{R}_{jk}^* \sqrt{m_i m_j} \right|^2 . \tag{3.42}$$

For the simple choice of $\mathcal{R}_{ij} = \delta_{ij}$, the above expression reduces to

$$\mathrm{BR}(\mu \to e\gamma) = \frac{3\alpha_{\rm em}}{4\pi G_F^2 M_\Phi^4} \frac{(16\pi^2)^2}{\lambda_{\Phi H}^2 v^4} \left| \sum_i \frac{\mathcal{F}(x_i)}{\mathcal{I}_i} U_{ei} U_{\mu i}^* m_i \right|^2 . \tag{3.43}$$

In the following analysis for $0\nu\beta\beta$, we took the current bounds on lepton flavor violating processes into account. The MEG experiment constrains (at 90% CL) [133]

$$\mathrm{BR}(\mu \to e\gamma) \leq 5.7 \times 10^{-13}, \tag{3.44}$$

which is about a factor of four better than the old MEG limit [136]

$$\mathrm{BR}(\mu \to e\gamma) \leq 2.4 \times 10^{-12} \tag{3.45}$$

(at 90% CL) that was taken into account in the analysis in [42]. Lepton flavor violating decays of heavier leptons have weaker constraints, with

$$\mathrm{BR}(\tau^\pm \to e^\pm\gamma) \leq 3.3 \times 10^{-8} \tag{3.46}$$

and

$$\mathrm{BR}(\tau^\pm \to \mu^\pm\gamma) \leq 4.4 \times 10^{-8}, \tag{3.47}$$

both at 90% CL [137].

3.2.3 The case of two color octet fermions

With two color octet fermions, one of the light neutrinos is massless, and the Casas–Ibarra matrix $\mathcal{R}$ depends only on one complex parameter ω. For normal hierarchy (NH) and for inverted hierarchy (IH), it can be given as

$$\mathcal{R}(\mathrm{NH}) = \begin{pmatrix} 0 & 0 \\ \sqrt{1-\omega^2} & -\omega \\ \omega & \sqrt{1-\omega^2} \end{pmatrix} \text{ and } \mathcal{R}(\mathrm{IH}) = \begin{pmatrix} \sqrt{1-\omega^2} & -\omega \\ \omega & \sqrt{1-\omega^2} \\ 0 & 0 \end{pmatrix}, \tag{3.48}$$

respectively.

Normal hierarchy

Let us have a look at the normal hierarchy first. For mass degenerate color octet fermions, i.e., $M_{\Psi_1} = M_{\Psi_2} \equiv M_\Psi$ and hence $\mathcal{I}_1 = \mathcal{I}_2 \equiv \mathcal{I}$, the Yukawas can be expressed as

$$Y_\nu = \sqrt{\frac{16\pi^2}{\lambda_{\Phi H}}} \frac{1}{v} U \,\mathrm{diag}(0, \sqrt{m_2}, \sqrt{m_3})\, \mathcal{R}\, \mathrm{diag}(\sqrt{\mathcal{I}^{-1}}, \sqrt{\mathcal{I}^{-1}})\,. \tag{3.49}$$

and the amplitude for the colored octet exchange is found to be

$$\mathcal{A}_{\mathrm{color}} = \frac{16\pi^2}{\lambda_{\Phi H} v^2} \frac{y_{11}^2}{M_\Phi^4 M_\Psi \mathcal{I}} \left| U_{e2}^2 m_2 + U_{e3}^2 m_3 \right|. \tag{3.50}$$

The expression for the amplitude is independent of the parameter ω, even though the Yukawa couplings depend strongly on it. Due to the degeneracy of the octet fermion masses, $\mathcal{A}_{\mathrm{color}}$ is also proportional to the effective mass

$$m_{0\nu\beta\beta} = \left| U_{e2}^2 m_2 + U_{e3}^2 m_3 \right|. \tag{3.51}$$

The color octet contribution therefore vanishes whenever the light neutrino exchange contribution vanishes due to cancelations coming from the Majorana phases. For a non-vanishing $m_{0\nu\beta\beta}$ however, the color octet contribution $\mathcal{A}_{\mathrm{color}}$ can basically be taken independent of $\mathcal{A}_{\mathrm{light}}$. This is due to the coupling $\lambda_{\Phi H}$, which is a free parameter and only present in the amplitude of the octet contribution.

There is viable parameter space where light neutrino masses can be achieved and a dominating (and even saturating the present half-life limits) contribution to $0\nu\beta\beta$ can still be obtained. See the original paper [42] for a more detailed discussion of the case of

two color octets. Note that the rate of $0\nu\beta\beta$ coming from light neutrino exchange is very small for normal hierarchy and way below the reach of next-generation experiments. However, in this setup, a dominant and saturating contribution can arise from the color octet exchange even in the normal hierarchy, such that $0\nu\beta\beta$ cannot be used to distinguish between hierarchies anymore.

The branching ratio for $\mu \to e\gamma$ is also independent of ω in this case and is given by

$$\mathrm{BR}(\mu \to e\gamma) = \frac{3\alpha_{\mathrm{em}}}{4\pi G_F^2 M_\Phi^4} \frac{(16\pi^2)^2}{\lambda_{\Phi H}^2 v^4} \left(\frac{\mathcal{F}(x)}{\mathcal{I}}\right)^2 \left| m_2 U_{e2} U_{\mu 2}^* + m_3 U_{e3} U_{\mu 3}^* \right|^2 . \tag{3.52}$$

It was shown in Ref. [42] that in this setup both the $0\nu\beta\beta$ bound and the bound from $\mu \to e\gamma$ can be saturated. Interestingly, if the lepton flavor violation bound is saturated, the color octet fermions can be within the reach of the LHC. If they are also required to give a saturating contribution to $0\nu\beta\beta$, their masses need to be higher.

Inverted hierarchy

In the inverted hierarchy, the amplitude for neutrinoless double beta decay is

$$\mathcal{A}_{\mathrm{color}} = \frac{16\pi^2}{\lambda_{\Phi H} v^2} \frac{y_{11}^2}{M_\Phi^4 M_\Psi \mathcal{I}} \left| U_{e1}^2 m_1 + U_{e2}^2 m_2 \right| , \tag{3.53}$$

and the branching ratio for $\mu \to e\gamma$ is

$$\mathrm{BR}(\mu \to e\gamma) = \frac{3\alpha_{\mathrm{em}}}{4\pi G_F^2 M_\Phi^4} \frac{(16\pi^2)^2}{\lambda_{\Phi H}^2 v^4} \left(\frac{\mathcal{F}(x)}{\mathcal{I}}\right)^2 \left| m_1 U_{e1} U_{\mu 1}^* + m_2 U_{e2} U_{\mu 2}^* \right|^2 . \tag{3.54}$$

A dominant $0\nu\beta\beta$ contribution can arise also in the inverted hierarchy, see Ref. [42] for more details.

Lepton flavor violation

The ratios of the branching ratios for different lepton flavor violating processes in this particular setup with two degenerate color octet fermions are

$$\frac{\mathrm{BR}(\tau \to e\gamma)}{\mathrm{BR}(\mu \to e\gamma)} = \frac{(U_{e2} U_{\tau 2}^* m_2 + U_{e3} U_{\tau 3}^* m_3)}{\left(U_{e2} U_{\mu 2}^* m_2 + U_{e3} U_{\mu 3}^* m_3\right)}, \tag{3.55}$$

$$\frac{\mathrm{BR}(\tau \to \mu\gamma)}{\mathrm{BR}(\mu \to e\gamma)} = \frac{(U_{\mu 2} U_{\tau 2}^* m_2 + U_{\mu 3} U_{\tau 3}^* m_3)}{\left(U_{e2} U_{\mu 2}^* m_2 + U_{e3} U_{\mu 3}^* m_3\right)} \tag{3.56}$$

for normal hierarchy, and

$$\frac{\mathrm{BR}(\tau \to e\gamma)}{\mathrm{BR}(\mu \to e\gamma)} = \frac{(U_{e1}U^*_{\tau 1}m_1 + U_{e2}U^*_{\tau 2}m_2)}{\left(U_{e1}U^*_{\mu 1}m_1 + U_{e2}U^*_{\mu 2}m_2\right)}, \tag{3.57}$$

$$\frac{\mathrm{BR}(\tau \to \mu\gamma)}{\mathrm{BR}(\mu \to e\gamma)} = \frac{(U_{\mu 1}U^*_{\tau 1}m_1 + U_{\mu 2}U^*_{\tau 2}m_2)}{\left(U_{e1}U^*_{\mu 1}m_1 + U_{e2}U^*_{\mu 2}m_2\right)} \tag{3.58}$$

for inverted hierarchy.

In this simple setup one therefore finds exact predictions for these ratios in terms of neutrino oscillation parameters and experimental measurements of these ratios can be used to check if the lepton flavor violation is solely due to the neutrino mass generation mechanism.

Not taking into account possible cancelations in Eqs. (3.55)–(3.58), the expressions are expected to be of order one. Thus, because the upper limit on the branching ratio for $\mu \to e\gamma$ is much more stringent than the limits on the other branching ratios, those are automatically fulfilled if $\mu \to e\gamma$ is fulfilled.

3.2.4 The case of three color octet fermions

We now turn to the three generation scenario, dropping in addition the assumption of degenerate octet fermions. Then, the color octet contribution to $0\nu\beta\beta$ is not proportional to $m_{0\nu\beta\beta}$ anymore, see Eq. (3.38). Thus, if the light neutrino contribution vanishes due to cancelations, the color octet contribution can still give a significant contribution.

In general, the color octet contribution has a significant dependence on the phases of the matrix $\mathcal{R}$. We do not address this issue here, because we encounter extreme cases even when choosing $\mathcal{R}_{ij} = \delta_{ij}$. The particle physics amplitude of $0\nu\beta\beta$ is then given by

$$\mathcal{A}_{\mathrm{color}} \simeq \frac{16\pi^2}{\lambda_{\Phi H} v^2} \frac{y_{11}^2}{M_\Phi^4} \left(\sum_i \frac{m_i U_{ei}^2}{M_{\Psi_i} \mathcal{I}_i} \right). \tag{3.59}$$

In what regards neutrino mixing, we keep things as simple as possible. We study a minimal deviation from tribimaximal mixing. Tribimaximal mixing [138, 139] is defined by a particular choice of the moduli-squared of the elements of the PMNS mixing matrix, i.e.,

$$\begin{pmatrix} |U_{e1}|^2 & |U_{e2}|^2 & |U_{e3}|^2 \\ |U_{\mu 1}|^2 & |U_{\mu 2}|^2 & |U_{\mu 3}|^2 \\ |U_{\tau 1}|^2 & |U_{\tau 2}|^2 & |U_{\tau 3}|^2 \end{pmatrix} \equiv \begin{pmatrix} \frac{2}{3} & \frac{1}{3} & 0 \\ \frac{1}{6} & \frac{1}{3} & \frac{1}{2} \\ \frac{1}{6} & \frac{1}{3} & \frac{1}{2} \end{pmatrix}, \tag{3.60}$$

and was consistent with neutrino data prior to the discovery of a large mixing angle θ_{13}. It can nevertheless still serve as a zeroth-order approximation to a more general neutrino mixing matrix.

Denoting $\sin\theta_{13} = \lambda$, the form of the PMNS mixing matrix that we use in the analysis is

$$U_{\text{PMNS}} \simeq \begin{pmatrix} -\frac{2}{\sqrt{6}} & \frac{1}{\sqrt{3}} & \lambda e^{-i\delta} \\ \frac{1}{\sqrt{6}} - \frac{\lambda}{\sqrt{3}} e^{i\delta} & \frac{1}{\sqrt{3}} + \frac{\lambda}{\sqrt{6}} e^{i\delta} & -\frac{1}{\sqrt{2}} \\ \frac{1}{\sqrt{6}} + \frac{\lambda}{\sqrt{6}} e^{i\delta} & \frac{1}{\sqrt{3}} - \frac{\lambda}{\sqrt{6}} e^{i\delta} & \frac{1}{\sqrt{2}} \end{pmatrix} \text{diag}(1, e^{i\alpha}, e^{i(\beta+\delta)}). \tag{3.61}$$

Note that we allow for a complex PMNS matrix in what follows. In this case, the amplitude for the light neutrino contribution to $0\nu\beta\beta$ is

$$\mathcal{A}_{\text{light}} \simeq \frac{G_F^2}{\langle p^2 \rangle} \left(\frac{2m_1}{3} + \frac{m_2}{3} e^{i2\alpha} + m_3 \lambda^2 e^{i2\beta} \right). \tag{3.62}$$

For the amplitude of $0\nu\beta\beta$ mediated by the color octet fermions and scalars, we have

$$\mathcal{A}_{\text{color}} \simeq \frac{y_{11}^2}{M_\Phi^4} \frac{16\pi^2}{\lambda_{\Phi H} v^2} \left(\frac{2m_1}{3\mathcal{I}_1 M_{\Psi_1}} + \frac{m_2 e^{i2\alpha}}{3\mathcal{I}_2 M_{\Psi_2}} + \frac{m_3 \lambda^2 e^{i2\beta}}{\mathcal{I}_3 M_{\Psi_3}} \right). \tag{3.63}$$

The branching ratio for the process $\mu \to e\gamma$ is given by

$$\begin{aligned} \text{BR}(\mu \to e\gamma) = \frac{2}{3} \frac{16\pi^3}{\lambda_{\Phi H}^2 v^4} \frac{\alpha_{\text{em}}}{G_F^2 M_\Phi^4} \Bigg| & (2e^{i\delta}\lambda - \sqrt{2}) \frac{m_1 \mathcal{F}(x_1)}{\mathcal{I}_1} \\ & + (\sqrt{2} e^{i2\alpha} + \lambda e^{i2\alpha + i\delta}) \frac{m_2 \mathcal{F}(x_2)}{\mathcal{I}_2} - 3 e^{i2\beta + i\delta} \lambda \frac{m_3 \mathcal{F}(x_3)}{\mathcal{I}_3} \Bigg|^2 . \end{aligned} \tag{3.64}$$

In Figs. 3.11 and 3.12, the ratio of $\mathcal{A}_{\text{color}}$ and $\mathcal{A}_{\text{light}}$ are plotted as a function of the smallest neutrino mass for normal and inverted hierarchy. For the different values of $\lambda_{\Phi H}$ used, this shows the relative size of the direct and indirect contributions to $0\nu\beta\beta$. Even for this simple example, the ratio of the amplitudes can be very large or very small, corresponding to the dominance of one of the contributions. For the figure, the mass of the color octet scalar was chosen to be $M_\Phi = 2\,\text{TeV}$, while the masses of the color octet fermions were varied inside the interval $M_{\Psi_i} \in [0.9\,\text{TeV}, 1.1\,\text{TeV}]$. No particular form of hierarchy was considered between the color octet fermions. The random variation inside this interval mainly assures that there is no exact degeneracy between the three fermions. The Yukawa coupling y_{11} was varied inside the interval $[0.001, 1.0]$. Additionally, all phases in the PMNS matrix have been varied in the interval $[0, 2\pi]$. The solar and atmospheric mass-squared differences, as well as the mixing angles were varied inside their presently allowed 3σ intervals [53], see Appendix A for

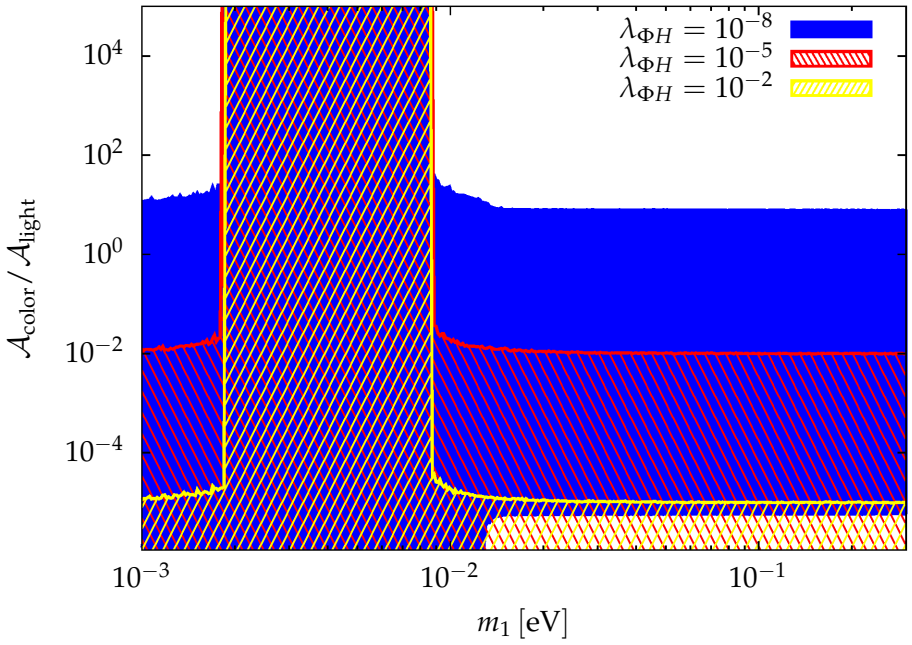

Figure 3.11: The ratio of the particle physics amplitudes $\mathcal{A}_{\rm color}/\mathcal{A}_{\rm light}$ for normal hierarchy as a function of the lightest neutrino mass $m_{\rm min} = m_1$ in the colored seesaw mechanism. The parameters used are given in the text. The colored areas give the allowed regions using the current MEG limit for $\mu \to e\gamma$. Note that the areas for different values of $\lambda_{\Phi H}$ overlap. The large increase in the ratio in the range $2 \times 10^{-3}\,\text{eV} < m_1 < 9 \times 10^{-3}\,\text{eV}$ is due to the cancellation in $\mathcal{A}_{\rm light}$. Here, all three regions overlap, and $\mathcal{A}_{\rm color}$ is non-zero and dominant.

the used values. The differently colored regions in this figure correspond to different $\lambda_{\Phi H}$ values as shown in the plot legend, all satisfying the current MEG limit [133]

$$\text{BR}(\mu \to e\gamma) < 5.7 \times 10^{-13}. \tag{3.65}$$

Note that as $\lambda_{\Phi H}$ increases, the ratio $\mathcal{A}_{\rm color}/\mathcal{A}_{\rm light}$ decreases. The large increase in $\mathcal{A}_{\rm color}/\mathcal{A}_{\rm light}$ for low values of $m_{\rm min}$ in normal hierarchy is an artifact of cancelations in $\mathcal{A}_{\rm light}$ due to conspiring Majorana phases.

Another way to visualize the direct contributions is to define a "color effective mass": noting that the usual effective mass $m_{0\nu\beta\beta}$ is obtained by multiplying $\mathcal{A}_{\rm light}$ with $\langle p^2\rangle/G_F^2$, we can define

$$m_{0\nu\beta\beta}^{\rm color} = \frac{\langle p^2\rangle}{G_F^2}\mathcal{A}_{\rm color}, \tag{3.66}$$

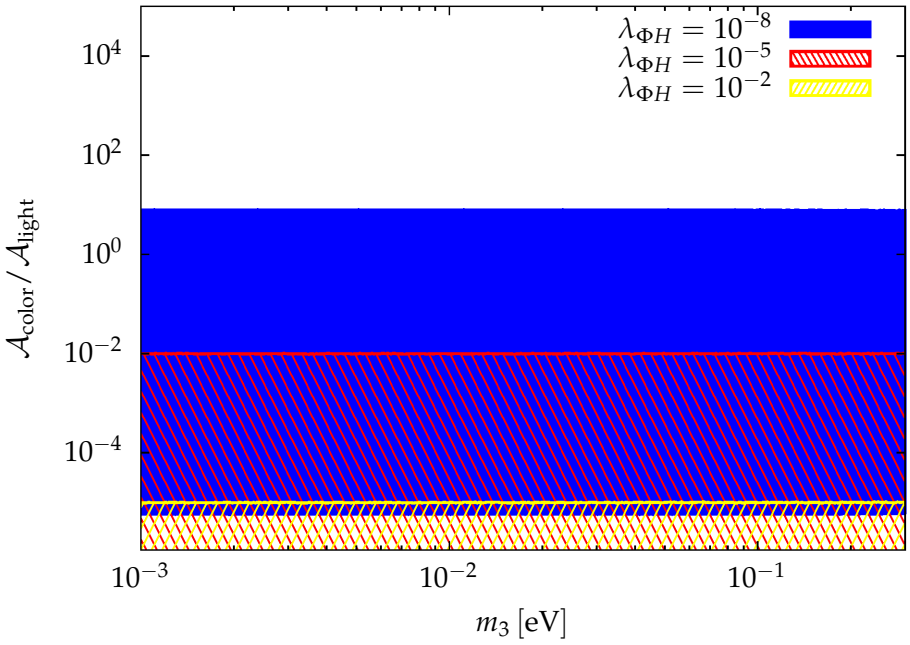

Figure 3.12: The ratio of particle physics amplitudes $\mathcal{A}_{\rm color}/\mathcal{A}_{\rm light}$ for inverted hierarchy as a function of the lightest neutrino mass $m_{\rm min} = m_3$ in the colored seesaw mechanism, similar to Fig. 3.11.

where $\mathcal{A}_{\rm color}$ is given in Eq. (3.63). In Fig. 3.13, the color effective mass is given as a function of the lightest neutrino mass eigenvalue. The usual phenomenology can be significantly modified. For instance, in the inverted hierarchy (negligible m_3) one expects $m_{0\nu\beta\beta} > 0.05\,\text{eV}$ for the exchange of light Majorana neutrinos. The direct contribution from the octets does approach 1 eV, and hence, even for the simple example considered here, limits coming from $0\nu\beta\beta$ experiments can be used to cut in the parameter space of couplings and masses. Note also that the predicted rate of $0\nu\beta\beta$ is very large even for normal hierarchy and almost comparable to that for inverted hierarchy, as pointed out earlier for the case of two color octets.

3.3 Consistency test of neutrinoless double beta decay with one isotope

Having discussed the $0\nu\beta\beta$ phenomenology of a particular model for lepton number violating physics beyond the SM in the last section, in this section we turn to a more

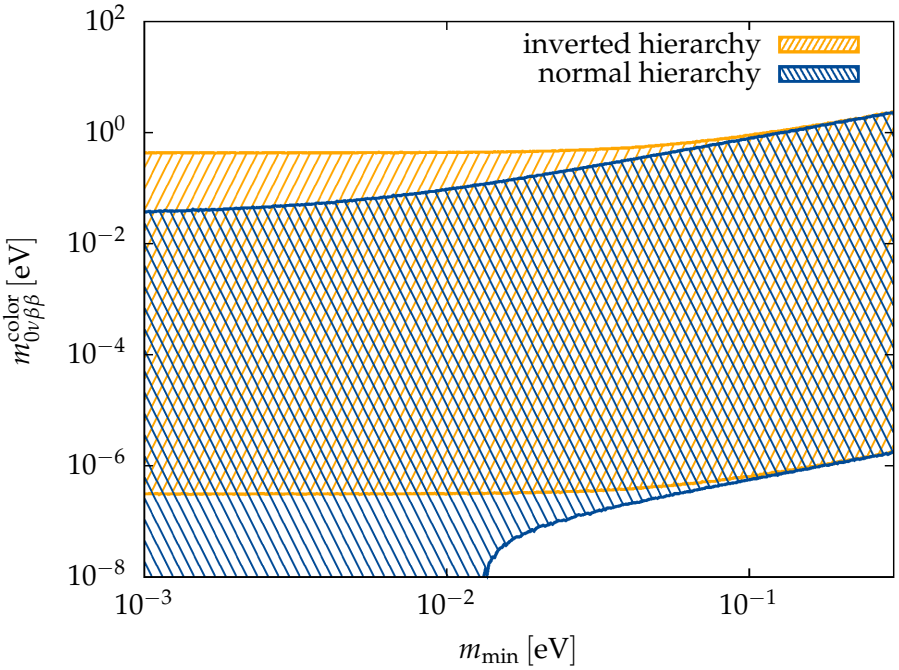

Figure 3.13: The "color effective mass" $m^{\text{color}}_{0\nu\beta\beta}$ as a function of the lightest neutrino mass eigenvalue, which has to be compared with the effective mass from the standard mechanism for $0\nu\beta\beta$ in Fig. 3.4. We use $\lambda_{\Phi H} = 10^{-8}$ for the plot. The normal ordering is given in blue and the inverted ordering in yellow. Best-fit values are used for the oscillation parameters, the other parameters are varied as before. Recall that the standard effective mass $m_{0\nu\beta\beta}$ would be observable in the next few years for values of $m_{\text{min}} > 0.3\,\text{eV}$, and the current limit on the half-life corresponds to about 1 eV for $m_{0\nu\beta\beta}$, which is also roughly the limit for $m^{\text{color}}_{0\nu\beta\beta}$.

experimental question. As stated before, experiments on $0\nu\beta\beta$ are currently the most promising attempts in the search for lepton number violation. Although the present round of experiments did not detect a signal [25–27], the next round of experiments might do so in the near future. Of course, in case one of the experiments finds a signal at the expected Q-value, it will be necessary to cross-check that indeed $0\nu\beta\beta$ was detected and not some unknown background line. Usually, a second isotope would then be used to also detect the decay. There are, however, other options.

Here, we discuss a consistency test which allows one to discriminate unknown nuclear background lines from neutrinoless double beta decay with only one isotope, i.e., within a single experiment. By considering both the transition to the ground

state (g.s. in equations and figures) and to the first excited 0^+ state (0_1^+ in equations and figures) of the daughter nucleus, a sufficiently large detector can reveal if indeed neutrinoless double beta decay or some other nuclear physics process is observed. Such a detector could therefore simultaneously provide a consistency test for a certain range of Majorana masses and be sensitive (without the consistency test, of course) to even lower values of the effective Majorana mass $m_{0\nu\beta\beta}$.

The results presented in this section were published together with Manfred Lindner and Kai Zuber in [43]. At that stage, a consistent set of phase space factors for the ground state transition and the transition to the first excited 0^+ state ($G^{0\nu}_{\text{g.s.}}$ and $G^{0\nu}_{0_1^+}$, respectively) was not available. We therefore approximated

$$\frac{G^{0\nu}_{0_1^+}}{G^{0\nu}_{\text{g.s.}}} \approx \frac{(Q - E(0_1^+))^5}{Q^5}, \tag{3.67}$$

where Q is the maximum energy that can be released in $0\nu\beta\beta$ to the ground state of the daughter nucleus (the so-called Q-value), and $E(0_1^+)$ is the energy of the first excited 0^+ state. For this thesis, the discussion was updated with the most recent IBM-2 matrix element calculations [115][5] using the now available complete sets of phase space factors [103, 104]. The plot for the effective neutrino mass was updated with the most recent global fit on neutrino oscillation data, provided in [53] and given in Appendix A for convenience.

3.3.1 Double beta decay to excited states

Usually, double beta decay to the ground state of the final nucleus is considered. However, practically all interesting nuclei, i.e., those with a Q-value above 2 MeV (see Tab. 3.3) have at least one excited 0^+ and one excited 2^+ state which are accessible by double beta decay as well. The level scheme of ^{76}Ge is given in Fig. 3.14 as an example. Transitions to excited 2^+ states might be dominated by potential contributions of $V + A$ interactions (see, however, [141]).

The decay rate to excited states is lower due to the lower Q-value of the decay. The ratio between the decay rate to the excited 0_1^+ state and the ground state is given by

$$\frac{\Gamma_{0_1^+}}{\Gamma_{\text{g.s.}}} = \frac{G^{0\nu}_{0_1^+}}{G^{0\nu}_{\text{g.s.}}} \times \left(\frac{\mathcal{M}^{0\nu}_{0_1^+}}{\mathcal{M}^{0\nu}_{\text{g.s.}}}\right)^2, \tag{3.68}$$

where $\mathcal{M}^{0\nu}_{\text{g.s.}}$ denotes the nuclear matrix element for the decay to the ground state, and $\mathcal{M}^{0\nu}_{0_1^+}$ denotes the nuclear matrix element for the decay to the first excited 0^+ state.

[5] In [43], the values for the nuclear matrix elements provided in [116, 140] were used. For a full list of matrix elements as of September 2010, see the online version of the corresponding talk at `http://www.ba.infn.it/~now/now2010/TALKS/sept.5/plenary/iachello-otranto.pdf`.

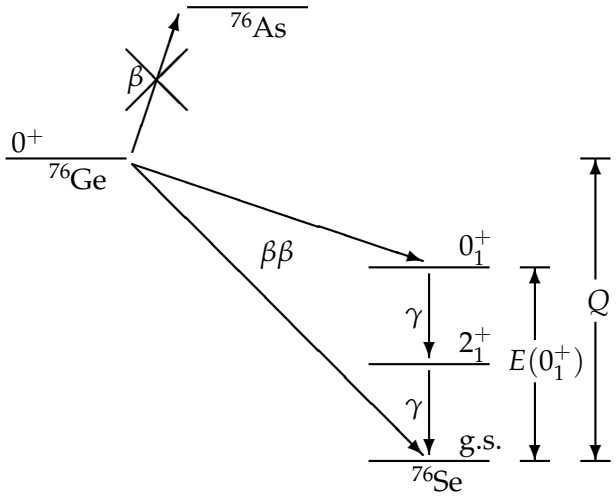

Figure 3.14: Level scheme of the double beta decay of ^{76}Ge. Single beta decay to ^{76}As is energetically forbidden, thus the only open decay channel is double beta decay. It may proceed in the two-neutrino mode, as well as in the neutrinoless mode. In addition to the transition to the ground state (g.s.) of the daughter nucleus ^{76}Se, we discuss the decay to the first excited 0^+ state, labeled by 0_1^+ .

Excited state transitions have been observed in ^{100}Mo (latest results given in [142]) and ^{150}Nd (latest results given in [143]), both considered to be $2\nu\beta\beta$ transitions.

The experimental signature of the decay to the first excited 0^+ state is quite distinctive, two gammas with well-defined energies and a known total electron energy different from the Q-value of the ground state transition. Therefore, the transition to the first excited 0^+ state could be used as a consistency check within the same isotope, i.e., within the same experiment, whether a ground state transition is observed. Such a test might be desirable in future large-scale experiments due to the involved costs. The ratio of rates to the first excited 0^+ and to the ground state for all double beta emitters with a Q-value of at least 2 MeV are compiled in Tab. 3.3.

With current values, the best choice (highest rate of decays to the first excited 0^+ state relative to the ground state transition) would be ^{48}Ca.[6] This isotope, however, has the lowest natural abundance of all $0\nu\beta\beta$ isotopes (0.187%, compare with 7.8% of ^{76}Ge). Currently, there is only one experiment using the isotope ^{48}Ca, CANDLES [145], which is in the R&D phase, and is not as developed as the ^{76}Ge experiment GERDA. In this

[6] In [43] it seemed that the two most suitable choices for such an internal consistency check would be ^{150}Nd and ^{76}Ge, the first being about a factor of two better than the latter.

Table 3.3: List of all double beta isotopes with a Q-value larger than 2 MeV, compare Tab. 3.2. We give the relevant parameters for the decay to the first excited 0^+ state (which we call 0_1^+ here): the energies $E(0_1^+)$ of this state, the nuclear matrix elements $\mathcal{M}^{0\nu}_{0_1^+}$ and phase space factors $G^{0\nu}_{0_1^+}$. The values of $E(0_1^+)$ are taken from Ref. [144]. The matrix elements are IBM-2 calculations [115]. The phase space factor for $^{124}_{50}$Sn is from Ref. [103], all other phase space factors are from the more recent calculation in Ref. [104]. For all isotopes, we calculate the ratio between the rates of the decay to the 0_1^+ state and the ground state, $\Gamma_{0_1^+}/\Gamma_{\text{g.s.}}$ by means of Eq. (3.68). Based on the ratio of rates, the best choices for the proposed consistency test are $^{48}_{20}$Ca and $^{76}_{32}$Ge.

Decay	$E(0_1^+)$ [keV] [144]	$\mathcal{M}^{0\nu}_{0_1^+}$ [115]	$G^{0\nu}_{0_1^+}$ [$g_A^4\,\text{yr}^{-1}$] [103, 104]	$\Gamma_{0_1^+}/\Gamma_{\text{g.s.}}$
$^{48}_{20}\text{Ca}\rightarrow{}^{48}_{22}\text{Ti}$	2997	5.83	3.05×10^{-16}	1.06×10^{-1}
$^{76}_{32}\text{Ge}\rightarrow{}^{76}_{34}\text{Se}$	1122	2.46	1.87×10^{-16}	1.65×10^{-2}
$^{82}_{34}\text{Se}\rightarrow{}^{82}_{36}\text{Kr}$	1488	1.32	9.17×10^{-16}	7.26×10^{-3}
$^{96}_{40}\text{Zr}\rightarrow{}^{96}_{42}\text{Mo}$	1148	0.04	3.30×10^{-15}	4.06×10^{-5}
$^{100}_{42}\text{Mo}\rightarrow{}^{100}_{44}\text{Ru}$	1130	0.99	3.07×10^{-15}	1.38×10^{-2}
$^{110}_{46}\text{Pd}\rightarrow{}^{110}_{48}\text{Cd}$	1473	0.46	1.08×10^{-16}	3.64×10^{-4}
$^{116}_{48}\text{Cd}\rightarrow{}^{116}_{50}\text{Sn}$	1757	0.85	7.19×10^{-16}	4.05×10^{-3}
$^{124}_{50}\text{Sn}\rightarrow{}^{124}_{52}\text{Te}$	1657	2.70	1.71×10^{-16}	1.13×10^{-2}
$^{130}_{52}\text{Te}\rightarrow{}^{130}_{54}\text{Xe}$	1794	3.07	3.57×10^{-16}	1.47×10^{-2}
$^{136}_{54}\text{Xe}\rightarrow{}^{136}_{56}\text{Ba}$	1579	1.82	6.59×10^{-16}	1.35×10^{-2}
$^{150}_{60}\text{Nd}\rightarrow{}^{150}_{62}\text{Sm}$	740	0.39	2.70×10^{-14}	1.23×10^{-2}

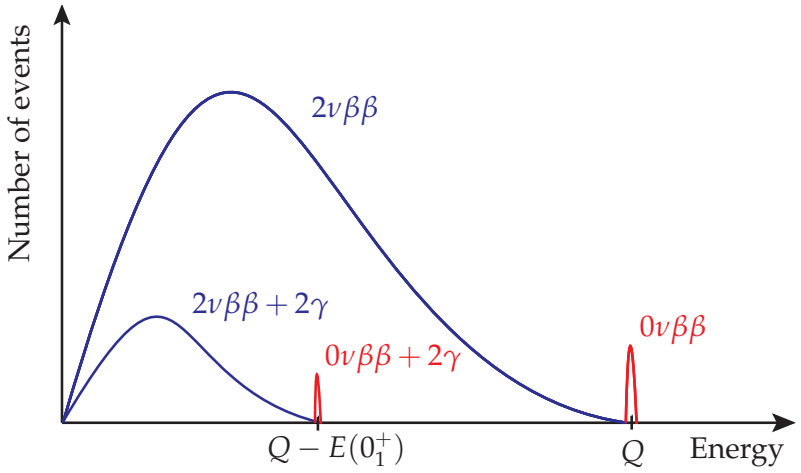

Figure 3.15: Schematic plot of the spectrum of the total energy of the emitted electrons for double beta decay to the ground state and to the first excited 0^+ state. The spectrum for double beta decay to the ground state was discussed before, see Fig. 3.2. For the decay to an excited final state, the diagrams are qualitatively the same. However, as energy is taken away by the emitted photons, the line for $0\nu\beta\beta$ decay lies at lower energies. Moreover, the number of decays to excited states is lower than the number of decays to the ground state.

thesis, we therefore focus on the second best option, which is ^{76}Ge, and discuss the prospects of a consistency test in this isotope in more detail.

A possible benefit of the proposed method is that the nuclear matrix elements of the transition to the ground state and to the excited state may have common uncertainties, which would cancel in the ratio. Improvement of the nuclear matrix elements will thus allow for a more precise extraction of $m_{0\nu\beta\beta}$ from half-life measurements.

3.3.2 Experimental considerations and possible backgrounds

The expected signature for the required additional decay channel into the excited 0_1^+ state of the daughter nucleus is two electrons and two gammas with defined energies, in contrast to the ground state transition emitting only two electrons with a defined total kinetic energy (see Fig. 3.15 for a comparison of the corresponding energy spectra). Therefore, the gammas must be clearly separated from the emitted electrons in the experiment, otherwise the excited state transition would look like a decay to the ground state. Hence, a purely calorimetric approach without spatial resolution to determine the individual gammas will fail. Consequently, in a large homogeneous detector, there

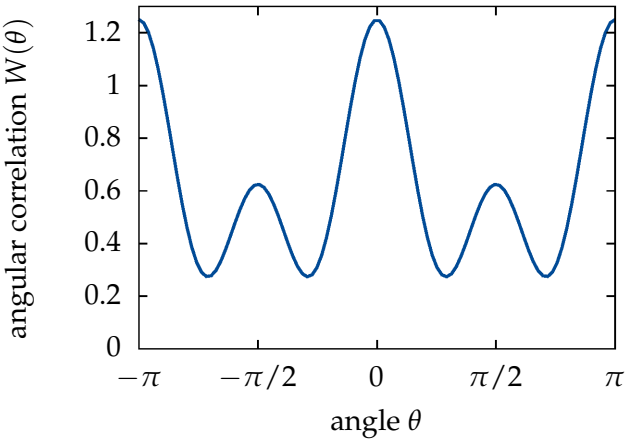

Figure 3.16: Angular correlation of the emitted gammas in double beta decay to the first excited 0^+ state, see Eq. (3.69) for the function $W(\theta)$.

must be spatial resolution to see the gammas independently from the emitted electrons. In a high granularity detector, the granularity should be chosen such that both gammas can leave the crystal containing the decay without any interaction, making it possible to search for coincidences with high efficiency.

All double beta decays into the first excited 0^+ state will de-excite via the sequence of $0^+ \rightarrow 2^+ \rightarrow 0^+$, compare the level scheme of ^{76}Ge in Fig. 3.14, so there will be an angular correlation between the emitted gammas. For this particular angular momentum sequence, the angular correlation is given by

$$W(\theta) = \frac{5}{8} \times (1 - 3\cos^2\theta + 4\cos^4\theta). \tag{3.69}$$

The function $W(\theta)$ is plotted in Fig. 3.16. It is easy to see that the angles 0 and π have the highest probability.

Due to the low count rates expected in $0\nu\beta\beta$ experiments, the reduction of possible backgrounds is an important part of the experimental efforts. As usual in $0\nu\beta\beta$, the major background for the consistency test also is the $2\nu\beta\beta$ decay into the 0_1^+ excited state, observed so far for two isotopes [142, 143]. Since the high energy tail of the continuous two-neutrino spectrum can mimic the signal of the neutrinoless transition, energy resolution is the crucial experimental quantity for rejecting this background.

The consistency test relies on even lower backgrounds than regular $0\nu\beta\beta$ experiments, so small background contributions also have to be taken into account. One possible type of background can arise because double beta emitters are surrounded by unstable

isotopes in the chart of nuclides. The intermediate nucleus in the double beta system, which may be produced by (p, n) reactions on the double beta emitter, is also unstable and its beta decay into excited states leads to the same gamma-signature. The energy spectrum of the single beta decay is continuous but overlapping with the double beta electron signal. The fraction of beta electrons in the peak range depends on the energy difference of the ground states of the double beta emitter and the intermediate nucleus. If it is small, only electrons close to the endpoint of the beta spectrum contribute. If it is large, more electrons contribute. A detailed estimate depends also on the quantum numbers of the ground state of the intermediate nucleus, as allowed or forbidden beta decays lead to different electron energy spectra. Thus, it is essential to measure the electron energy accurately or to build a detector which is able to discriminate one and two electrons, typically done in detectors with tracking capabilities. Normally, there are no free protons in an underground experiment, so the aforementioned (p, n) reactions are not an issue. Free protons could be produced by (n, p) reactions on a nucleus. Underground, high energy neutrons are dominantly produced by muon interactions in or close to the experiment. These neutrons in principle have enough energy to trigger (n, p) reactions. A detailed estimation depends on the actual cross section for (n, p) reactions (which is in the region of millibarn for neutron energies below 100 MeV) and the following (p, n) reactions (which is in the region of millibarn to barn, depending on the proton energy).

External backgrounds may also be an issue. The signal of a decay into excited states, however, will be a triple coincidence with well-defined energies of all involved particles. Additionally, angular correlation exists between the gammas, and the total sum of particle energies must correspond to the Q-value of the double beta decay. These constraints make the search for a signal more or less background free, depending of course on the detector technology used, but a more detailed discussion is beyond the scope of this thesis. Especially in the case of ^{76}Ge detectors with their excellent energy resolution, the triple coincidence is so sharply defined that it cannot be mimicked by any other process. Decay sequences with the same gamma energies are very unlikely, and furthermore the electron in such a sequence would be continuous, and only a small fraction will have the right energy. Triple Compton events (note that we have three different energy depositions) are als very unlikely. In any case, applying the equation of Compton scattering to the three energy depositions will immediately tell whether this is consistent with Compton scattering or not.

3.3.3 A consistency test with germanium

We discuss the prospects of a consistency test for the case of ^{76}Ge, which is used in the GERDA [27] and MAJORANA [146] experiments, in more detail. In addition to

the signal in the spectrum of the total energy of the emitted electrons in the form of a peak at 2039 keV as an indication of the ground state transition, the decay into the first excited 0^+ state would be indicated by a total energy of the electrons of 917 keV, associated with two gammas of 559.1 keV and 563.2 keV, respectively. A coincidence measurement would be preferential for this form of decay. Even ignoring the angular correlation among the photons, see Eq. (3.69), this channel should be basically free of background. In this case, one or two events would indicate an observation, which, however, implies 61–122 neutrinoless ground state transitions (compare the rates in Tab. 3.3).

The emitted gammas can be detected quite efficiently. Monte Carlo simulations[7] show that about 60% of the gammas are expected to leave the crystal without interaction for ^{76}Ge detectors in the form of disks of 15 cm diameter and 1 cm thickness. These photons might be detected in neighboring ^{76}Ge detectors or an active medium surrounding the crystals.

Let us check whether the necessary number of counts (several hundred, see above) can be reached for the decay into the ground state in future detectors. In case the half-life $T_{1/2}$ of the isotope under consideration is much longer than the measuring time t, we can write the number of double beta decays as

$$N_{\beta\beta} = \frac{\ln 2 a M t N_A}{T_{1/2}}\,, \tag{3.70}$$

where a is the isotopical abundance of the nuclide of interest, M is the used mass and $N_A = 6.022 \times 10^{23}\,/\mathrm{mol}$ is the Avogadro constant. However, in experiments, we may be confronted with background, such that there are two different possible dependencies of the expected half-life sensitivity:

$$(T_{1/2})^{-1} \propto a M \epsilon t \quad \text{(background free)} \tag{3.71}$$

or

$$(T_{1/2})^{-1} \propto a \epsilon \sqrt{\frac{Mt}{B\Delta E}} \quad \text{(background limited)}\,. \tag{3.72}$$

Here, ϵ is the efficiency for detection, B is the background index [in counts/(keV kg y)], and ΔE is the energy resolution at the peak position. See [147] for a more detailed discussion on $0\nu\beta\beta$ experiments.

Consider a future ^{76}Ge detector. Two scenarios are thinkable: the Klapdor claim $T^{0\nu}_{1/2} = 2.23 \times 10^{25}$ y [90] is right, so that one only would have to reach this half-life. However, it is not improbable that the effective Majorana neutrino mass is as low as 50 meV, where the inverted hierarchy begins (cf. Fig. 3.17). Results for the running

[7] The simulations were performed by B. Lehnert.

Table 3.4: Running times that have to be accumulated to perform the proposed consistency test in a future ^{76}Ge detector for two possible scenarios: checking Klapdor's claim [90] and with an effective mass of $m_{0\nu\beta\beta} = 50\,\text{meV}$.

Klapdor's claim $T^{0\nu}_{1/2} = 2.23 \times 10^{25}\,\text{y}$ [90]:	
background free	$Mt = 0.92\,\text{ton y}$
background limited	$Mt = 25.3\,\text{ton y}$
$m_{0\nu\beta\beta} = 50\,\text{meV}$:	
background free	$Mt = 25.7\,\text{ton y}$
background limited	$Mt = 19.6\,\text{kton y}$

Table 3.5: Experimental parameters of the ^{76}Ge $0\nu\beta\beta$ experiment GERDA [27] used in the calculations. The nuclear matrix element is calculated in IBM-2 [115], and the phase space factor is taken from Ref. [104]. In the calculations, we use an axial coupling of $g_A = 1.25$.

Isotopical abundance a $[m_u^{-1}]$	86%
Efficiency ϵ	60%
Number of decays to the ground state $N_{\beta\beta}$	122
Background B [counts/(keV kg y)]	0.01
Energy resolution at peak position ΔE	3 keV
$\mathcal{M}^{0\nu}$	5.42
$G^{0\nu}$ $[g_A^4\,\text{y}^{-1}]$	2.34×10^{-15}
Typical mass [kg]	1000

times that need to be accumulated in order to be able to use the proposed consistency test in both scenarios are given in Tab. 3.4. All parameters used in the calculations are given in Tab. 3.5.

What is the largest half-life, so that the proposed consistency check can be used in a running time of 10 years? This means that we need at least 122 decays to the ground state in ^{76}Ge. Assuming a background-free experiment, and using the values from Tab. 3.5, for a ^{76}Ge detector of 1 ton, the maximal half-life where this number of decays to the ground state is reached is

$$T_{1/2} = 2.43 \times 10^{26}\,\mathrm{y}\,. \tag{3.73}$$

This corresponds (using the matrix elements and phase space factors in Tab. 3.5) to an effective Majorana neutrino mass of

$$m_{0\nu\beta\beta} = 79\,\mathrm{meV}. \tag{3.74}$$

For other isotopes with their typical mass ranges, results are expected to be similar. Thus, for the next generation of detectors of the size of several hundred kilograms up to 1 ton, the method should work down to an effective mass below 100 meV. See Fig. 3.17 for the reach of the consistency test in a future 1 ton ^{76}Ge experiment.

3.4 Summary

In this chapter, we have provided a discussion of neutrinoless double beta decay, which is one of the most promising searches for lepton number violation at the moment. We discussed the standard interpretation of this decay, i.e., the virtual exchange of light Majorana neutrinos, in some detail and mentioned possible beyond the SM mechanisms discussed in the literature. After that, we presented two original results. First, we discussed neutrinoless double beta decay and lepton flavor violation processes such as $\mu \to e\gamma$ in the so-called colored seesaw mechanism in Section 3.2. In this model, color octet scalars and fermions generate Majorana masses for the light neutrinos via a one-loop diagram, and the same fields can directly mediate neutrinoless double beta decay and lepton flavor violating processes.

We compared the direct contribution of the color octet particles with the standard contribution to neutrinoless double beta decay, namely the exchange of light Majorana neutrinos, whose masses are generated by the color octet particles. In this sense, the latter contribution is an indirect one of the new colored fields. Extreme cases are easily possible, in the sense that both contributions can be either dominant or negligible. Studying only simple examples, we found interesting features: it is possible that the octet states saturate the limits on both $\mu \to e\gamma$ and $0\nu\beta\beta$. If the octet fermions are

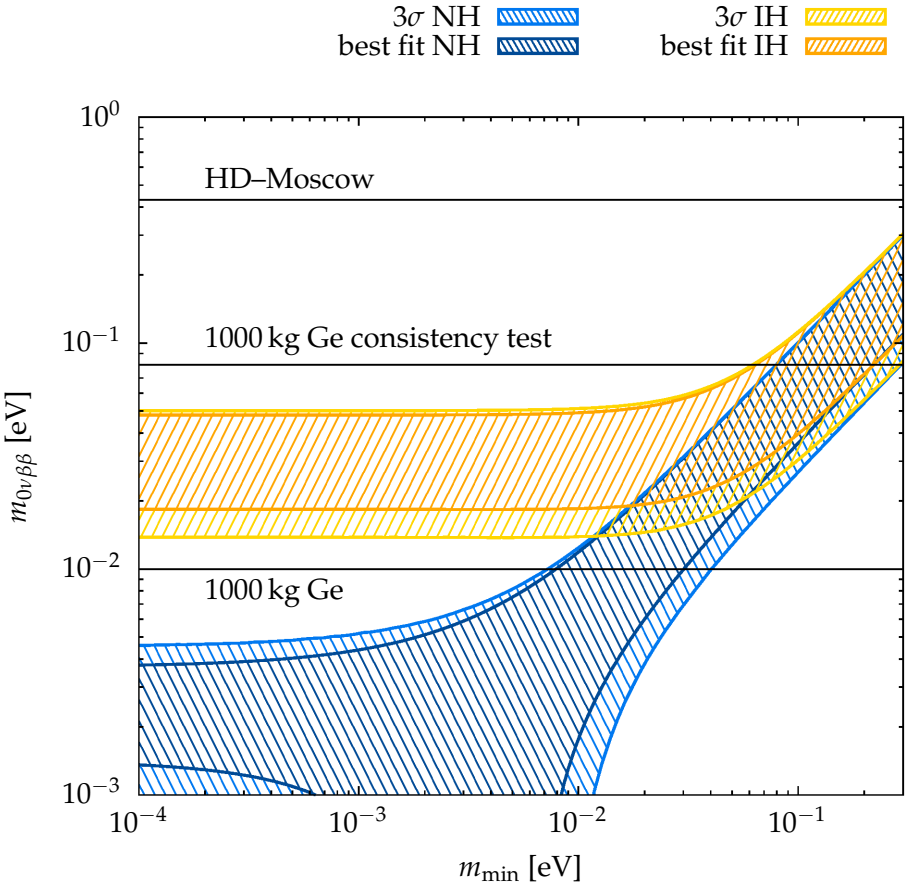

Figure 3.17: The effective Majorana mass $m_{0\nu\beta\beta}$ as a function of the lightest neutrino mass eigenvalue, just as in Fig. 3.4, given here to show the reach of the proposed consistency test. The best fit value $m_{0\nu\beta\beta} = 0.34\,\text{eV}$ obtained in the Heidelberg–Moscow experiment [89] is marked. A future 1 ton ^{76}Ge experiment [148] could probe the inverted hierarchy down to $m_{0\nu\beta\beta} = 0.01\,\text{eV}$. Using this experiment for the consistency test, the probed value for $m_{0\nu\beta\beta}$ would be higher, due to the lower rate of the decay to excited states, but could still cover the mass-degenerate regime.

degenerate in mass, then the contributions to $0\nu\beta\beta$ from the octets and the light neutrinos are both proportional to the effective mass $m_{0\nu\beta\beta}$, with their relative importance depending on the model parameters.

Second, we proposed a method to check within a single experiment whether a possibly observed signal in a future $0\nu\beta\beta$ detector is really due to $0\nu\beta\beta$ or due to some unknown background line in Section 3.3. This question will arise if a positive signal is seen in one of the next-generation experiments. Usually, it is argued that another experiment with a different isotope can settle the question. We pointed out that it is also possible to combine effort into one large detector, instead of using various different isotopes. Such a detector would therefore serve two purposes: it would have sensitivity to lower values of $m_{0\nu\beta\beta}$ and it would be able to cross-check a claim for larger values of $m_{0\nu\beta\beta}$ due to the very characteristic features described before. It is clear that the proposed consistency test is only viable for relatively large effective neutrino mass (see Fig. 3.17). Should we really have to cover the whole inverted hierarchy, or even go down to normal hierarchy, one large detector may not be viable due to the large amount of material needed, and a set of various isotopes in smaller detectors may be preferable to check for consistency.

Part II

Gauge theories for baryon and lepton numbers

Chapter 4

A gauge theory for baryon and lepton numbers with leptoquarks

In Part I of this thesis, we were concerned with two manifestations of lepton number violation by two units: Majorana neutrino masses and neutrinoless double beta decay. Now, in Part II, we have a closer look at the origin of this accidental global symmetry lepton number. Additionally, we include baryon number, the second accidental global symmetry of the SM, in the discussion. In this context, accidental means that both baryon and lepton number turn out to be symmetries of the renormalizable and gauge-invariant couplings of the SM Lagrangian, without imposing these symmetries when constructing the model.

As we already discussed in the introduction in Chapter 1, there are hints that both symmetries may actually not be conserved in nature. One way to include a violation of, e.g., lepton number into a particle physics model is an explicit breaking of the symmetry at the level of the Lagrangian: when writing down all renormalizable and gauge-invariant couplings of a model with a particular field content, one can include couplings that do not respect lepton number, in the sense that any assignment of such a number to the field content of the model leads to lepton number violation. This is exactly what we did in Part I of this thesis: all the models we discussed violate lepton number explicitly by two units.

There is no reason to object to the aforementioned approach if it leads to a phenomenologically viable model, but there is a more interesting way to include a violation of baryon and/or lepton number into a particle physics theory: promoting the accidental global symmetries to local gauge symmetries. These gauge symmetries can then be broken spontaneously by the vacuum expectation value of a scalar field. Thus, the quantum numbers of the fields breaking the local gauge symmetries dictate which processes will be allowed after symmetry breaking. The breaking of baryon number has to be done in a way that does not introduce dangerous baryon number violating operators mediating proton decay, see Section 2.2 for a discussion of these operators.

Of course, unwanted baryon number violating processes can always be suppressed

by postulating a great desert between the electroweak scale and a high scale where the baryon number violating processes have their origin. This is somewhat unsatisfying, and now, in Part II of this thesis, we are concerned with models where we can understand the breaking of baryon and lepton number at a low scale, with still suppressed dangerous baryon number violating processes.

The goal of this chapter is to define an anomaly-free theory based on the gauge group[1]

$$G_{BL} = SU(3)_C \otimes SU(2)_L \otimes U(1)_Y \otimes U(1)_B \otimes U(1)_L. \tag{4.1}$$

With the SM particle content given in Tab. 2.1, however, baryon and lepton numbers are not free of anomalies and therefore cannot be gauged separately immediately.[2] In Section 4.1 of this chapter, we discuss the promotion of the global $U(1)_B$ and $U(1)_L$ symmetries to local gauge symmetries, and present the anomalies that have to be canceled to do so consistently. Then, in Section 4.2, we revisit the attempts in the literature to build models where the baryon and lepton numbers are local gauge symmetries that are spontaneously broken at a low scale (e.g., TeV scale). We will see that all of them are ruled out by current collider results or by cosmological data. Aim of this exercise is of course to find guidance in building a viable extension of the Standard Model, which we will do in Section 4.3 (and in Chapter 5 in a left–right symmetric framework). We will take into account all experimental and observational constraints.

We then consider the theoretical framework of the simplest scenario, i.e., colorless fermionic leptoquarks, in Section 4.4. As desired, the local baryonic and leptonic gauge symmetries can be broken at a scale close to the electroweak scale without the need to postulate the existence of a great desert in order to satisfy the experimental constraints on baryon number violating processes such as proton decay. In this setup, the seesaw mechanism for neutrino masses can be realized easily, and no flavor-changing neutral currents arise at tree level. Furthermore, there is a stable DM candidate, whose stability is a consequence of the gauge theory and therefore does not have to be put into the model by hand. We summarize the main results of this chapter in Section 4.5.

The model presented in this chapter was published in collaboration with Pavel Fileviez Pérez and Mark B. Wise in Ref. [44] and the discussion presented here is an extension of the one in the paper. A more detailed analysis of the phenomenology of the model is work in progress together with Pavel Fileviez Pérez.

[1] As mentioned before, the "L" in $SU(2)_L$ refers the left-handedness of the weak interaction, whereas the "L" in $U(1)_L$ refers to lepton number.

[2] Baryon minus lepton number ($B - L$) is anomaly-free in the SM with three right-handed neutrinos, and can therefore be gauged without the introduction of additional fermions beyond these SM singlets, see the discussion in Section 4.1.2.

4.1 Relevant anomalies

4.1.1 Standard Model anomalies

The SM fermionic fields and their transformation properties under the SM gauge group G_{SM}, see Eq. (2.1), can be found in Tab. 2.1. With this field content, the SM gauge group is free of anomalies. This is important, because the chiral couplings of the theory can lead to problems at the one-loop level: an axial current that is conserved classically can obtain a non-zero divergence through one-loop triangle diagrams, coupling the axial current to two gauge currents. In a theory in which gauge bosons couple to a chiral current these contributions show up in the one-loop corrections to the vertex of three gauge bosons. Such a theory can be gauge invariant only if the anomalous contributions cancel.

The anomalous triangle diagram of three gauge bosons A^a_μ, A^b_ν, and A^c_ρ is proportional to

$$\text{Tr}\left(\pm t^a t^b t^c\right), \tag{4.2}$$

where t^a, t^b, and t^c are the corresponding representation matrices and the trace is taken over all fermion species circulating in the loop. Of course, also the diagram with the fermions circulating in opposite direction has to be taken into account. The $\pm$ accounts for the fact that left-handed and right-handed contributions contribute with a different sign. Therefore, all anomalies automatically cancel in theories where the gauge bosons couple to left-handed and right-handed in the same way, as is the case in, e.g., quantum chromodynamics and quantum electrodynamics.

Triangle diagrams containing three $SU(2)_L$ currents vanish identically. Diagrams containing only one $SU(2)_L$ or one $SU(3)_C$ current also vanish because of $\text{Tr}(t^a) = 0$ for all corresponding representation matrices t^a. Triangle diagrams containing only one external gravitational field also vanish [149]. See Tab. 4.1 and Fig. 4.1 for the non-trivial SM anomalies. When extending the particle content in extensions of the SM, we have to make sure not to introduce non-zero values for any of these anomalies.

In what follows, we are concerned with gauging the symmetries $U(1)_B$ and $U(1)_L$ individually. We start to do so by considering the gauge group given in Eq. (4.1) in this chapter. See Refs. [34–36] for earlier attempts to gauge baryon and lepton numbers in this way, and Refs. [150, 151] for early related studies. In Chapter 5, we will move to a left–right symmetric setup using the gauge group

$$G^{BL}_{LR} = SU(2)_L \otimes SU(2)_R \otimes U(1)_B \otimes U(1)_L \otimes \mathcal{P}, \tag{4.3}$$

where $\mathcal{P}$ is the discrete left–right parity transformation, and we omitted the QCD gauge group $SU(3)_C$ for simplicity. This gauge group was used in Ref. [152], where

Table 4.1: Non-trivial SM anomalies. The SM is an anomaly-free gauge theory and therefore, with the fermionic field content given in Tab. 2.1, all of these anomalies vanish. When extending the SM field content by additional fermions, as we will do in this chapter and the following ones to gauge baryon and lepton numbers, we have to make sure not to introduce non-zero values for one or more of these anomalies.

Anomaly	SM value
$\mathcal{A}_1^{\mathrm{SM}}\left(U(1)_Y^3\right)$	0
$\mathcal{A}_2^{\mathrm{SM}}\left(SU(3)_C^2 \otimes U(1)_Y\right)$	0
$\mathcal{A}_3^{\mathrm{SM}}\left(SU(2)_L^2 \otimes U(1)_Y\right)$	0
$\mathcal{A}_4^{\mathrm{SM}}\left(\mathrm{gravity}^2 \otimes U(1)_Y\right)$	0

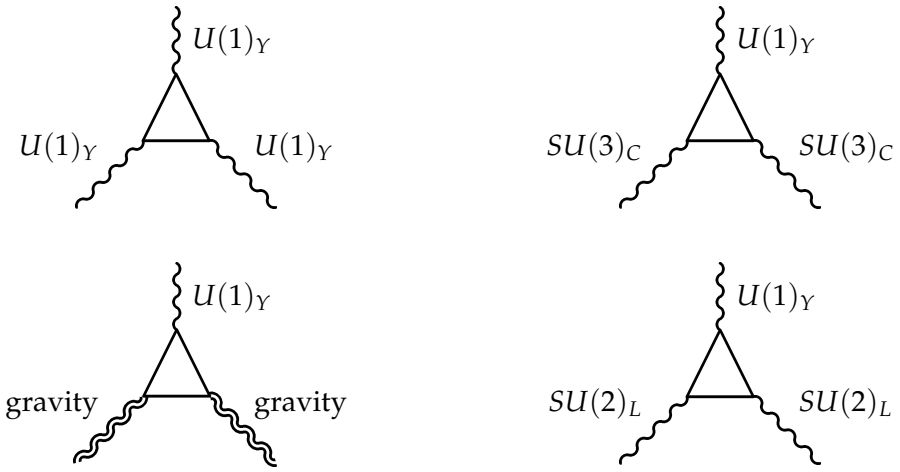

Figure 4.1: Triangle diagrams of the non-trivial anomalies of the SM, see also Tab. 4.1. Figures clock-wise from top left: $\mathcal{A}_1^{\mathrm{SM}}(U(1)_Y^3)$, $\mathcal{A}_2^{\mathrm{SM}}(SU(3)_C^2 \otimes U(1)_Y)$, $\mathcal{A}_3^{\mathrm{SM}}(SU(2)_L^2 \otimes U(1)_Y)$, $\mathcal{A}_3^{\mathrm{SM}}(\mathrm{gravity}^2 \otimes U(1)_Y)$.

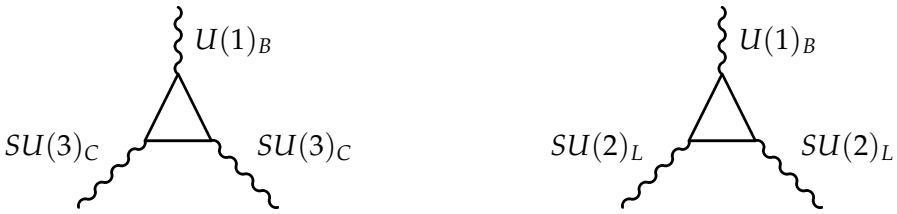

Figure 4.2: Triangle diagrams of the baryonic anomalies that are calculated in the text: $\mathcal{A}_1\left(SU(3)_C^2 \otimes U(1)_B\right)$ and $\mathcal{A}_2\left(SU(2)_L^2 \otimes U(1)_B\right)$.

the authors discussed some solutions for the cancelation of anomalies, and we shortly present these solutions in Chapter 5.

From now on, we take the right-handed neutrinos to be part of the (slightly extended) SM fermionic spectrum, having the following transformation properties under the gauge group G_{BL}:

$$\nu_R^\alpha \sim (\mathbf{1}, \mathbf{1}, 0, 0, 1)\,. \tag{4.4}$$

The introduction of these right-handed neutrinos of course affects the values of anomalies involving $U(1)_L$, but leaves the SM anomalies in Tab. 4.1 untouched, because the right-handed neutrinos are total singlets under the SM gauge group G_{SM}.

4.1.2 Baryonic and leptonic anomalies

The additional anomalies (baryonic, leptonic, and mixed) that need to be canceled are presented in Tab. 4.2, together with their values with the SM particle content plus right-handed neutrinos. The mixed anomalies become important when we deal with particles charged both under $U(1)_B$ and $U(1)_L$, the so-called leptoquarks that we introduce later.

Let us calculate the SM values of $\mathcal{A}_1\left(SU(3)_C^2 \otimes U(1)_B\right)$ and $\mathcal{A}_2\left(SU(2)_L^2 \otimes U(1)_B\right)$ from Tab. 4.2 as an example. The corresponding triangle diagrams are given in Fig. 4.2. To $\mathcal{A}_1$, all SM fermions in a non-trivial representation of $SU(3)_C$ and a non-zero baryon number contribute, i.e., all SM quarks. We obtain (t^a, $a = 1, \ldots, 8$, are the matrices of the corresponding $SU(3)_C$ representation)

$$\mathcal{A}_1\left(SU(3)_C^2 \otimes U(1)_B\right)\delta^{ab} \equiv \text{Tr}(t^a t^b B) = \frac{1}{2}\delta^{ab}\sum_i B_i, \tag{4.5}$$

where the sum runs over all SM quarks with an extra minus for the right-handed quarks:

$$\sum_i B_i = 3\left(2\cdot\frac{1}{3} - \frac{1}{3} - \frac{1}{3}\right) = 0. \tag{4.6}$$

Table 4.2: Purely baryonic, purely leptonic, and mixed anomalies and their values in the SM with right-handed neutrinos. To be able to gauge baryon and lepton numbers consistently, the non-zero anomalies have to be canceled by new fermions and non-zero values for the vanishing ones may not be introduced. See Ref. [34] for a first detailed discussion of these anomalies.

Type	Anomaly	SM value
Baryonic	$\mathcal{A}_1\left(SU(3)_C^2 \otimes U(1)_B\right)$	0
	$\mathcal{A}_2\left(SU(2)_L^2 \otimes U(1)_B\right)$	$\frac{3}{2}$
	$\mathcal{A}_3\left(U(1)_Y^2 \otimes U(1)_B\right)$	$-\frac{3}{2}$
	$\mathcal{A}_4\left(U(1)_Y \otimes U(1)_B^2\right)$	0
	$\mathcal{A}_5\left(\text{gravity}^2 \otimes U(1)_B\right)$	0
	$\mathcal{A}_6\left(U(1)_B^3\right)$	0
Leptonic	$\mathcal{A}_7\left(SU(3)_C^2 \otimes U(1)_L\right)$	0
	$\mathcal{A}_8\left(SU(2)_L^2 \otimes U(1)_L\right)$	$\frac{3}{2}$
	$\mathcal{A}_9\left(U(1)_Y^2 \otimes U(1)_L\right)$	$-\frac{3}{2}$
	$\mathcal{A}_{10}\left(U(1)_Y \otimes U(1)_L^2\right)$	0
	$\mathcal{A}_{11}\left(\text{gravity}^2 \otimes (U(1)_L\right)$	0
	$\mathcal{A}_{12}\left(U(1)_L^3\right)$	0
Mixed	$\mathcal{A}_{13}\left(U(1)_B^2 \otimes U(1)_L\right)$	0
	$\mathcal{A}_{14}\left(U(1)_L^2 \otimes U(1)_B\right)$	0
	$\mathcal{A}_{15}\left(U(1)_Y \otimes U(1)_L \otimes U(1)_B\right)$	0

The factor of 3 accounts for the three quark families. To $\mathcal{A}_2\left(SU(2)_L^2 \otimes U(1)_B\right)$, only the quarks in a non-trivial representation of $SU(2)_L$ contribute, i.e., the left-handed quark doublets. We thus find (τ^a, $a = 1, 2, 3$, are the matrices of the corresponding $SU(2)_L$ representation)

$$\mathcal{A}_2\left(SU(2)_L^2 \otimes U(1)_B\right)\delta^{ab} \equiv \mathrm{Tr}(\tau^a\tau^b B) = 3 \cdot 3 \cdot \frac{1}{3} \cdot \frac{1}{2}\delta^{ab} = \frac{3}{2}\delta^{ab}. \tag{4.7}$$

One factor of 3 comes from color, the second one represents the three quark families.

The anomalies $\mathcal{A}_2\left(SU(2)_L^2 \otimes U(1)_B\right)$ and $\mathcal{A}_8\left(SU(2)_L^2 \otimes U(1)_L\right)$ cannot be canceled in the SM, because each SM family contains only one quark doublet and one lepton doublet. Therefore, we need to introduce new fermions with non-trivial transformation properties under $SU(2)_L$ to cancel these anomalies. It is worth to point out that $\mathcal{A}_{11}\left(\text{gravity}^2 \otimes U(1)_L\right)$ and $\mathcal{A}_{12}\left(U(1)_L^3\right)$ are only canceled after we extend the SM particle content by right-handed neutrinos.

It is obvious from Tab. 4.2 that the gauge group

$$G_{B-L} = SU(3)_C \otimes SU(2)_L \otimes U(1)_Y \otimes U(1)_{B-L} \tag{4.8}$$

is free of anomalies with the SM field content (extended by right-handed neutrinos). Compare the values of $\mathcal{A}_2\left(SU(2)_L^2 \otimes U(1)_B\right)$ and $\mathcal{A}_8\left(SU(2)_L^2 \otimes U(1)_L\right)$, as well as the ones of $\mathcal{A}_3\left(U(1)_Y^2 \otimes U(1)_B\right)$ and $\mathcal{A}_9\left(U(1)_Y^2 \otimes U(1)_L\right)$. G_{B-L} can therefore be gauged without the introduction of new fermionic fields. Since our ultimate aim is to write down gauge theories for baryon and lepton number without the need to assume a great desert to suppress baryon number violating processes, it is of no use to follow this direction: the dimension-6 proton decay operators given in Section 2.2 invariant under $B - L$. We will thus not discuss such models in more detail in this thesis.

4.2 Attempts in the literature to gauge baryon and lepton numbers

Different solutions of the equations that ensure the cancelation of the anomalies presented in Tab. 4.2 were studied in the literature [34–37]. Early attempts to gauge baryon and lepton numbers can be found in Refs. [150, 151, 153–155]. By current experimental results, however, all of the models in [34–37] are ruled out. We nevertheless present them here to serve as a guideline for model building, which we will do later in this chapter and in Chapter 5.

Table 4.3: Field content of a sequential family and the corresponding transformation properties under the gauge group G_{BL} [34, 35]. The new quarks transform like the SM quarks under the SM gauge group, but have baryon number $B_{Q'_L} = B_{u'_R} = B_{d'_R} = -1$. The new leptons transform like the SM leptons under the SM gauge group, but have lepton number $L_{\ell'_L} = L_{e'_R} = L_{\nu'_R} = -3$.

Field	$SU(3)_C$	$SU(2)_L$	$U(1)_Y$	$U(1)_B$	$U(1)_L$
Q'_L	**3**	**2**	$\frac{1}{6}$	$B_{Q'_L}$	0
u'_R	**3**	**1**	$\frac{2}{3}$	$B_{u'_R}$	0
d'_R	**3**	**1**	$-\frac{1}{3}$	$B_{d'_R}$	0
ℓ'_L	**1**	**2**	$-\frac{1}{2}$	0	$L_{\ell'_L}$
e'_R	**1**	**1**	-1	0	$L_{e'_R}$
ν'_R	**1**	**1**	0	0	$L_{\nu'_R}$

4.2.1 Sequential or mirror family of quarks and leptons

In Refs. [34, 35], two solutions were presented: a sequential family and a mirror family of quarks and leptons. The corresponding particle contents are presented in Tabs. 4.3 and 4.4. In the sequential family, the new quarks have baryon number

$$B_{Q'_L} = B_{u'_R} = B_{d'_R} = -1, \tag{4.9}$$

and the new leptons have lepton number

$$L_{\ell'_L} = L_{e'_R} = L_{\nu'_R} = -3, \tag{4.10}$$

which is their only difference from the corresponding SM fields.[3] In the mirror family, the new quarks have baryon number

$$B_{Q'_R} = B_{u'_L} = B_{d'_L} = 1, \tag{4.11}$$

and the new leptons have lepton number

$$L_{\ell'_R} = L_{e'_L} = L_{\nu'_L} = 3. \tag{4.12}$$

The factor of three in comparison to the SM fields is somewhat obvious, because one family of new fermions has to cancel the contribution of three SM families.

[3] A similar charge assignment was used before in the context of gauging baryon number only [154].

Table 4.4: Field content of a mirror family and the corresponding transformation properties under the gauge group G_{BL} [34, 35]. The new quarks transform like SM quarks of opposite chirality under the SM gauge group, but have baryon number $B_{Q'_R} = B_{u'_L} = B_{d'_L} = 1$. The new leptons transform like SM leptons of opposite chirality under the SM gauge group, but have lepton number $L_{\ell'_R} = L_{e'_L} = L_{\nu'_L} = 3$.

Field	$SU(3)_C$	$SU(2)_L$	$U(1)_Y$	$U(1)_B$	$U(1)_L$
Q'_R	**3**	**2**	$\frac{1}{6}$	$B_{Q'_R}$	0
u'_L	**3**	**1**	$\frac{2}{3}$	$B_{u'_L}$	0
d'_L	**3**	**1**	$-\frac{1}{3}$	$B_{d'_L}$	0
ℓ'_R	**1**	**2**	$-\frac{1}{2}$	0	$L_{\ell'_R}$
e'_L	**1**	**1**	-1	0	$L_{e'_L}$
ν'_L	**1**	**1**	0	0	$L_{\nu'_L}$

All the baryonic and leptonic anomalies in Tab. 4.2 cancel in both setups. The mixed anomalies do not play a role because fields are either charged under $U(1)_B$ or $U(1)_L$, but not under both symmetries. The anomalies of the SM gauge group do not pose a problem because a full new family is introduced.

Unfortunately, both solutions are ruled out today by LHC data. LHC bounds on the masses of the new quarks are strong: a CMS search excludes mass-degenerate fourth-generation quarks with masses below 685 GeV at 95% CL [156]. Because these quark masses can only come from Yukawa interactions with the SM Higgs, the fourth generation Yukawa couplings have to be quite large, changing the gluon fusion Higgs production by a factor of 9 [157]. This is in disagreement with the recent LHC results, where Higgs production is well described by the SM [158]. Additionally, the Yukawas have to be so large that one enters the regime of non-perturbativity, expecting Landau poles for the new Yukawa couplings in the TeV region [159]. A current two-loop analysis for a 126 GeV Higgs shows that perturbation theory is useful for the new quark masses of the order 600 GeV, but becomes to be marginal at masses $\geq$ 900 GeV [160].

4.2.2 Vector-like family of quarks and leptons

The problem of too large Yukawa couplings occurred in the case of a sequential or a mirror family because the particles could get their masses only from the SM Higgs. By introducing a vector-like family of quarks and leptons (vector-like with regard to the

SM gauge group), this problem can be avoided.[4] In Ref. [36] anomalies were canceled using vector-like fermions, consisting of a sequential and a mirror family, see Tabs. 4.3 and 4.4. In this case, all anomalies are canceled provided

$$B_{Q'_L} = B_{u'_R} = B_{d'_R}, \tag{4.13}$$
$$B_{Q'_R} = B_{u'_L} = B_{d'_L}, \tag{4.14}$$
$$B_{Q'_L} - B_{Q'_R} = -1 \tag{4.15}$$

for the baryon numbers of the new quarks and

$$L_{\ell'_L} = L_{e'_R} = L_{\nu'_R}, \tag{4.16}$$
$$L_{\ell'_R} = L_{e'_L} = L_{\nu'_L}, \tag{4.17}$$
$$L_{\ell'_L} - L_{\ell'_R} = -3 \tag{4.18}$$

for the lepton numbers of the new leptons.

In addition to the Yukawa couplings to the SM Higgs, one can then write down the couplings

$$-\mathcal{L}_{\text{vec}} = \lambda_Q \overline{Q'_L} Q'_R S_B + \lambda_u \overline{u'_R} u'_L S_B + \lambda_d \overline{d'_R} d'_L S_B + \text{h.c.}, \tag{4.19}$$

where

$$S_B \sim (\mathbf{1}, \mathbf{1}, 0, -1, 0) \tag{4.20}$$

is the scalar that eventually obtains a VEV and breaks $U(1)_B$, thereby generating vector-like masses for the new quarks. Thus, in this setup, the masses of the new quarks can be large without the need of large Yukawa couplings to the SM Higgs. The model can therefore be free of non-perturbative Yukawa couplings up to the Planck scale and the Higgs production channels are not modified by the new quarks.

In the setup used in Ref. [36], the neutrino masses are generated through the type I seesaw and the new charged leptons get mass only from the SM Higgs VEV. The corresponding Lagrangian is

$$\begin{aligned} -\mathcal{L}_\ell = {} & h'_e \overline{\ell'_L} H e'_R + h''_e \overline{\ell'_R} H e'_L + h'_\nu \overline{\ell'_L} \tilde{H} \nu'_R + h''_\nu \overline{\ell'_R} \tilde{H} \nu'_L \\ & + Y_e \overline{\ell_L} H e_R + Y_\nu \overline{\ell_L} \tilde{H} \nu_R + \lambda \overline{(\nu_R)^c} \nu_R S_L + \text{h.c.}, \end{aligned} \tag{4.21}$$

where the new scalar transforms as

$$S_L \sim (\mathbf{1}, \mathbf{1}, 0, 0, -2)\,. \tag{4.22}$$

[4] Vector-like means that left- and right-handed fields transform in the same way under the SM gauge group.

After S_L acquires its VEV, the right-handed neutrinos obtain a Majorana mass term. Therefore, in this model the lepton number is broken by two units and one does never generate proton decay. Unfortunately, the new charged leptons reduce the Higgs branching ratio into gamma gamma [161] by about a factor of 3. This model therefore disagrees with the recent LHC results where the newly discovered boson is SM-like.

One can modify this model by adding a second new Higgs boson with lepton number

$$S'_L \sim (\mathbf{1}, \mathbf{1}, 0, 0, -3) \tag{4.23}$$

to generate vector-like masses for the charged leptons via

$$-\mathcal{L}^{\ell}_{\text{vec}} = \lambda_{\ell} \overline{\ell'_L} \ell'_R S'_L + \lambda_e \overline{e'_R} e'_L S'_L + \lambda_\nu \overline{\nu'_R} \nu'_L S'_L + \text{h.c.} \tag{4.24}$$

after spontaneous symmetry breaking, when S'_L obtained its VEV. Then, one will generate dimension nine operators mediating proton decay, e.g.,

$$\mathcal{O}_9 = \frac{c_9}{\Lambda^5} \left(u_R u_R d_R e_R\right) S_B S_L^{\dagger} S'_L. \tag{4.25}$$

Assuming that $c_9 \sim 1$ and that the VEVs of S_B, S_L, and S'_L are around TeV, one finds that $\Lambda \geq 10^{7-8}\,\text{GeV}$. This means that we still have to postulate half of the desert (on a logarithmic scale) in order to satisfy the proton decay bounds. Of course, we could also assume that c_9 is very small. We will not discuss this model further but instead look for solutions, where proton decay is absent and we do not have to postulate the existence of a desert.

4.2.3 Family of fermionic leptoquarks

Instead of introducing a full family of quarks and a full family of leptons, it is natural to think about canceling the B and L anomalies by adding fermionic leptoquarks, i.e., particles that carry both baryon and lepton numbers. A generic starting point can be the assignment of quantum numbers provided in Tab. 4.5, where, for simplicity, all new fields are in the same representation $\boldsymbol{N}$ of $SU(3)_C$ and the $SU(2)_L$ structure is similar to the one of a SM family of quarks and leptons (one left-handed doublet and two right-handed singlets). The conditions obtained from the requirement of anomaly cancelation then lead to a unique model, up to different choices for $\boldsymbol{N}$.

The combination of $\mathcal{A}_5$ $\left(\text{gravity}^2 \otimes U(1)_B\right)$ and $\mathcal{A}_6$ $\left(U(1)_B^3\right)$ allows for two assignments of baryon numbers B_1, B_2, B_3:

$$B_1 = 0,\ B_2 = -B_3 \ \text{ or } \ B_1 = B_2 = B_3 \equiv B. \tag{4.26}$$

Let us consider the second assignment. Similarly, for the lepton numbers, we are led to

$$L_1 = L_2 = L_3 \equiv L. \tag{4.27}$$

Table 4.5: Generic assignment of quantum numbers for a family of leptoquarks. For simplicity, all new fields are in the same representation $\boldsymbol{N}$ of $SU(3)_C$, which will fix the baryon and lepton numbers of the fields. For simplicity, the $SU(2)_L$ structure is similar to the one of a SM family of quarks or leptons: one left-handed doublet and two right-handed singlets.

Field	$SU(3)_C$	$SU(2)_L$	$U(1)_Y$	$U(1)_B$	$U(1)_L$
Ψ_L	$\boldsymbol{N}$	$\mathbf{2}$	Y_1	B_1	L_1
η_R	$\boldsymbol{N}$	$\mathbf{1}$	Y_2	B_2	L_2
χ_R	$\boldsymbol{N}$	$\mathbf{1}$	Y_3	B_3	L_3

Then, $\mathcal{A}_2\left(SU(2)_L^2 \otimes U(1)_B\right)$ and $\mathcal{A}_8\left(SU(2)_L^2 \otimes U(1)_L\right)$ immediately fix B and L to be

$$B = L = -\frac{3}{N}. \tag{4.28}$$

The combination of $\mathcal{A}_1^{\text{SM}}\left(U(1)_Y^3\right)$ and $\mathcal{A}_4^{\text{SM}}\left(\text{gravity}^2 \otimes U(1)_Y\right)$ leads to two possible combinations (compare the discussion for baryon and lepton numbers above):

$$Y_1 = 0,\ Y_2 = -Y_3 \ \text{ or } \ Y_1 = Y_2 = Y_3. \tag{4.29}$$

Combining this condition with the one obtained from $\mathcal{A}_3\left(U(1)_Y^2 \otimes U(1)_B\right)$, the unique assignment of hypercharges is

$$Y_1 = 0,\ Y_2 = \pm\frac{1}{2} = -Y_3. \tag{4.30}$$

This discussion nicely illustrates the power of anomaly cancelation in fixing the quantum numbers of the additional fields.

For the choice $N = 3$, this is just the model which was presented in Ref. [37], where the authors introduced the fields

$$F_L \sim (\mathbf{3}, \mathbf{2}, 0, -1, -1)\,, \tag{4.31}$$

$$j_R \sim \left(\mathbf{3}, \mathbf{1}, \frac{1}{2}, -1, -1\right), \tag{4.32}$$

$$k_R \sim \left(\mathbf{3}, \mathbf{1}, -\frac{1}{2}, -1, -1\right), \tag{4.33}$$

in addition to the SM fermion content given before. This simple particle content cancels all relevant anomalies. Of course, one could similarly introduce a set of "mirror"

leptoquarks with opposite chirality and lepton and baryon numbers $B = L = +1$, also canceling all anomalies. The new particles have exotic electric charges, $Q_j = 1/2$ and $Q_k = -1/2$, and one predicts the existence of stable charged fields. This model is therefore ruled out by cosmology. In the next section, we present different solutions with particles having both baryon and lepton numbers, in which one can avoid this problem.

4.3 Vector-like family of fermionic leptoquarks

In the last section, we saw that all models proposed in the literature to gauge baryon and lepton numbers are by now ruled out by observations. In the case of sequential and mirror families, as well as the vector-like family, LHC data rules out the setups; the case of a family of leptoquarks is ruled out by cosmology. In this section, we build a viable model that can satisfy all current constraints. We combine the advantages of the different models presented before, namely vector-like fermions and leptoquark fields that carry both lepton and baryon numbers.

4.3.1 Anomaly cancelation

As we have seen in the last chapter, there are different possibilities to cancel all relevant anomalies to gauge B and L. However, it is difficult to write a consistent model which is in agreement with collider data and cosmology without the need to postulate the existence of a large desert. In order to find viable scenarios, we consider the particle content listed in Tab. 4.6. We consider different possibilities for the quantum numbers of the new fields under $SU(3)_C$ and use the conditions for the cancelation of anomalies to determine the quantum numbers under $U(1)_Y$, $U(1)_B$, and $U(1)_L$. The anomalies $\mathcal{A}_2(SU(2)_L^2 \otimes U(1)_B)$ and $\mathcal{A}_8(SU(2)_L^2 \otimes U(1)_L)$, see Tab. 4.2, can only be canceled by a field charged under $SU(2)$, most conveniently by a doublet. We therefore fix the $SU(2)_L$ quantum numbers of the new particles to be similar to a SM family of quarks or leptons (one $SU(2)_L$ doublet and two singlets). To not spoil the SM anomaly cancelation, see the non-trivial anomalies in Tab. 4.1, we choose the new fields to be vector-like under the SM gauge group.

Starting with the cancelation of $\mathcal{A}_2(SU(2)_L^2 \otimes U(1)_B)$, one finds the condition

$$B_1 - B_4 = -\frac{3}{N}, \tag{4.34}$$

and for simplicity we use

$$B_1 = -B_4 = -\frac{3}{2N} \tag{4.35}$$

Table 4.6: Generic assignment of quantum numbers for a vector-like family of leptoquarks. Compare with the single family of leptoquarks presented before, see Tab. 4.5. For simplicity, all new fields are in the same representation $\boldsymbol{N}$ of $SU(3)_C$, which will fix the baryon and lepton numbers using the constraints that come from the cancelation of anomalies, see the discussion in Section 4.3.1. For simplicity, the $SU(2)_L$ structure is similar to the one of a SM family of quarks or leptons: one left-handed doublet and two right-handed singlets.

Field	$SU(3)_C$	$SU(2)_L$	$U(1)_Y$	$U(1)_B$	$U(1)_L$
Ψ_L	$\boldsymbol{N}$	$\mathbf{2}$	Y_1	$B_1 = -\frac{3}{2N}$	$L_1 = -\frac{3}{2N}$
η_R	$\boldsymbol{N}$	$\mathbf{1}$	Y_2	$B_2 = -\frac{3}{2N}$	$L_2 = -\frac{3}{2N}$
χ_R	$\boldsymbol{N}$	$\mathbf{1}$	Y_3	$B_3 = -\frac{3}{2N}$	$L_3 = -\frac{3}{2N}$
Ψ_R	$\boldsymbol{N}$	$\mathbf{2}$	Y_1	$B_4 = +\frac{3}{2N}$	$L_4 = +\frac{3}{2N}$
η_L	$\boldsymbol{N}$	$\mathbf{1}$	Y_2	$B_5 = +\frac{3}{2N}$	$L_5 = +\frac{3}{2N}$
χ_L	$\boldsymbol{N}$	$\mathbf{1}$	Y_3	$B_6 = +\frac{3}{2N}$	$L_6 = +\frac{3}{2N}$

The same applies to the corresponding leptonic anomaly $\mathcal{A}_8(SU(2)_L^2 \otimes U(1)_L)$, and we have

$$L_1 = -L_4 = -\frac{3}{2N}. \tag{4.36}$$

To cancel $\mathcal{A}_5(\text{gravity}^2 \otimes U(1)_B)$, one needs to impose the condition

$$2(B_1 - B_4) - (B_2 - B_5) - (B_3 - B_6) = 0. \tag{4.37}$$

Using

$$B_5 = -B_2 \text{ and } B_6 = -B_3, \tag{4.38}$$

this reduces to

$$2B_1 - B_2 - B_3 = 0, \tag{4.39}$$

which is most easily canceled by the choice

$$B_1 = B_2 = B_3. \tag{4.40}$$

Similarly, a good choice for the lepton numbers is

$$L_5 = -L_2, L_6 = -L_3, \text{ and } L_1 = L_2 = L_3. \tag{4.41}$$

Finally, we have to cancel the anomalies with weak hypercharge. The anomalies $\mathcal{A}_4\left(U(1)_Y \otimes U(1)_B^2\right)$ and $\mathcal{A}_{10}\left(U(1)_Y \otimes U(1)_L^2\right)$ are always canceled with the above used assignment of baryon and lepton numbers, and do not provide a condition for the hypercharges. From $\mathcal{A}_3(U(1)_Y^2 \otimes U(1)_B)$, we obtain the condition

$$Y_2^2 + Y_3^2 - 2Y_1^2 = \frac{1}{2}. \tag{4.42}$$

A useful set of solutions for this equation is

$$(Y_1, Y_2, Y_3) \in \left\{ \left(\pm\frac{1}{2}, \pm 1, 0\right), \left(\pm\frac{1}{6}, \pm\frac{2}{3}, \pm\frac{1}{3}\right), \left(0, \pm\frac{1}{2}, \pm\frac{1}{2}\right) \right\}. \tag{4.43}$$

It is easy to check that, using any of these choices, all baryonic and leptonic anomalies are canceled. Since the new particles are vector-like with respect to the SM gauge group, the SM anomalies do not pose a problem. Additionally, it can be checked that the mixed anomalies $\mathcal{A}_{13}(U(1)_L \otimes U(1)_B^2)$, $\mathcal{A}_{14}(U(1)_L^2 \otimes U(1)_B)$, and $\mathcal{A}_{15}(U(1)_Y \otimes U(1)_L \otimes U(1)_B)$ are canceled as well. These could be relevant because we deal with particles charged both under $U(1)_B$ and $U(1)_L$.

In the following three subsections, we discuss the possible scenarios for different values of N in some detail. For a viable model, one has to avoid scenarios with a stable electrically charged or a stable colored field; this can most easily be done if we either demand that the new fields should have a direct coupling to the SM fermions to allow for a decay channel, or that the lightest particle in the new sector is neutral and stable.

4.3.2 Color singlets

In the case of $N = 1$, i.e., if the new fields do not feel the strong interaction, both the solutions with the hypercharge assignments $(Y_1, Y_2, Y_3) = (\pm 1/6, \pm 2/3, \pm 1/3)$ and $(Y_1, Y_2, Y_3) = (0, \pm 1/2, \pm 1/2)$ contain a stable electrically charged field (compare the leptoquark discussion in the last section). The only solution which allows for a stable neutral field in the new sector is $(Y_1, Y_2, Y_3) = (\pm 1/2, \pm 1, 0)$. This neutral particle can then be a dark matter candidate. This is a very interesting setup, and we discuss this solution in Section 4.4 in more detail.

4.3.3 Color triplets

In the case $N = 3$, both the solutions $(Y_1, Y_2, Y_3) = (0, \pm 1/2, \pm 1/2)$ and $(Y_1, Y_2, Y_3) = (\pm 1/2, \pm 1, 0)$ do not allow for a decay of the new colored fields to SM particles and/or electrically neutral and colorless fields. A stable colored field can be avoided if one

uses the weak hypercharge assignment $(Y_1, Y_2, Y_3) = (\pm 1/6, \pm 2/3, \pm 1/3)$, because part of the new leptoquarks can decay to the SM quarks and a new scalar SM singlet

$$X \sim \left(\mathbf{1}, \mathbf{1}, 0, -\frac{1}{6}, -\frac{1}{2}\right) \tag{4.44}$$

via the following coupling

$$-\mathcal{L} \supset \lambda_Q X \overline{Q_L} \Psi_R + \lambda_u X \overline{u_R} \eta_L + \lambda_d X \overline{d_R} \chi_L + \text{h.c.} \tag{4.45}$$

Additionally, one can introduce a new scalar

$$S_{BL} \sim (\mathbf{1}, \mathbf{1}, 0, -1, -1) \tag{4.46}$$

that couples to the new leptoquarks as

$$-\mathcal{L} \supset \lambda_\Psi S_{BL} \overline{\Psi_L} \Psi_R + \lambda_\eta S_{BL} \overline{\eta_R} \eta_L + \lambda_\chi S_{BL} \overline{\chi_R} \chi_L + \text{h.c.} \tag{4.47}$$

If the new scalar X does not acquire a VEV, no mass mixing between the SM quarks and the new leptoquarks will be induced. Actually, if X is the lightest new particle with baryon number, it will be a stable DM candidate. This is ensured by a global $U(1)$ symmetry where the new leptoquarks and X are multiplied by a phase. It is worth pointing out that this symmetry does not have to be put in by hand because it is an automatic consequence of the particle content of the model and the underlying gauge symmetry. The VEV of S_{BL} will break $U(1)_B$ and $U(1)_L$ and give vector-like masses to the leptoquarks. Unfortunately, with S_{BL} one generates dimension seven operators mediating proton decay, e.g.,

$$\mathcal{O}_7 = \frac{c_7}{\Lambda^3} (e_R u_R u_R d_R) S_{BL}. \tag{4.48}$$

Assuming that the VEV of S_{BL} is around TeV and that $c_7 \approx 1$, one finds that $\Lambda > 10^{11}$ GeV, such that one has to still postulate a large desert to account for the large proton lifetime. Therefore, we will not pursue this model further in this thesis.

4.3.4 Color octets

This scenario with $N = 8$ also is viable if one chooses

$$(Y_1, Y_2, Y_3) = \left(\pm\frac{1}{2}, \pm 1, 0\right), \tag{4.49}$$

such that the leptoquarks couple to the SM fermions via

$$-\mathcal{L} \supset \lambda_1 \overline{\Psi_R} \ell_L S + \lambda_2 \overline{\eta_L} e_R S + \lambda_3 \overline{\chi_L} \nu_R S + \text{h.c.}, \tag{4.50}$$

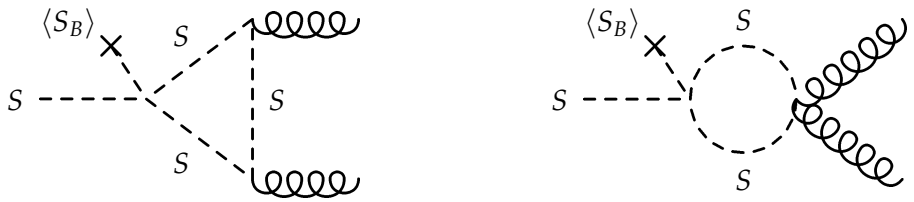

Figure 4.3: Decay of the scalar S to two gluons at one loop.

introducing the extra colored scalar field

$$S \sim \left(\mathbf{8}, \mathbf{1}, 0, \frac{3}{16}, -\frac{13}{16}\right). \tag{4.51}$$

By additionally introducing a scalar SM singlet with non-zero baryon and lepton numbers

$$S_B \sim \left(\mathbf{1}, \mathbf{1}, 0, B', L'\right) \tag{4.52}$$

that will break B and L once it obtains a VEV, one can allow for a term $\mathrm{Tr}(S^3 S_B)$ in the scalar potential that fixes B' and L'. Then, after spontaneous symmetry breaking, S can decay at one loop to a pair of gluons [82]; see the corresponding Feynman diagrams in Fig. 4.3.

Although this setup is interesting, we do not consider $N = 8$ further in this thesis, but instead present the simplest possible model with $N = 1$ in the following sections in more detail.

4.4 Color singlets: framework and phenomenology

4.4.1 Particle content and interactions

The additional fields of the solution with colorless leptoquarks are given in Tab. 4.7. The new fermions are exactly the ones necessary to cancel all relevant anomalies to be able to gauge $U(1)_B$ and $U(1)_L$. We call these fields leptoquarks even though they do not couple to quarks and leptons because they have baryon and lepton numbers $\pm 3/2$. Because we need to break both local gauge symmetries, we need to introduce two additional scalar fields, S_{BL} and S_L. Their quantum numbers are also given in Tab. 4.7.

The Lagrangian of the model can be written as

$$\mathcal{L} = \mathcal{L}_{\text{scalar}} + \mathcal{L}_{\text{kin}}^{\text{gauge}} + \mathcal{L}_{\text{kin}}^{\text{fermion}} + \mathcal{L}_{\text{Yuk}}, \tag{4.53}$$

where $\mathcal{L}_{\text{scalar}}$ defines the scalar sector of the model, $\mathcal{L}_{\text{kin}}^{\text{gauge}}$ contains the kinetic terms of the gauge bosons, $\mathcal{L}_{\text{kin}}^{\text{fermion}}$ contains the kinetic terms of the fermions (SM quarks

Table 4.7: The extra particle content of the simplest model with colorless leptoquarks and the corresponding transformation properties under the gauge group G_{BL}. The leptoquark fields Ψ_L, η_R, χ_R, Ψ_R, η_L, and χ_L cancel all relevant anomalies. The scalar fields S_{BL} and S_L will obtain VEVs and contribute to the breaking of $U(1)_B$ and $U(1)_L$.

Field	$SU(3)$	$SU(2)$	$U(1)_Y$	$U(1)_B$	$U(1)_L$
Ψ_L	**1**	**2**	$\pm\frac{1}{2}$	$-\frac{3}{2}$	$-\frac{3}{2}$
η_R	**1**	**1**	± 1	$-\frac{3}{2}$	$-\frac{3}{2}$
χ_R	**1**	**1**	0	$-\frac{3}{2}$	$-\frac{3}{2}$
Ψ_R	**1**	**2**	$\pm\frac{1}{2}$	$+\frac{3}{2}$	$+\frac{3}{2}$
η_L	**1**	**1**	± 1	$+\frac{3}{2}$	$+\frac{3}{2}$
χ_L	**1**	**1**	0	$+\frac{3}{2}$	$+\frac{3}{2}$
S_{BL}	**1**	**1**	0	-3	-3
S_L	**1**	**1**	0	0	-2

and leptons as well as leptoquarks), and $\mathcal{L}_{\text{Yuk}}$ contains all Yukawa couplings of the SM quarks and leptons as well as of the new leptoquarks.

The scalar sector is defined by

$$\mathcal{L}_{\text{scalar}} = \left(D_\mu H\right)^\dagger D^\mu H + \left(D_\mu S_{BL}\right)^\dagger D^\mu S_{BL} + \left(D_\mu S_L\right)^\dagger D^\mu S_L - \mathcal{V}(H, S_{BL}, S_L) \quad (4.54)$$

with the scalar potential

$$\begin{aligned}\mathcal{V}(H, S_{BL}, S_L) = {} & m_1^2 H^\dagger H + m_2^2 S_{BL}^\dagger S_{BL} + m_3^2 S_L^\dagger S_L + \mu_1 (H^\dagger H)^2 + \mu_2 (S_{BL}^\dagger S_{BL})^2 \\ & + \mu_3 (S_L^\dagger S_L)^2 + \mu_4 (H^\dagger H)(S_{BL}^\dagger S_{BL}) + \mu_5 (H^\dagger H)(S_L^\dagger S_L) + \mu_6 (S_{BL}^\dagger S_{BL})(S_L^\dagger S_L). \quad (4.55)\end{aligned}$$

The general covariant derivative is given by (sum over repeated index a implied)

$$D_\mu = \partial_\mu + i g t^a W_\mu^a + i g' Y B_\mu + i g_L L B_\mu^L + i g_B B B_\mu^B. \quad (4.56)$$

For symmetry breaking, we use the parameterization of complex scalars in terms of real scalars and pseudoscalars:

$$H^0 = \frac{1}{\sqrt{2}}(v + h) + \frac{i}{\sqrt{2}} A, \quad (4.57)$$

$$S_L = \frac{1}{\sqrt{2}}(v_L + h_L) + \frac{i}{\sqrt{2}}A_L, \tag{4.58}$$

$$S_{BL} = \frac{1}{\sqrt{2}}(v_{BL} + h_{BL}) + \frac{i}{\sqrt{2}}A_{BL}. \tag{4.59}$$

The local baryonic and leptonic symmetries, $U(1)_B$ and $U(1)_L$, are broken by the VEV v_{BL} of S_{BL}, while the VEV v_L of S_L only contributes to the breaking of $U(1)_L$. After symmetry breaking, the two new physical scalars h_L and h_{BL} mix with each other and with the Standard Model Higgs boson to form three real scalars.

Ignoring the kinetic mixing with $U(1)_Y$, which has to be small, the kinetic terms of the gauge bosons are given by

$$\mathcal{L}_{\text{kin}}^{\text{gauge}} = \mathcal{L}_{\text{kin}}^{\text{SM gauge}} - \frac{1}{4}F_{B\,\mu\nu}F_B^{\mu\nu} - \frac{1}{4}F_{L\,\mu\nu}^{L}F_L^{\mu\nu} - \frac{\epsilon_{BL}}{2}F_{\mu\nu}^{B}F_L^{\mu\nu}, \tag{4.60}$$

where $\mathcal{L}_{\text{kin}}^{\text{SM gauge}}$ is the usual SM gauge boson term and

$$F_{\mu\nu}^{L} = \partial_\mu B_\nu^L - \partial_\nu B_\mu^L, \tag{4.61}$$

$$F_{\mu\nu}^{B} = \partial_\mu B_\nu^B - \partial_\nu B_\mu^B. \tag{4.62}$$

The kinetic terms of the fermions are given by

$$\begin{aligned}\mathcal{L}_{\text{kin}}^{\text{fermion}} = {} & i\overline{Q_L}\not{D}Q_L + i\overline{u_R}\not{D}u_R + i\overline{d_R}\not{D}d_R + i\overline{\ell_L}\not{D}\ell_L + i\overline{e_R}\not{D}e_R + i\overline{\nu_R}\not{D}\nu_R \\ & + i\overline{\Psi_L}\not{D}\Psi_L + i\overline{\Psi_R}\not{D}\Psi_R + i\overline{\eta_L}\not{D}\eta_L + i\overline{\eta_R}\not{D}\eta_R + i\overline{\chi_L}\not{D}\chi_L + i\overline{\chi_R}\not{D}\chi_R,\end{aligned} \tag{4.63}$$

where $\not{D} = \gamma_\mu D^\mu$. The corresponding covariant derivatives for each fermionic field can be obtained from Eq. (4.56).

The Yukawa interactions are given by

$$\begin{aligned}-\mathcal{L}_{\text{Yuk}} = {} & Y_d\overline{Q_L}Hd_R + Y_u\overline{Q_L}\tilde{H}u_R + Y_e\overline{l_L}He_R + h_1\overline{\Psi_L}H\eta_R + h_2\overline{\Psi_L}\tilde{H}\chi_R \\ & + h_3\overline{\Psi_R}H\eta_L + h_4\overline{\Psi_R}\tilde{H}\chi_L + \lambda_1\overline{\Psi_L}\Psi_R S_{BL} + \lambda_2\overline{\eta_R}\eta_L S_{BL} + \lambda_3\overline{\chi_R}\chi_L S_{BL} \\ & + a_1\overline{(\chi_L)^c}\chi_L S_{BL} + a_2\overline{(\chi_R)^c}\chi_R S_{BL}^\dagger + Y_\nu\overline{\ell_L}\tilde{H}\nu_R + \frac{\lambda_R}{2}\overline{(\nu_R)^c}\nu_R S_L + \text{h.c.},\end{aligned} \tag{4.64}$$

with $\tilde{H} = i\sigma_2 H^*$. Terms proportional to a_i $(i = 1, 2)$ give Majorana masses for the neutral fields after symmetry breaking, and all interactions proportional to the λ_i $(i = 1, 2, 3)$ couplings generate vector-like mass terms for the new fermions. Note that the quantum numbers of the Higgs fields S_L and S_{BL} that break $U(1)_B$ and $U(1)_L$ are totally fixed by these interactions, see Tab. 4.7 for their values. Thus, after symmetry breaking there will be interactions that violate baryon number by three units (therefore not allowing for proton decay) and/or violate lepton number by two or three units.

4.4.2 Neutrinos

In this model, it is very easy to realize the type I seesaw [14–18] mechanism (even at the weak scale) for neutrino masses by introducing the new Higgs S_L, see Tab. 4.7 for its quantum numbers. The interactions providing neutrino masses are given by

$$-\mathcal{L}_\nu = Y_\nu \overline{\ell}_L \tilde{H} \nu_R + \frac{\lambda_R}{2} \overline{(\nu_R)^c} \nu_R S_L + \text{h.c.} \tag{4.65}$$

After symmetry breaking, the mass terms for the neutrinos are

$$-\mathcal{L}_\nu^{\text{mass}} = \frac{1}{2} \left(\overline{\nu_L} M_\text{D} \nu_R + \overline{(\nu_R)^c} M_\text{D}^T (\nu_L)^c + \overline{(\nu_R)^c} M_R \nu_R \right) + \text{h.c.}, \tag{4.66}$$

where the Dirac mass term is given by

$$M_\text{D} = \frac{1}{\sqrt{2}} Y_\nu v \tag{4.67}$$

and the Majorana mass term of the right-handed neutrinos is given by

$$M_R = \frac{1}{\sqrt{2}} \lambda_R v_L. \tag{4.68}$$

4.4.3 Fermionic leptoquarks

After symmetry breaking, we have four neutral and four charged chiral fermions in the leptoquark sector. It is important to remember that the new fermions, since they have a different baryon number, do not couple to the SM fermions and one never generates new sources of flavor violation in the SM quark and lepton sectors.

Let us denote the leptoquark doublets as

$$\Psi_L = \begin{pmatrix} \psi_L^0 \\ \psi_L^- \end{pmatrix} \quad \text{and} \quad \Psi_R = \begin{pmatrix} \psi_R^0 \\ \psi_R^- \end{pmatrix}. \tag{4.69}$$

Then, the charged lepton mass term is

$$-\mathcal{L}_\text{mass}^\text{charged} = \overline{(\psi_L^- \ \eta_L)} \mathcal{M}_\text{charged} \begin{pmatrix} \eta_R \\ \psi_R^- \end{pmatrix} + \text{h.c.} \tag{4.70}$$

with

$$\mathcal{M}_\text{charged} = \frac{1}{\sqrt{2}} \begin{pmatrix} h_1 v & \lambda_1 v_{BL} \\ \lambda_2 v_{BL} & h_3 v \end{pmatrix}. \tag{4.71}$$

The neutral lepton mass term is

$$-\mathcal{L}_{\text{mass}}^{\text{neutral}} = \overline{\left(\psi_L^0\,(\chi_R)^c\,(\psi_R^0)^c\,\chi_L\right)}\mathcal{M}_{\text{neutral}}\begin{pmatrix}(\psi_L^0)^c\\ \chi_R\\ \psi_R^0\\ (\chi_L)^c\end{pmatrix} \tag{4.72}$$

with

$$\mathcal{M}_{\text{neutral}} = \frac{1}{\sqrt{2}}\begin{pmatrix}0 & h_2 v & \lambda_1 v_{BL} & 0\\ h_2 v & 2a_2 v_{BL} & 0 & \lambda_3 v_{BL}\\ \lambda_1 v_{BL} & 0 & 0 & h_4 v\\ 0 & \lambda_3 v_{BL} & h_4 v & 2a_1 v_{BL}\end{pmatrix}. \tag{4.73}$$

The mass matrices can be diagonalized via

$$\mathcal{M}_{\text{charged}}^{\text{diag}} = V_L^\dagger \mathcal{M}_{\text{charged}} V_R, \tag{4.74}$$

$$\mathcal{M}_{\text{neutral}}^{\text{diag}} = R^T \mathcal{M}_{\text{neutral}} R, \tag{4.75}$$

where V_L and V_R are unitary matrices and R is an orthogonal matrix.

4.4.4 Gauge sector

The mass matrix of the new gauge bosons in the basis $(B_\mu^B\ B_\mu^L)$ is given by

$$\mathcal{M}_{\text{gauge}}^2 = \begin{pmatrix}\frac{9}{2}g_B^2 v_{BL}^2 & \frac{9}{2}g_B g_L v_{BL}^2\\ \frac{9}{2}g_B g_L v_{BL}^2 & \frac{9}{2}g_L^2 v_{BL}^2 + 2v_L^2 g_L^2\end{pmatrix} \tag{4.76}$$

This matrix can be diagonalized by

$$\left(\mathcal{M}_{\text{gauge}}^{\text{diag}}\right)^2 = U^T \mathcal{M}_{\text{gauge}}^2 U, \tag{4.77}$$

where

$$U = \begin{pmatrix}\cos\theta & -\sin\theta\\ \sin\theta & \cos\theta\end{pmatrix}, \tag{4.78}$$

with

$$\tan 2\theta = \frac{9 g_B g_L v_{BL}^2}{\frac{9}{2}(g_B^2 - g_L^2)v_{BL}^2 - 2v_L^2 g_L^2}. \tag{4.79}$$

The new mass eigenstates are

$$\begin{pmatrix} Z'_{1\mu} \\ Z'_{2\mu} \end{pmatrix} = U^T \begin{pmatrix} B_\mu^B \\ B_\mu^L \end{pmatrix} \text{ or } \begin{pmatrix} B_\mu^B \\ B_\mu^L \end{pmatrix} = U \begin{pmatrix} Z'_{1\mu} \\ Z'_{2\mu} \end{pmatrix}. \tag{4.80}$$

4.4.5 Scalar sector

Minimizing the scalar potential in Eq. (4.55), we find the conditions

$$m_1^2 = -(\mu_1 v^2 + \frac{\mu_4}{2} v_{BL}^2 + \frac{\mu_5}{2} v_L^2), \tag{4.81}$$

$$m_2^2 = -(\mu_2 v_{BL}^2 + \frac{\mu_4}{2} v^2 + \frac{\mu_6}{2} v_L^2), \tag{4.82}$$

$$m_3^2 = -(\mu_3 v_L^2 + \frac{\mu_5}{2} v^2 + \frac{\mu_6}{2} v_{BL}^2). \tag{4.83}$$

The scalar potential is bounded from below if

$$\mu_1, \mu_2, \mu_3 \geq 0, \tag{4.84}$$

$$\frac{\mu_4}{2} + \sqrt{\mu_1 \mu_2} \geq 0, \tag{4.85}$$

$$\frac{\mu_5}{2} + \sqrt{\mu_1 \mu_3} \geq 0, \tag{4.86}$$

$$\frac{\mu_6}{2} + \sqrt{\mu_2 \mu_3} \geq 0, \tag{4.87}$$

$$\tag{4.88}$$

and

$$\det \begin{pmatrix} \mu_1 & \mu_4/2 & \mu_5/2 \\ \mu_4/2 & \mu_2 & \mu_6/2 \\ \mu_5/2 & \mu_6/2 & \mu_3 \end{pmatrix} \geq 0, \tag{4.89}$$

where the last condition is equivalent to

$$\frac{\mu_4}{2}\sqrt{\mu_3} + \frac{\mu_5}{2}\sqrt{\mu_2} + \frac{\mu_6}{2}\sqrt{\mu_1} + \sqrt{\mu_1 \mu_2 \mu_3} \geq 0. \tag{4.90}$$

After spontaneous symmetry breaking, the Higgs mass term is given by

$$\mathcal{L}^{h}_{\text{mass}} = \frac{1}{2}(h\, h_{BL}\, h_L)\mathcal{M}^2_{\text{Higgs}} \begin{pmatrix} h \\ h_{BL} \\ h_L \end{pmatrix} \tag{4.91}$$

with the CP-even Higgs mass matrix

$$\mathcal{M}^2_{\text{Higgs}} = \begin{pmatrix} 2\mu_1 v^2 & \mu_4 v v_{BL} & \mu_5 v v_L \\ \mu_4 v v_{BL} & 2\mu_2 v_{BL}^2 & \mu_6 v_{BL} v_L \\ \mu_5 v v_L & \mu_6 v_{BL} v_L & 2\mu_3 v_L^2 \end{pmatrix}. \tag{4.92}$$

4.4.6 Dark matter candidate

The lightest fermionic field in the new sector is automatically stable and a candidate for the cold dark matter of the Universe if it is electrically neutral. The dark matter stability is a consequence of the gauge symmetry and we do not need to impose any discrete symmetry by hand to obtain a stable particle. Indeed, after the breaking of the local $U(1)_L$ and $U(1)_B$ symmetries we obtain a $\mathcal{Z}_2$ symmetry as a remnant, under which the new fermions transform as

$$\mathcal{Z}_2 : \ \Psi_{L,R} \to -\Psi_{L,R},\ \eta_{L,R} \to -\eta_{L,R},\ \text{ and } \ \chi_{L,R} \to -\chi_{L,R}. \tag{4.93}$$

All other fields are even under this $\mathcal{Z}_2$. The DM candidate carries baryon number, such that we have "baryonic dark matter." The idea of having a DM candidate with baryon number was already discussed in the early papers for gauge theories of baryon and lepton numbers, see, e.g., Ref. [34].

The careful study of the properties of the dark matter candidate in this model is beyond the scope of this thesis. We cannot discuss the relic density calculations and the constraints coming from direct and indirect detection in detail. Let us nevertheless shortly mention how the direct detection constraints can be satisfied and the right relic density can be achieved. The dark matter candidate, Ψ_{DM}, couples to the new neutral gauge bosons in the theory, Z'_1 and Z'_2, and to the new scalars, h_L and h_{BL}. It will be possible to achieve the right annihilation cross section, and therefore the right relic density by using one of these resonances, e.g., a DM mass of

$$m_{\Psi_{\text{DM}}} \simeq \frac{1}{2} M_{Z'_i}. \tag{4.94}$$

DM direct detection will also be possible through the couplings of the DM to the Z and the Z'_i. There is quite some freedom in choosing the parameters of the model, so there should be no problem to satisfy the experimental constraints. A detailed analysis of the DM sector of this model is work in progress.

An analysis of the DM sector of a simplified version of this model was performed recently together with Pavel Fileviez Pérez in Ref. [50]. We only considered baryon number, and therefore used the gauge group

$$G_B = SU(3)_C \otimes SU(2)_L \otimes U(1)_Y \otimes U(1)_B. \tag{4.95}$$

We discussed the case of a SM singlet-like Dirac fermion as a DM candidate, which carries baryon number and therefore couples to the new gauge boson Z_B related to baryon number. The new gauge Z_B boson also couples to the quarks, and this is crucial for the relic density and for direct detection: the DM particle can annihilate into two SM quarks via the exchange of Z_B, and the same interaction allows for direct detection of the DM particles. See Ref. [50] for a detailed discussion of the DM relic density and direct detection in this simplified model. A relevant result of the numerical survey is that in this case one does not have to be on the resonance to achieve the correct relic density and consistent scenarios with the results of DM direct detection experiments can easily be achieved. Additionally, this model only has four free parameters and is therefore fully testable by comparing dark matter and collider experiments.

Related work exists in the literature: a discussion of the DM candidate in a model with vector-like leptons can be found in Ref. [162], where also the impact of the new fields on the SM Higgs decays and the constraints from electroweak precision observables were studied. A recent publication uses a model similar to ours, however only taking into account gauged lepton number and ignoring baryon number [163]. They obtain a Dirac electroweak (mostly) singlet neutrino as a DM candidate and show its viability. Of course, the phenomenology of the model presented here is quite different from theirs, due to the baryon number that our DM candidate carries.

4.4.7 Baryon and lepton number violating processes

The new Higgs field S_{BL} breaks baryon number by three units, therefore non-renormalizable operators that cause proton decay do not occur. Thus, there is no need to postulate a large desert between the electroweak scale and the scale where baryon number violation occurs. The field S_L breaks lepton number in two units, so one generates a $\Delta L = 2$ Majorana mass term for the light neutrinos as we discussed before, and we have the usual constraints coming from neutrinoless double beta decay; see the discussion of this experimental test of lepton number violation in Chapter 3 of

this thesis. The lowest-dimensional B and L violating operator that contains only SM fermions after symmetry breaking is

$$\mathcal{O}_{19} = \frac{c_{19}}{\Lambda^{15}} \left(u_R u_R d_R e_R\right)^3 S_{BL}. \tag{4.96}$$

It has dimension nineteen, and therefore B and L violating processes are strongly suppressed even if the cut-off Λ of the theory is quite low.

4.5 Summary and outlook

In this chapter, we proposed viable models for gauging B and L in an anomaly-free theory and spontaneously breaking these gauge symmetries at a low scale (e.g., TeV scale). We found that using leptoquarks, i.e., particles carrying baryon and lepton numbers, one can cancel all anomalies and generate masses for all fields in the theory. Various setups were briefly introduced, and the simplest scenario with colorless leptoquarks was discussed in some detail, by presenting the full Lagrangian of the model and discussing some phenomenology. In this setup, there is a fermionic dark matter candidate whose stability is an automatic consequence of the breaking of the gauge symmetry. The new leptoquarks do not induce flavor violation and after symmetry breaking one only generates $\Delta L = \pm 2, \pm 3$ and $\Delta B = \pm 3$ interactions. Therefore, non-renormalizable operators that cause proton (and baryon number violating neutron) decay do not occur and there is no need to assume a large desert between the electroweak scale and the scale where we can understand the origin of the baryon number violating interactions. Due to limitations of time and space, a complete survey of the model is beyond the scope of this thesis and left for future investigation.

We outlined that a viable DM candidate can arise in this model, which is a fermion that carries baryon number. Due to the freedom in parameter space of the model, it should be possible to achieve the correct relic density and be in agreement with direct detection experiments. Of course, the collider phenomenology and the predictions for indirect DM detection of this model should also be investigated, and we plan to do so in the future.

Potentially more difficult is the generation of a cosmological baryon excess because B and L are broken at a low scale in this model. It has however been shown before [35] that it is in principle possible to generate a non-zero baryon asymmetry in such models even though B and L are broken at a low scale, e.g., by making use of accidental global symmetries of the renormalizable couplings in the model.

Chapter 5

A left–right symmetric theory for baryon and lepton numbers

In this chapter, we extend the idea of gauging baryon and lepton numbers as independent symmetries to left–right symmetric models. We present solutions of the equations that ensure the cancelation of the relevant anomalies for the gauge group

$$G_{LR}^{BL} = SU(2)_L \otimes SU(2)_R \otimes U(1)_B \otimes U(1)_L \otimes \mathcal{P}, \tag{5.1}$$

where the QCD gauge group $SU(3)_C$ is omitted for simplicity and $\mathcal{P}$ is the discrete left–right parity. We discuss the minimal model based on this gauge group in detail and show that the new leptoquark fields introduced to obtain an anomaly-free theory also generate neutrino masses via the type III seesaw mechanism. The spectrum of neutrinos and some phenomenological aspects of the model are presented. Without assuming any extra symmetries, the model contains two light sterile neutrinos.

Just as in Chapter 4, where we extended the Standard Model gauge group by a factor $U(1)_B \otimes U(1)_L$, the latter symmetries can be broken at a low scale in this setup. There is no need to postulate the existence of a large desert between the left–right scale and the high scale where one can understand the origin of higher-dimensional operators inducing baryon number violating processes such as proton decay. The breaking scale of B and L can be as low as a few TeV, such that there is hope that this theory may be tested at the LHC. Another of extending the discussion to left–right symmetric theories is that the spontaneous breaking of parity can be related to the spontaneous breaking of baryon and lepton numbers.

The outline of the chapter is as follows: to set the grounds for our new model, we start this chapter with a short discussion of left–right symmetric theories in Section 5.1, focussing on the generation of neutrino masses. Then, in Section 5.2, we discuss the anomalies that have to be canceled to gauge the group G_{LR}^{BL}. We review possible solutions regarding the additional particle content, and present a new solution with fermionic triplets, which have exactly the right quantum numbers to generate neutrino masses via the type III seesaw mechanism. We discuss the implementation of the

type III seesaw mechanism in this setup and the resulting spectrum of neutrinos in Section 5.3. Further aspects of our solution are presented in Section 5.4, and we summarize the main results of this chapter in Section 5.5.

The original results presented in this chapter were published in collaboration with Pavel Fileviez Pérez and Manfred Lindner in [45].

5.1 Left–right symmetric theories

Left–right symmetric theories [14, 15, 23, 38–41] are very appealing candidates for physics beyond the SM. These theories provide a natural framework to understand the maximal parity violation, i.e., the $V - A$ structure of the weak interaction observed at low energy, as a result of the spontaneous breaking of the gauge group [39–41]. Later versions of these theories [14, 15, 23] additionally connect the spontaneous breakdown of parity to the origin of neutrino masses.

In general, one cannot predict the scale above which the left–right symmetry is restored, which also sets the mass scale of the right-handed gauge bosons W_R. If this scale is as low as a few TeV, this can lead to very interesting signals at the LHC. In particular, if the right-handed neutrinos are Majorana particles and lighter than the right-handed gauge bosons, one could observe the "smoking gun" signal of same-sign dileptons plus two jets without missing energy [164],

$$W_R \longrightarrow \ell^\pm \ell^\pm jj. \tag{5.2}$$

For recent phenomenological studies of left–right symmetric models in the context of LHC physics, see, e.g., Refs. [165–167]. In particular, LHC searches constrain the masses of W_R to be of the order TeV or larger, see the Particle Data Group for a listing of recent bounds [57].

5.1.1 General framework

The original left–right symmetric theories [38–40] are based on the gauge group

$$G_{LR} = SU(2)_L \otimes SU(2)_R \otimes U(1)_{B-L}, \tag{5.3}$$

omitting the QCD gauge group $SU(3)_C$ for simplicity. As before, $B - L$ is baryon minus lepton number. Quarks and leptons are organized in doublets of $SU(2)_L$ and $SU(2)_R$ with the following transformation properties under G_{LR}:

$$Q_L = \begin{pmatrix} u_L \\ d_L \end{pmatrix} \sim \left(\mathbf{2}, \mathbf{1}, \frac{1}{3}\right), \qquad Q_R = \begin{pmatrix} u_R \\ d_R \end{pmatrix} \sim \left(\mathbf{1}, \mathbf{2}, \frac{1}{3}\right), \tag{5.4}$$

$$\ell_L = \begin{pmatrix} \nu_L \\ e_L \end{pmatrix} \sim (\mathbf{2}, \mathbf{1}, -1)\,, \qquad \ell_R = \begin{pmatrix} \nu_R \\ e_R \end{pmatrix} \sim (\mathbf{1}, \mathbf{2}, -1)\,. \tag{5.5}$$

The left–right symmetry directly predicts the existence of right-handed neutrinos and allows for the implementation of neutrino masses in a simple way. In this sense, massive neutrinos are a prediction of left–right symmetric models.

Under the discrete left–right parity $\mathcal{P}$, the fields transform as

$$Q_L \overset{\mathcal{P}}{\longleftrightarrow} Q_R \text{ and } \ell_L \overset{\mathcal{P}}{\longleftrightarrow} \ell_R, \tag{5.6}$$

and electric charge is defined as

$$Q = T_{3L} + T_{3R} + \frac{B-L}{2}, \tag{5.7}$$

where T_{3L} and T_{3R} are the isospin under $SU(2)_L$ and $SU(2)_R$, respectively.

Fermion masses can be generated if a Higgs bidoublet is introduced

$$\Phi = \begin{pmatrix} \phi_1^0 & \phi_2^+ \\ \phi_1^- & \phi_2^0 \end{pmatrix} \sim (\mathbf{2}, \mathbf{2}, 0)\,, \tag{5.8}$$

which transforms as

$$\Phi \overset{\mathcal{P}}{\longleftrightarrow} \Phi^\dagger \tag{5.9}$$

under the left–right parity transformation. This allows for the Yukawa interactions

$$-\mathcal{L}_Y = \overline{Q_L}\left(Y_1\Phi + Y_2\tilde{\Phi}\right) Q_R + \overline{\ell_L}\left(Y_3\Phi + Y_4\tilde{\Phi}\right)\ell_R + \text{h.c.}, \tag{5.10}$$

where

$$\tilde{\Phi} = \sigma_2\Phi^*\sigma_2 \tag{5.11}$$

again is a bidoublet. After the bidoublet Φ obtains its VEV

$$\langle\Phi\rangle = \begin{pmatrix} v_1 & 0 \\ 0 & v_2 \end{pmatrix}, \tag{5.12}$$

with $v_1^2 + v_2^2 = (174\,\text{GeV})^2$, we find the fermion mass matrices to be

$$M_u = Y_1 v_1 + Y_2 v_2^*, \tag{5.13}$$

$$M_d = Y_1 v_2 + Y_2 v_1^*, \tag{5.14}$$

$$M_e = Y_3 v_2 + Y_4 v_1^*, \tag{5.15}$$

$$M_\nu^D = Y_3 v_1 + Y_4 v_2^*. \tag{5.16}$$

In the limit $v_2 \ll v_1$, where the mixing between the left-handed and right-handed charged gauge bosons is small[1] (see the mass matrix of the charged gauge bosons below in Eq. (5.22)), this allows to have small Dirac neutrino masses only for tiny couplings Y_3. This is somewhat similar to the SM when right-handed neutrinos are introduced with tiny Yukawa couplings and is of course not fully satisfying from a theoretical point of view. We fix this issue in the next subsection, where the small neutrino masses are generated by the seesaw mechanism.

To complete symmetry breaking, additional Higgs fields have to be introduced

$$H_L = \begin{pmatrix} h_L^+ \\ h_L^0 \end{pmatrix} \sim (\mathbf{2}, \mathbf{1}, 1)\,, \tag{5.17}$$

$$H_R = \begin{pmatrix} h_R^+ \\ h_R^0 \end{pmatrix} \sim (\mathbf{1}, \mathbf{2}, 1)\,. \tag{5.18}$$

It can be shown that for some range of coupling parameters, the absolute minimum of the left–right symmetric scalar potential can found to be [41]

$$\langle H_L \rangle = \begin{pmatrix} 0 \\ 0 \end{pmatrix}, \text{ and } \langle H_R \rangle = \begin{pmatrix} 0 \\ v_R/\sqrt{2} \end{pmatrix}, \tag{5.19}$$

together with Eq. (5.12), such that the breaking of gauge symmetry leads to spontaneous parity violation. The breaking sequence is therefore

$$G_{LR} \xrightarrow{\langle H_R \rangle} SU(2)_L \otimes U(1)' \xrightarrow{\langle \Phi \rangle} U(1)_{\mathrm{EM}}, \tag{5.20}$$

where the generator of the $U(1)'$ is

$$\frac{1}{2} Y' = T_{3R} + \frac{1}{2}(B - L). \tag{5.21}$$

After symmetry breaking, the mass matrix of the charged gauge bosons in the basis $(W_L^\pm, W_R^\pm)$ is given by [41]

$$\mathcal{M}_\pm^2 = \begin{pmatrix} \frac{g^2}{4}\left(v_1^2 + v_2^2\right) & -\frac{g^2}{2} v_1 v_2 \\ -\frac{g^2}{2} v_1 v_2 & \frac{g^2}{4}\left(v_1^2 + v_2^2 + v_R^2\right) \end{pmatrix} \tag{5.22}$$

[1] Defining the lighter mass eigenstate as $W_1 = W_L \cos\xi - W_R \sin\xi$, the mixing angle can be constrained to be $\xi < 10^{-2}$ [57].

where $g_L = g_R \equiv g$, with the equality of the gauge couplings being a consequence of the left–right symmetry. The VEV v_R, which is much larger than v_1 and v_2, gives mass to the right-handed gauge bosons, so the absence of right-handed weak currents in low energy experiments can easily be understood due to the large mass of these gauge bosons.

5.1.2 Majorana neutrino masses

It is very easy to incorporate the seesaw mechanism into left–right symmetric models, such that there is an explanation for the tiny neutrino masses, beyond a small coupling chosen by nature. In extensions of the original left–right symmetric theories, neutrino masses are generated through a combination of type I and type II seesaw mechanisms [14, 15, 23]. Then, these theories connect the maximal violation of parity that is observed in low-energy processes to the smallness of neutrino masses. We explain this in more detail here.

Instead of introducing left- and right-handed Higgs doublets H_L and H_R that were used before to break left–right symmetry in the above discussion, see Eqs. (5.17) and (5.18), one can also introduce two Higgs triplets [14, 15, 23]

$$\Delta_L = \begin{pmatrix} \frac{1}{\sqrt{2}}\delta_L^+ & \delta_L^{++} \\ \delta_L^0 & -\frac{1}{\sqrt{2}}\delta_L^+ \end{pmatrix} \sim (\mathbf{3},\mathbf{1},2)\,, \tag{5.23}$$

$$\Delta_R = \begin{pmatrix} \frac{1}{\sqrt{2}}\delta_R^+ & \delta_R^{++} \\ \delta_R^0 & -\frac{1}{\sqrt{2}}\delta_R^+ \end{pmatrix} \sim (\mathbf{1},\mathbf{3},2)\,, \tag{5.24}$$

which transform under the left–right parity as

$$\Delta_L \overset{\mathcal{P}}{\longleftrightarrow} \Delta_R. \tag{5.25}$$

The relevant interactions of the neutrinos are

$$-\mathcal{L}_\nu = \overline{\ell}_L \left(Y_3\Phi + Y_4\tilde{\Phi}\right)\ell_R + \lambda_\Delta\left(\ell_L^T C i\sigma_2 \Delta_L \ell_L + \ell_R^T C i\sigma_2 \Delta_R \ell_R\right) + \text{h.c.} \tag{5.26}$$

After the triplets have obtained the VEVs

$$\langle \delta_{L,R}^0 \rangle = \frac{1}{\sqrt{2}}\kappa_{L,R}, \tag{5.27}$$

we find the neutrino mass matrix to be

$$\mathcal{M}_\nu = \begin{pmatrix} \sqrt{2}\lambda_\Delta \kappa_L & M_D^* \\ M_D^\dagger & -\sqrt{2}\lambda_\Delta^\dagger \kappa_R^* \end{pmatrix} \tag{5.28}$$

in the basis $(\nu_L, (\nu_R)^c)$. Diagonalizing this matrix in the seesaw limit

$$\lambda_\Delta \kappa_R \gg M_D, \tag{5.29}$$

one finds the Majorana mass matrix for the three light active neutrinos to be

$$M_{\nu_L} = \sqrt{2}\lambda_\Delta \kappa_L - M_D^\dagger (\sqrt{2}\lambda_\Delta^\dagger \kappa_R^*)^{-1} M_D^*. \tag{5.30}$$

The given VEVs are the most general ones in agreement with electromagnetic gauge invariance. It can be shown that this solution corresponds to an absolute minimum of the left–right symmetric potential, where the VEVs are related by [23]

$$\kappa_L = \gamma \frac{v_1^2}{\kappa_R}, \tag{5.31}$$

with γ being a constant to be calculated from the scalar potential.

Thus, the smallness of neutrino masses can directly be understood from a large value of κ_R (or, equivalently, m_{W_R}). Especially, when $\kappa_R \to \infty$, the masses of the light neutrinos vanish. This is the promised connection between tiny neutrino masses and maximal parity violation [15].

The type III seesaw also can be nicely implemented in the left–right symmetric context, see Ref. [70]. We do so in the next section, when we gauge baryon and lepton numbers individually, which forces us to introduce fermionic triplets that just have the right quantum numbers to give Majorana masses to the neutrinos.

5.2 Gauging baryon and lepton numbers in left–right symmetric models

5.2.1 Anomaly cancelation

Now, we go beyond the original left–right symmetric setup and define a simple theory where we can investigate the spontaneous breaking of baryon and lepton numbers as well as parity based on the gauge group G_{LR}^{BL} given in Eq. (5.1).

Under G_{LR}^{BL}, the quarks and leptons transform as [compare to the transformation properties under G_{LR} given in Eqs. (5.4) and (5.5)]

$$Q_L = \begin{pmatrix} u_L \\ d_L \end{pmatrix} \sim (\mathbf{2}, \mathbf{1}, 1/3, 0)\,, \qquad Q_R = \begin{pmatrix} u_R \\ d_R \end{pmatrix} \sim (\mathbf{1}, \mathbf{2}, 1/3, 0)\,, \tag{5.32}$$

$$\ell_L = \begin{pmatrix} \nu_L \\ e_L \end{pmatrix} \sim (\mathbf{2}, \mathbf{1}, 0, 1)\,, \qquad \ell_R = \begin{pmatrix} \nu_R \\ e_R \end{pmatrix} \sim (\mathbf{1}, \mathbf{2}, 0, 1)\,. \tag{5.33}$$

As before, under the left–right discrete parity, the quarks and leptons transform as

$$Q_L \overset{\mathcal{P}}{\longleftrightarrow} Q_R \text{ and } \ell_L \overset{\mathcal{P}}{\longleftrightarrow} \ell_R \tag{5.34}$$

and the electric charge is defined as in Eq. (5.7).

The set of non-trivial anomalies that have to be canceled in order to be able to define an anomaly-free theory is quite small in this setup. As always, triangle diagrams containing only one $SU(3)_C$ or only one $SU(2)_{L,R}$ current vanish, due to a vanishing trace of the corresponding representation matrices. Additionally, the fermionic fields presented before are either in a non-trivial representation of $SU(2)_L$ or $SU(2)_R$, such that mixed anomalies between these gauge groups cannot play a role. Due to the manifest left–right symmetry of the theory, any further anomaly not containing exactly two $SU(2)_L$ or exactly two $SU(2)_R$ currents also vanishes. This means that (see Tab. 4.2 in Chapter 4)

$$\mathcal{A}_1\left(SU(3)_C^2 \otimes U(1)_B\right) = \mathcal{A}_7\left(SU(3)_C^2 \otimes U(1)_L\right) = 0, \tag{5.35}$$

and that also the purely baryonic, purely leptonic, and mixed anomalies vanish (see also Tab. 4.2 in Chapter 4):

$$\mathcal{A}_5\left(\text{gravity}^2 \otimes U(1)_B\right) = \mathcal{A}_{11}\left(\text{gravity}^2 \otimes U(1)_L\right) = 0, \tag{5.36}$$
$$\mathcal{A}_6\left(U(1)_B^3\right) = \mathcal{A}_{12}\left(U(1)_L^3\right) = 0, \tag{5.37}$$
$$\mathcal{A}_{13}\left(U(1)_B^2 \otimes U(1)_L\right) = \mathcal{A}_{14}\left(U(1)_L^2 \otimes U(1)_B\right) = 0. \tag{5.38}$$

Thus, the only non-trivial anomalies that have to be canceled by new fermionic degrees of freedom are

$$\mathcal{A}_1^{LR}\left(SU(2)_L^2 \otimes U(1)_B\right) = 3/2, \tag{5.39}$$
$$\mathcal{A}_2^{LR}\left(SU(2)_L^2 \otimes U(1)_L\right) = 3/2, \tag{5.40}$$
$$\mathcal{A}_3^{LR}\left(SU(2)_R^2 \otimes U(1)_B\right) = -3/2, \tag{5.41}$$
$$\mathcal{A}_4^{LR}\left(SU(2)_R^2 \otimes U(1)_L\right) = -3/2. \tag{5.42}$$

5.2.2 Solutions in the literature

Some solutions for the cancelation of these anomalies were studied in [152], where the gauge group G_{LR}^{BL} was considered for the first time. The aim of the authors of [152] was to discuss solutions that contain equal numbers of singlets and triplets under $SU(3)_C$, similar to the conventional fermion families. They discussed solutions where the fermions either have baryon or lepton number (mirror fermions and fermions in different representations of $SU(2)_{L,R}$) and also solutions where the new fermions have

both baryon and lepton numbers. Of course, these solutions are motivated by the family structure found in the SM quarks and leptons, and are not minimal in the sense of the number of fields necessary for a cancelation of all anomalies.

Additionally, they found two very simple solutions (for n families of conventional quarks and leptons). Two singlets F_L^1 and F_R^1 of $SU(3)_C$ that transform under G_{BL}^{LR} as

$$F_L^1 \sim (\mathbf{2}, \mathbf{1}, -n, -n)\,, \tag{5.43}$$

$$F_R^1 \sim (\mathbf{1}, \mathbf{2}, -n, -n)\,, \tag{5.44}$$

or two triplets F_L^3 and F_R^3 of $SU(3)_C$ that transform under G_{BL}^{LR} as

$$F_L^3 \sim \left(\mathbf{2}, \mathbf{1}, -\frac{n}{3}, -\frac{n}{3}\right), \tag{5.45}$$

$$F_R^3 \sim \left(\mathbf{1}, \mathbf{2}, -\frac{n}{3}, -\frac{n}{3}\right). \tag{5.46}$$

This of course can be generalized to exotic fermions transforming as a representation $\boldsymbol{N}$ of $SU(3)_C$. Then,

$$F_L^N \sim \left(\mathbf{2}, \mathbf{1}, -\frac{n}{N}, -\frac{n}{N}\right), \tag{5.47}$$

$$F_R^N \sim \left(\mathbf{1}, \mathbf{2}, -\frac{n}{N}, -\frac{n}{N}\right). \tag{5.48}$$

These solutions are more minimal than the ones mentioned before with an equal number of triplets and singlets under $SU(3)_C$. Yet, we do not consider them in more detail, because neutrinos are Dirac particles in this setup. Thus, the nice implementation of the seesaw mechanism that is characteristic for left–right symmetric models is not possible and one would only rely on tiny Yukawa couplings for light neutrinos. We thus opt for another solution that will allow for the implementation of the type III seesaw mechanism, which we present in the following subsection.

5.2.3 New solution: fermionic leptoquarks

Let us discuss a different solution in this subsection, sticking to extra fields that do not feel the strong interaction. The introduction of the triplet fields

$$\rho_L = \frac{1}{2}\begin{pmatrix} \rho_L^0 & \sqrt{2}\rho_L^+ \\ \sqrt{2}\rho_L^- & -\rho_L^0 \end{pmatrix} \sim (\mathbf{3}, \mathbf{1}, B, L)\,, \tag{5.49}$$

$$\rho_R = \frac{1}{2}\begin{pmatrix} \rho_R^0 & \sqrt{2}\rho_R^+ \\ \sqrt{2}\rho_R^- & -\rho_R^0 \end{pmatrix} \sim (\mathbf{1}, \mathbf{3}, B, L)\,, \tag{5.50}$$

allows for a cancelation of all four anomalies $\mathcal{A}_i^{LR}$, and due the left–right symmetry does not introduce non-zero values for any of the other relevant ones. Again, anomaly conditions allow for a unique determination of the values of B and L. Consider

$$\mathcal{A}_1^{LR}\left(SU(2)_L^2 \otimes U(1)_B\right) = \frac{3}{2} + 2B \stackrel{!}{=} 0, \tag{5.51}$$

where the factor 2 comes from the trace over the matrices of the adjoint representation. Thus we obtain

$$B = -\frac{3}{4} \text{ and } L = -\frac{3}{4}, \tag{5.52}$$

using a similar calculation for the lepton numbers L. Thus, the full transformation properties of the new fields are

$$\rho_L \sim \left(\mathbf{3}, \mathbf{1}, -\frac{3}{4}, -\frac{3}{4}\right), \tag{5.53}$$

$$\rho_R \sim \left(\mathbf{1}, \mathbf{3}, -\frac{3}{4}, -\frac{3}{4}\right). \tag{5.54}$$

Under the discrete left–right parity, the new fields transform as

$$\rho_L \stackrel{\mathcal{P}}{\longleftrightarrow} \rho_R. \tag{5.55}$$

These leptoquarks introduced for anomaly cancelation have just the right quantum numbers to generate neutrino masses through the type III seesaw mechanism in this left–right setup, see Ref. [70] for a first implementation of this without gauging baryon and lepton numbers. Let us note here that even in the SM, the introduction of a triplet fermion per family leads to an anomaly-free $U(1)_X$ symmetry that may be gauged [168, 169]. This is somewhat similar to the anomaly-free $U(1)_{B-L}$ in the SM with three right-handed neutrinos.

This solution is the simplest left–right symmetric theory based on the gauge group G_{LR}^{BL} that allows us to generate masses for all fields and we discuss its phenomenology in more detail in the following sections.

5.3 Neutrino masses via the type III seesaw mechanism

Let us now discuss the implementation of the type III seesaw for the solution presented before. This is similar to the implementation given in Ref. [70]. Introducing the Higgs fields

$$\Phi = \begin{pmatrix} \phi_1^0 & \phi_2^+ \\ \phi_1^- & \phi_2^0 \end{pmatrix} \sim (\mathbf{2}, \mathbf{2}, 0, 0), \tag{5.56}$$

$$H_L = \begin{pmatrix} h_L^+ \\ h_L^0 \end{pmatrix} \sim \left(\mathbf{2}, \mathbf{1}, \frac{3}{4}, -\frac{1}{4}\right), \tag{5.57}$$

$$H_R = \begin{pmatrix} h_R^+ \\ h_R^0 \end{pmatrix} \sim \left(\mathbf{1}, \mathbf{2}, \frac{3}{4}, -\frac{1}{4}\right), \tag{5.58}$$

$$S_{BL} \sim \left(\mathbf{1}, \mathbf{1}, \frac{3}{2}, \frac{3}{2}\right), \tag{5.59}$$

the relevant interactions are

$$\begin{aligned} -\mathcal{L} \supset\ & \overline{\ell_L}\left(Y_3\Phi + Y_4\tilde{\Phi}\right)\ell_R + \lambda_D\left(\ell_L^T C i\sigma_2 \rho_L H_L\ +\ \ell_R^T C i\sigma_2 \rho_R H_R\right) \\ & + \lambda_\rho\ \mathrm{Tr}\left(\rho_L^T C \rho_L + \rho_R^T C \rho_R\right) S_{BL}\ +\ \text{h.c.}, \end{aligned} \tag{5.60}$$

and, as always, $\tilde{\Phi} = \sigma_2 \Phi^* \sigma_2$. Notice that the Higgs sector is quite simple. Under the left–right parity the Higgs fields transform as

$$\Phi \overset{\mathcal{P}}{\longleftrightarrow} \Phi^\dagger, H_L \overset{\mathcal{P}}{\longleftrightarrow} H_R. \tag{5.61}$$

For spontaneous symmetry breaking, the Higgs fields obtain the VEVs

$$\langle H_L \rangle = \begin{pmatrix} 0 \\ v_L/\sqrt{2} \end{pmatrix}, \langle H_R \rangle = \begin{pmatrix} 0 \\ v_R/\sqrt{2} \end{pmatrix}, \tag{5.62}$$

$$\langle \Phi \rangle = \begin{pmatrix} v_1 & 0 \\ 0 & v_2 \end{pmatrix}, \langle S_{BL} \rangle = v_{BL}/\sqrt{2}. \tag{5.63}$$

The hierarchy of the VEVs, and therefore the symmetry breaking sequence, is determined by the constraints on the model. v_R is giving mass to the right-handed gauge bosons, which have to be heavy (beyond TeV scale). H_L and Φ have $SU(2)_L$ quantum numbers and will therefore participate in electroweak symmetry breaking. The sum of their VEVs can therefore not be beyond the electroweak scale, and we have to fulfill

$$v_1^2 + v_2^2 + \frac{1}{2} v_L^2 = (174\,\mathrm{GeV})^2. \tag{5.64}$$

Furthermore, because Φ directly gives mass to the charged leptons à la SM Higgs,

$$v_L \ll v_1, v_2. \tag{5.65}$$

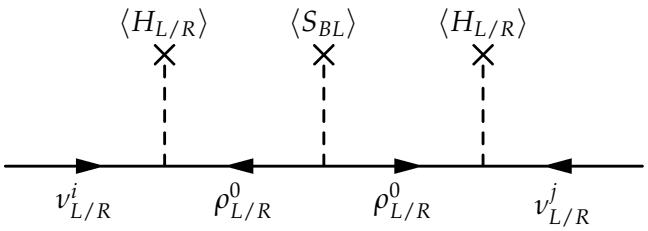

Figure 5.1: Type III seesaw for the left-handed and right-handed neutrinos.

A combination of all these constraints directly leads to parity violation

$$v_L \ll v_R. \tag{5.66}$$

Finally, v_{BL} gives mass to ρ_L and ρ_R, see Eq. (5.60), which have to be a hundred GeV or larger; for a recent discussion of these fields at the LHC, see Ref. [69]. In our setup, we want to use type II seesaw mechanism also for the right-handed neutrinos, see Fig. 5.1, such that we have to demand

$$v_{BL} \gg v_R. \tag{5.67}$$

After spontaneous symmetry breaking, we can integrate out ρ^0_L and ρ^0_R and obtain the relevant Lagrangian for the neutrino masses

$$-\mathcal{L}_\nu = M^D_\nu \overline{\nu_L} \nu_R - \frac{1}{2} M^{III}_{\nu_L} \nu^T_L C \nu_L - \frac{1}{2} M^{III}_{\nu_R} \nu^T_R C \nu_R + \text{h.c.}, \tag{5.68}$$

where the masses are given by

$$\left(M^D_\nu\right)^{ij} = Y^{ij}_3 v_1 + Y^{ij}_4 v_2, \tag{5.69}$$

$$\left(M^{III}_{\nu_L}\right)^{ij} = \frac{\lambda^i_D \lambda^j_D v_L^2}{4\sqrt{2}\lambda_\rho v_{BL}}, \tag{5.70}$$

$$\left(M^{III}_{\nu_R}\right)^{ij} = \frac{\lambda^i_D \lambda^j_D v_R^2}{4\sqrt{2}\lambda_\rho v_{BL}}. \tag{5.71}$$

The Feynman diagrams of these mass terms are given in Fig. 5.1. Both mass terms $M^{III}_{\nu_L}$ and $M^{III}_{\nu_R}$ are generated through the type III seesaw mechanism and there is a simple relation between them:

$$M^{III}_{\nu_L} = \frac{v_L^2}{v_R^2} M^{III}_{\nu_R}. \tag{5.72}$$

Now, parity violation, $v_L \ll v_R$, tells us that

$$M^{III}_{\nu_L} \ll M^{III}_{\nu_R}. \tag{5.73}$$

This is the first consequence of having the type III seesaw mechanism in this context. The second consequence is that the Majorana mass matrix for the right-handed neutrinos given by $M_{\nu_R}^{III}$ has rank one. Therefore, only one of the three right-handed neutrinos will have a non-zero Majorana mass. We can rotate the right-handed neutrinos via $\nu_R \to U_R \nu_R$, and obtain

$$-\mathcal{L}_\nu = \tilde{M}_\nu^D \overline{\nu_L} \nu_R - \frac{1}{2} M_{\nu_L}^{III} \nu_L^T C \nu_L - \frac{1}{2} M_R \nu_R^{3T} C \nu_R^3 + \text{h.c.}, \tag{5.74}$$

where $\tilde{M}_\nu^D = M_\nu^D U_R$. Then, ν_R^3 will generate an additional Majorana mass for the left-handed neutrinos via type I seesaw, such that we arrive at

$$-\mathcal{L}_\nu = -\frac{1}{2} M_{\nu_L}^{LL} \nu_L^T C \nu_L + \left(\tilde{M}_\nu^D\right)^{i\alpha} \overline{\nu_L^i} \nu_R^\alpha + \text{h.c.}, \tag{5.75}$$

where $\alpha = 1, 2$, after integrating out ν_R^3. The mass of the left-handed neutrinos is given by

$$\left(M_{\nu_L}^{LL}\right)^{ij} = \left(M_{\nu_L}^{III}\right)^{ij} - \frac{1}{M_R} \left(\tilde{M}_\nu^D\right)^{i3} \left(\tilde{M}_\nu^D\right)^{j3}. \tag{5.76}$$

We can go to the basis where the matrix $M_{\nu_L}^{LL}$ is diagonal and write the mass matrix for the light neutrinos in the theory as

$$\mathcal{M}_\nu^{3+2} = \begin{pmatrix} 0 & 0 & 0 & m_D^1 & m_D^2 \\ 0 & m_1 & 0 & m_D^3 & m_D^4 \\ 0 & 0 & m_2 & m_D^5 & m_D^6 \\ m_D^1 & m_D^3 & m_D^5 & 0 & 0 \\ m_D^2 & m_D^4 & m_D^6 & 0 & 0 \end{pmatrix}, \tag{5.77}$$

which is of full rank and leads to five massive states. This matrix is similar to the neutrino mass matrix discussed in a SUSY setup in Refs. [170, 171].

This simple matrix defines the mixing between the SM active neutrinos and the two extra sterile neutrinos. The theory does not predict the masses in the above matrix, but one expects that the two extra sterile neutrinos can have mass below or at the eV scale. See Ref. [172] for the constraints on sterile neutrinos with mass around the eV scale. In the interesting limit $m_D^i \to 0$, the sterile neutrinos decouple and one of the active neutrinos is massless.

5.4 Further aspects of the model

After having implemented the type III seesaw mechanism and discussed the resulting neutrino spectrum, let us discuss some further aspects of the model with fermionic triplets. In particular, we check higher-dimensional operators and loop corrections, and have a look at cosmological constraints on the model.

5.4.1 Higher-dimensional operators and loop corrections

In this subsection, we discuss possible corrections to the discussion we presented before. In particular, the mass matrices of the neutrinos may receive corrections from higher-dimensional operators and loop diagrams. Let us first discuss possible higher-dimensional operators. With the particle content of the model, one can write down the higher-dimensional operator

$$\mathcal{O}_{\nu_L} = \frac{c_L}{\Lambda^2} \ell_L \ell_L H_L H_L S_{BL}^\dagger, \tag{5.78}$$

which generates neutrino masses of the order

$$M_{\nu_L} \sim v_L^2 v_{BL} / \Lambda^2 \tag{5.79}$$

for $c_L \approx 1$. Thus, using $v_L \sim 1\,\text{GeV}$ and $v_{BL} \sim 10\,\text{TeV}$, one needs

$$\Lambda \gtrsim 3 \times 10^3\,\text{TeV} \tag{5.80}$$

to avoid a neutrino mass above 1 eV. The value of v_L can of course be much smaller, such that this is a very naive bound on Λ. A similar operator can generate masses for the right-handed neutrinos,

$$\mathcal{O}_{\nu_R} = \frac{c_R}{\Lambda^2} \ell_R \ell_R H_R H_R S_{BL}^\dagger, \tag{5.81}$$

which generates a right-handed neutrino mass of the order

$$M_{\nu_R} \sim v_R^2 v_{BL} / \Lambda^2 \tag{5.82}$$

for $c_R \approx 1$. Using $v_R \sim 1\,\text{TeV}$, $v_{BL} \sim 10\,\text{TeV}$, and the above bound for Λ, one finds $M_{\nu_R} < 1\,\text{MeV}$, which is a not too large correction. Notice that the two operators $\mathcal{O}_{\nu_R}$ and $\mathcal{O}_{\nu_L}$ are connected by the left–right parity.

There are higher-dimensional operators that induce baryon number violation in the quark sector, e.g.,

$$\mathcal{O}_{20} = \frac{c_{20}}{\Lambda^{16}} \left(Q_L Q_L Q_L \ell_L\right)^3 S_{BL}^\dagger S_{BL}^\dagger, \tag{5.83}$$

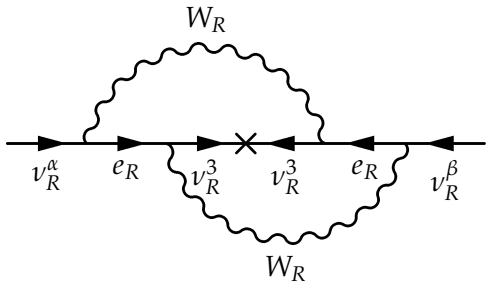

Figure 5.2: Two-loop correction to the right-handed neutrino mass matrix.

which however is of dimension 20 and therefore strongly suppressed. Due to the quantum numbers of the fields breaking $U(1)_L$ and $U(1)_B$, proton decay is not induced. Hence, there is no need to postulate a large desert in this scenario.

Possible radiative corrections should also be taken into account. The smallest one arises at two-loop level, see Fig. 5.2. A very naive estimation of the mass correction induced by this diagram is

$$M_{\nu_R}^{ij} \sim \frac{g^4}{(16\pi^2)^2} \frac{M_\tau^4}{M_{W_R}^4} M_{\nu_R^3} \sim 7 \times 10^{-17} M_{\nu_R^3}, \tag{5.84}$$

where M_τ is the mass of the τ lepton, and therefore negligibly small. $g = g_L = g_R$ is the $SU(2)$ gauge coupling.

5.4.2 Cosmological constraints

The extra light neutrino degrees of freedom that appear in the model presented above contribute to the radiation content of the Universe, and we should therefore check the corresponding cosmological constraints. Such extra radiation is parameterized in the value of N_{eff}, the effective number of thermalized neutrino species. The Planck Collaboration [56] has recently set a new limit on this parameter (for a certain combination of data sets)

$$N_{\text{eff}} = 3.30 \pm 0.27, \tag{5.85}$$

which is compatible with the standard value coming from three active neutrinos only,

$$N_{\text{eff}}^{\text{SM}} = 3.046. \tag{5.86}$$

Two mechanisms control the thermalization of the extra sterile neutrinos and therefore control their contribution to N_{eff} in our setup: Interactions with the new gauge bosons, which can be in thermal equilibrium with the SM plasma, and active–sterile oscillations. Taking into account the first mechanism, the contribution of the extra

neutrinos to N_{eff} depends on the mass of the new gauge bosons, Z_1, Z_2, and W_R. In Refs. [173] and [174], the constraints on the new forces that keep the right-handed neutrinos in thermal equilibrium were investigated, see also Ref. [175] for a recent study in a different context. It was shown that one does not have a large contribution to the effective number of relativistic degrees of freedom because the neutrinos decouple very early if the masses of the new gauge bosons are in the TeV region. LHC limits constrain the masses of the new gauge bosons to be of that order, and the cosmological constraints are therefore expected to be satisfied. Active–sterile oscillations are important for the case $m_i \sim m_D^i$ in the matrix given in Eq. (5.77), i.e., when the active–sterile mixing is large. Then, oscillations will put the two sterile neutrinos in thermal equilibrium and they are in strong tension with cosmology. Large mixing of eV sterile neutrinos is necessary to resolve the existing oscillation anomalies, see Ref. [172] for more details, such that these cannot be resolved in this model. Note, however, that the presence of these extra sterile states is a prediction of the model, and was not introduced to resolve any anomaly.

5.5 Summary and outlook

In this chapter, we investigated the possibility of defining a simple theory for the spontaneous breaking of parity, baryon and lepton numbers at a low scale without generating interactions that mediate proton decay and make a great desert necessary. We have found that the leptoquark fields introduced for anomaly cancelation also generate masses for the left-handed and right-handed neutrinos through the type III seesaw mechanism. The theory presented in this chapter can be considered as the simplest theory with these features.

The spectrum for neutrinos in this theory was studied in detail, showing that one predicts the existence of two light right-handed neutrinos. The existence of these light degrees of freedom can change the phenomenology of the new gauge bosons at colliders. In particular, the neutral gauge bosons can decay into the extra right-handed light neutrinos, $Z_i \to \bar{\nu}_R \nu_R$, and more important, the decays $W_R \to \bar{\nu}_R e_R$ are allowed. These decays can change the present collider bounds on the W_R mass based on the lepton number violating decays of the right-handed neutrinos and will be investigated in the future.

Chapter 6

Summary and outlook

In this thesis, we discussed the role of lepton and baryon numbers as windows to physics beyond the SM of particle physics. The text was separated into two parts: in Part I, we discussed the special case of lepton number violation by two units, and in Part II we focussed on promoting the accidental global symmetries baryon and lepton number of the SM Lagrangian to local gauge symmetries.

We saw in Chapter 2 that a violation of lepton number could allow for neutrinos to be Majorana particles. Then, the seesaw mechanism in one of its variants offers the possibility of explaining the smallness of neutrino masses by adding heavy new particles to the SM particle content without the necessity of tiny Yukawa couplings in the neutrino sector. The "naturalness" of the seesaw mechanism is of course no solid argument for the Majorana nature of neutrinos, but it would be fantastic if the discovery of neutrino mass revealed deeper insights into the lepton sector of the SM than a preference of nature for small couplings. The downside of the seesaw mechanism, at least in its canonical form, is its testability. The large mass scales involved (for order one couplings) make an experimental test impossible, and this lead us to explore alternatives that allow for an experimental test at current or future facilities. Radiative neutrino mass models, or more exotic setups such as a mini-seesaw mechanism in warped space, contained low-scale physics (around TeV) and still allowed to generate neutrino masses of the desired eV order without invoking unnaturally small couplings. LHC experiments or searches for lepton flavor violation could provide a test of these models in the near future.

In Chapter 3, we discussed a very prominent experimental test of lepton number violation, the neutrinoless mode of double beta decay. While mentioning that the standard mechanism, namely the exchange of light Majorana neutrinos, is a well-motivated possibility of realizing this decay and would connect it directly to neutrino masses, we focused on mechanisms beyond the SM. We discussed the contributions of color octet particles in the colored seesaw mechanism in detail in Section 3.2. We found that, depending on the parameters of the model, both the direct and the indirect contribution could be dominant. The presence of various mechanisms at the same time is a generic

problem of neutrinoless double beta decay in models beyond the SM, and depending on the choice of parameters different mechanisms can be dominant, see also Ref. [128] for a recent study in left–right symmetric models, which we also shortly discussed in this thesis. It should be clear that much work is left to be done here. Assuming the dominance of one particular mechanism, the lower limits on the $0\nu\beta\beta$ half-life obtained so far in all experiments can be transformed into limits on the parameters of new physics models (or upper limits on neutrino masses, in the case of light Majorana neutrino exchange). However, interference effects between different decay modes are easily thinkable and would alter the picture completely. In case this rare decay should indeed be observed in some future experiment, additional importance must be given to the determination of the underlying mechanism. First of all, the observation of $0\nu\beta\beta$ shows the violation of lepton number in nature. The connection to neutrino masses is an indirect one and is based on a particular interpretation of the decay. Ideas exist of how to distinguish different mechanisms in $0\nu\beta\beta$ experiments: measurements in different nuclei [176] or using the angular correlation of the emitted electrons [98, 177] might allow for a discrimination. Most likely, only a combination of $0\nu\beta\beta$ experiments with the LHC or other experiments may be able to provide a complete picture. This requires of course that the scale of lepton number violation is reachable by the experiments, and we saw that TeV-scale physics might give contributions to $0\nu\beta\beta$ at the same order of magnitude as the light neutrino exchange. Additionally, in Section 3.3, we discussed a cross check that would allow for an unambiguous test for $0\nu\beta\beta$ in future large-scale experiments. Using the decay to the first excited 0^+ state in addition to the ground state transition, a very characteristic experimental signature could be found. However, due to the low rates of $0\nu\beta\beta$ to excited states, this will only work to a size of the effective Majorana neutrino mass of about $m_{0\nu\beta\beta} \approx 80\,\text{meV}$ for ton-scale experiments.

Part II of this thesis was dedicated to the origin of the accidental symmetries baryon and lepton number in the SM. We promoted the global symmetries to local gauge symmetries and explored the implications of doing so. In order to define anomaly-free gauge theories, we needed to introduce additional particles, and deep consequences resulted from this simple task: a DM candidate arose, whose stability was a consequence of the breaking of the gauge symmetries and did not have to be put in by hand by demanding a discrete symmetry, see Chapter 4, and neutrino masses could be implemented in a simple manner via the type III seesaw mechanism in a left–right symmetric setup, see Chapter 5. It is important to point out that the models presented in Chapters 4 and 5 allow for a low breaking scale of baryon and lepton numbers and there is no need to postulate the existence of a large desert in order to be consistent with the bounds from proton decay. This is in the spirit of Part I, where we tried to lower the scale of new physics to allow for an experimental test of the models underlying neutrino masses and neutrinoless double beta decay. We were able to highlight some

of the phenomenology of the proposed models, but a full exploration is beyond the scope of this thesis.

In the model presented in Chapter 4, we outlined the phenomenology of the fermionic DM candidate that carries baryon number. We also mentioned that similar models allow for a successful generation of the baryon excess in the Universe, even though baryon and lepton numbers are broken at a low scale. It is an interesting question whether this can be implemented in our model, too, and we will tackle this question in the future. Also a detailed collider phenomenology of the model is an interesting direction of investigation.

In the model presented in Chapter 5, we discussed the implementation of the type III seesaw and the corresponding neutrino mass matrix. Without imposing any extra symmetries, the model contains two light sterile neutrinos. The extra light sterile neutrinos have implications at colliders and can change the phenomenology of the new gauge bosons considerably. This will also be investigated in the future.

To finally summarize, we addressed various issues that remain unexplained in the Standard Model. One prominent issue was the phenomenon of neutrino masses that originates from the observation of neutrino oscillations. The related question whether lepton number is broken in nature was also discussed, and we presented some detailed phenomenology of a corresponding rare decay, neutrinoless double beta decay. The dark matter observed in the Universe requires a neutral particle that is stable on cosmological time scales. We mentioned how such a particle can be achieved in the models we presented in this thesis. The origin of the accidental global symmetries of baryon and lepton numbers was discussed by promoting them to local gauge symmetries and a plethora of interesting implications was the result, resolving some of the aforementioned issues. All in all, we can conclude that baryon and lepton numbers provide us with a very interesting window to physics beyond the Standard Model.

Appendix

Appendix A

Neutrino oscillation parameters

The neutrino oscillation parameters (in the three-neutrino picture) used throughout this thesis are obtained in a global fit of all experimental neutrino data [53] and are given in Tab. A.1 for convenience. These are the most current values, including the non-zero reactor mixing angle θ_{13} measured by the reactor neutrino experiments Daya Bay [178], RENO [179], and Double Chooz [180]. We use the values where reactor fluxes were left free in the fits and short-baseline reactor data are used (see Ref. [53] for more details).

Table A.1: Neutrino oscillation parameters used throughout this thesis [53]. The chosen convention is such that always the larger mass-squared difference is given, which is Δm^2_{31} for normal hierarchy (NH) and Δm^2_{32} for inverted hierarchy (IH).

Parameter	best fit $\pm 1\sigma$	3σ range
$\sin^2\theta_{12}$	$0.302^{+0.013}_{-0.012}$	$0.267 \to 0.344$
$\sin^2\theta_{23}$	$0.413^{+0.037}_{-0.025} \oplus 0.594^{+0.021}_{-0.022}$	$0.342 \to 0.667$
$\sin^2\theta_{13}$	$0.0227^{+0.0023}_{-0.0024}$	$0.0156 \to 0.0299$
$\Delta m^2_{21}\,[10^{-5}\,\mathrm{eV}^2]$	$7.50^{+0.18}_{-0.19}$	$7.00 \to 8.09$
$\Delta m^2_{31}\,[10^{-3}\,\mathrm{eV}^2]$ (NH)	$+2.473^{+0.070}_{-0.067}$	$+2.276 \to +2.695$
$\Delta m^2_{32}\,[10^{-3}\,\mathrm{eV}^2]$ (IH)	$-2.427^{+0.042}_{-0.065}$	$-2.649 \to -2.242$

List of Abbreviations and Acronyms

$0\nu\beta\beta$	Neutrinoless Double Beta Decay
$2\nu\beta\beta$	Two-Neutrino Double Beta Decay
ATLAS	A Toroidal LHC Apparatus
BR	Branching Ratio
CANDLES	Calcium Flouride for the Study of Neutrinos and Dark Matters by Low Energy Spectrometer
CDF	Collider Detector at Fermilab
CERN	Conseil Européen pour la Recherche Nucléaire; official name in English: European Organization for Nuclear Research
CKM	Cabibbo–Kobayashi–Maskawa
CL	Confidence Level
CMS	Compact Muon Solenoid
CP	Charge Parity
DM	Dark Matter
EC	Electron Capture
EM	Electromagnetic
EW	Electroweak
EXO	Enriched Xenon Observatory
g.s.	ground state
GERDA	Germanium Detector Array
GUT	Grand Unified Theory

HdM ..... Heidelberg–Moscow

IBM ..... Interacting Boson Model

IGEX ..... International Germanium Experiment

IH ..... Inverted Hierarchy

KamLAND-Zen .... Kamioka Liquid Scintillator Antineutrino Detector – Zero-Neutrino Double-Beta Decay

KATRIN ..... Karlsruhe Tritium Neutrino Experiment

LHC ..... Large Hadron Collider

LR ..... Left–Right

MEG ..... Mu to E Gamma

MFV ..... Minimal Flavor Violation

MuLan ..... Muon Lifetime Analysis

NH ..... Normal Hierarchy

PMNS ..... Pontecorvo–Maki–Nakagawa–Sakata

QCD ..... Quantum Chromodynamics

R&D ..... Research & Development

RENO ..... Reactor Experiment for Neutrino Oscillation

SM ..... Standard Model (of particle physics)

SUSY ..... Supersymmetry

UV ..... Ultra-Violet

VEV ..... Vacuum Expectation Value

WIMP ..... Weakly Interacting Massive Particle

List of Figures

List of Tables

Bibliography

[1] S. L. Glashow, *Partial-symmetries of weak interactions*, Nucl. Phys. **22** (1961) 579.

[2] S. Weinberg, *A model of leptons*, Phys. Rev. Lett. **19** (1967) 1264.

[3] A. Salam, *Weak and electromagnetic interactions*, in *Elementary Particle Theory: Proceedings of the 8th Nobel Symposium at Lerum, Sweden (1968)*, edited by N. Svartholm (Almqvist and Wiksell, Stockholm, 1968), p. 367.

[4] CDF Collaboration, F. Abe *et al.*, *Observation of top quark production in $\bar{p}p$ collisions with the Collider Detector at Fermilab*, Phys. Rev. Lett. **74** (1995) 2626, arXiv:hep-ex/9503002.

[5] DØ Collaboration, S. Abachi *et al.*, *Observation of the top quark*, Phys. Rev. Lett. **74** (1995) 2632, arXiv:hep-ex/9503003.

[6] P. W. Higgs, *Broken symmetries and the masses of gauge bosons*, Phys. Rev. Lett. **13** (1964) 508.

[7] F. Englert and R. Brout, *Broken symmetry and the mass of gauge vector mesons*, Phys. Rev. Lett. **13** (1964) 321.

[8] G. S. Guralnik, C. R. Hagen, and T. W. B. Kibble, *Global conservation laws and massless particles*, Phys. Rev. Lett. **13** (1964) 585.

[9] ATLAS Collaboration, G. Aad *et al.*, *Observation of a new particle in the search for the Standard Model Higgs boson with the ATLAS detector at the LHC*, Phys. Lett. B **716** (2012) 1, arXiv:1207.7214 [hep-ex].

[10] CMS Collaboration, S. Chatrchyan *et al.*, *Observation of a new boson at a mass of 125 GeV with the CMS experiment at the LHC*, Phys. Lett. B **716** (2012) 30, arXiv:1207.7235 [hep-ex].

[11] Super-Kamiokande Collaboration, Y. Fukuda *et al.*, *Evidence for oscillation of atmospheric neutrinos*, Phys. Rev. Lett. **81** (1998) 1562, arXiv:hep-ex/9807003.

[12] KamLAND Collaboration, K. Eguchi *et al.*, *First results from KamLAND: Evidence for reactor antineutrino disappearance*, Phys. Rev. Lett. **90** (2003) 021802, arXiv:hep-ex/0212021.

[13] SNO Collaboration, Q. R. Ahmad *et al.*, *Direct evidence for neutrino flavor transformation from neutral-current interactions in the Sudbury Neutrino Observatory*, Phys. Rev. Lett. **89** (2002) 011301, arXiv:nucl-ex/0204008.

[14] P. Minkowski, *$\mu \to e\gamma$ at a rate of one out of 10^9 muon decays?*, Phys. Lett. B **67** (1977) 421.

[15] R. N. Mohapatra and G. Senjanović, *Neutrino mass and spontaneous parity nonconservation*, Phys. Rev. Lett. **44** (1980) 912.

[16] T. Yanagida, *Horizontal gauge symmetry and masses of neutrinos*, in *Proceedings of the Workshop on the Unified Theory and the Baryon Number in the Universe*, edited by O. Sawada and A. Sugamoto (KEK report 79-18, Tsukuba, Japan, 1979), p. 95.

[17] M. Gell-Mann, P. Ramond, and R. Slansky, *Complex spinors and unified theories*, in *Supergravity*, edited by P. van Nieuwenhuizen and D. Z. Freedman (North Holland Publ. Co., Amsterdam, 1979), p. 315, arXiv:1306.4669 [hep-th].

[18] S. L. Glashow, *The future of elementary particle physics*, in *Quarks and Leptons: Proceedings of the 1979 Cargèse Summer Institute*, edited by M. Lévy *et al.* (Plenum Press, New York, 1980), NATO Advanced Study Institutes Series, p. 687.

[19] W. Konetschny and W. Kummer, *Nonconservation of total lepton number with scalar bosons*, Phys. Lett. B **70** (1977) 433.

[20] T. P. Cheng and L.-F. Li, *Neutrino masses, mixings, and oscillations in $SU(2) \times U(1)$ models of electroweak interactions*, Phys. Rev. D **22** (1980) 2860.

[21] G. Lazarides, Q. Shafi, and C. Wetterich, *Proton lifetime and fermion masses in an $SO(10)$ model*, Nucl. Phys. B **181** (1981) 287.

[22] J. Schechter and J. W. F. Valle, *Neutrino masses in $SU(2) \otimes U(1)$ theories*, Phys. Rev. D **22** (1980) 2227.

[23] R. N. Mohapatra and G. Senjanović, *Neutrino masses and mixings in gauge models with spontaneous parity violation*, Phys. Rev. D **23** (1981) 165.

[24] R. Foot, H. Lew, X.-G. He, and G. C. Joshi, *See-saw neutrino masses induced by a triplet of leptons*, Z. Phys. C **44** (1989) 441.

[25] EXO Collaboration, M. Auger *et al.*, *Search for neutrinoless double-beta decay in ^{136}Xe with EXO-200*, Phys. Rev. Lett. **109** (2012) 032505, arXiv:1205.5608 [hep-ex].

[26] KamLAND-Zen Collaboration, A. Gando *et al.*, *Limit on neutrinoless $\beta\beta$ decay of ^{136}Xe from the first phase of KamLAND-Zen and comparison with the positive claim in ^{76}Ge*, Phys. Rev. Lett. **110** (2013) 062502, arXiv:1211.3863 [hep-ex].

[27] GERDA Collaboration, M. Agostini *et al.*, *Results on neutrinoless double-β decay of ^{76}Ge from phase I of the* GERDA *experiment*, Phys. Rev. Lett. **111** (2013) 122503, arXiv:1307.4720 [nucl-ex].

[28] F. Zwicky, *Die Rotverschiebung von extragalaktischen Nebeln*, Helv. Phys. Acta **6** (1933) 110.

[29] G. Bertone, D. Hooper, and J. Silk, *Particle dark matter: evidence, candidates and constraints*, Phys. Rept. **405** (2005) 279, arXiv:hep-ph/0404175.

[30] M. Milgrom, *A modification of the Newtonian dynamics as a possible alternative to the hidden mass hypothesis*, Astrophys. J. **270** (1983) 365.

[31] G. Jungman, M. Kamionkowski, and K. Griest, *Supersymmetric dark matter*, Phys. Rept. **267** (1996) 195, arXiv:hep-ph/9506380.

[32] S. Weinberg, *Baryon- and lepton-nonconserving processes*, Phys. Rev. Lett. **43** (1979) 1566.

[33] F. Wilczek and A. Zee, *Operator analysis of nucleon decay*, Phys. Rev. Lett. **43** (1979) 1571.

[34] P. Fileviez Pérez and M. B. Wise, *Baryon and lepton number as local gauge symmetries*, Phys. Rev. D **82** (2010) 011901, Erratum ibid. D **82** (2010) 079901, arXiv:1002.1754 [hep-ph].

[35] T. R. Dulaney, P. Fileviez Pérez, and M. B. Wise, *Dark matter, baryon asymmetry, and spontaneous B and L breaking*, Phys. Rev. D **83** (2011) 023520, arXiv:1005.0617 [hep-ph].

[36] P. Fileviez Pérez and M. B. Wise, *Breaking local baryon and lepton number at the TeV scale*, JHEP **08** (2011) 068, arXiv:1106.0343 [hep-ph].

[37] P. V. Dong and H. N. Long, *A simple model of gauged lepton and baryon charges*, arXiv:1010.3818 [hep-ph].

[38] J. C. Pati and A. Salam, *Lepton number as the fourth "color"*, Phys. Rev. D **10** (1974) 275, Erratum ibid. D **11** (1975) 703.

[39] R. N. Mohapatra and J. C. Pati, *"Natural" left-right symmetry*, Phys. Rev. D **11** (1975) 2558.

[40] G. Senjanović and R. N. Mohapatra, *Exact left-right symmetry and spontaneous violation of parity*, Phys. Rev. D **12** (1975) 1502.

[41] G. Senjanović, *Spontaneous breakdown of parity in a class of gauge theories*, Nucl. Phys. B **153** (1979) 334.

[42] S. Choubey, M. Duerr, M. Mitra, and W. Rodejohann, *Lepton number and lepton flavor violation through color octet states*, JHEP **05** (2012) 017, arXiv:1201.3031 [hep-ph].

[43] M. Duerr, M. Lindner, and K. Zuber, *Consistency test of neutrinoless double beta decay with one isotope*, Phys. Rev. D **84** (2011) 093004, arXiv:1103.4735 [hep-ph].

[44] M. Duerr, P. Fileviez Pérez, and M. B. Wise, *Gauge theory for baryon and lepton numbers with leptoquarks*, Phys. Rev. Lett. **110** (2013) 231801, arXiv:1304.0576 [hep-ph].

[45] M. Duerr, P. Fileviez Pérez, and M. Lindner, *Left–right symmetric theory with light sterile neutrinos*, Phys. Rev. D **88** (2013) 051701, arXiv:1306.0568 [hep-ph].

[46] M. Duerr, *Neutrinoless double beta decay and neutrino masses*, AIP Conf. Proc. **1467** (2012) 235, arXiv:1206.0565 [hep-ph].

[47] M. Duerr, *Lepton number violating new physics and neutrinoless double beta decay*, Nucl. Phys. B (Proc. Suppl.) **237–238** (2013) 24.

[48] M. Duerr, D. P. George, and K. L. McDonald, *Neutrino mass and $\mu \to e + \gamma$ from a mini-seesaw*, JHEP **07** (2011) 103, arXiv:1105.0593 [hep-ph].

[49] M. Aoki, M. Duerr, J. Kubo, and H. Takano, *Multicomponent dark matter systems and their observation prospects*, Phys. Rev. D **86** (2012) 076015, arXiv:1207.3318 [hep-ph].

[50] M. Duerr and P. Fileviez Pérez, *Baryonic dark matter*, arXiv:1309.3970 [hep-ph].

[51] M. Duerr, M. Lindner, and A. Merle, *On the quantitative impact of the Schechter-Valle theorem*, JHEP **06** (2011) 091, arXiv:1105.0901 [hep-ph].

[52] MuLan Collaboration, D. M. Webber *et al.*, *Measurement of the positive muon lifetime and determination of the Fermi constant to part-per-million precision*, Phys. Rev. Lett. **106** (2011) 041803, Publisher's note: ibid. **106** (2011) 079901, arXiv:1010.0991 [hep-ex].

[53] M. C. Gonzalez-Garcia, M. Maltoni, J. Salvado, and T. Schwetz, *Global fit to three neutrino mixing: critical look at present precision*, JHEP **12** (2012) 123, arXiv:1209.3023 [hep-ph].

[54] C. Kraus, B. Bornschein, L. Bornschein, J. Bonn, B. Flatt, A. Kovalik, B. Ostrick, E. W. Otten, J. P. Schall, T. Thümmler, and C. Weinheimer, *Final results from phase II of the Mainz neutrino mass search in tritium β decay*, Eur. Phys. J. C **40** (2005) 447, arXiv:hep-ex/0412056.

[55] KATRIN Collaboration, A. Osipowicz *et al.*, *KATRIN: A next generation tritium beta decay experiment with sub-eV sensitivity for the electron neutrino mass (letter of intent)*, arXiv:hep-ex/0109033.

[56] Planck Collaboration, P. A. R. Ade *et al.*, *Planck 2013 results. XVI. Cosmological parameters*, arXiv:1303.5076 [astro-ph.CO].

[57] Particle Data Group, J. Beringer *et al.*, *Review of particle physics*, Phys. Rev. D **86** (2012) 010001, and 2013 partial update for the 2014 edition (URL: http://pdg.lbl.gov).

[58] Super-Kamiokande Collaboration, H. Nishino *et al.*, *Search for proton decay via $p \to e^+\pi^0$ and $p \to \mu^+\pi^0$ in a large water cherenkov detector*, Phys. Rev. Lett. **102** (2009) 141801, arXiv:0903.0676 [hep-ex].

[59] E. Ma, *Pathways to naturally small neutrino masses*, Phys. Rev. Lett. **81** (1998) 1171, arXiv:hep-ph/9805219.

[60] B. Pontecorvo, *Mesonium and anti-mesonium*, Sov. Phys. JETP **6** (1957) 429, Zh. Eksp. Teor. Fiz. **33** (1957) 549.

[61] B. Pontecorvo, *Neutrino experiments and the problem of conservation of leptonic charge*, Sov. Phys. JETP **26** (1968) 984, Zh. Eksp. Teor. Fiz. **53** (1967) 1717.

[62] Z. Maki, M. Nakagawa, and S. Sakata, *Remarks on the unified model of elementary particles*, Prog. Theor. Phys. **28** (1962) 870.

[63] N. Cabibbo, *Unitary symmetry and leptonic decays*, Phys. Rev. Lett. **10** (1963) 531.

[64] M. Kobayashi and T. Maskawa, *CP-violation in the renormalizable theory of weak interaction*, Prog. Theor. Phys. **49** (1973) 652.

[65] P. Fileviez Pérez, T. Han, and T. Li, *Testability of the type I seesaw mechanism at the CERN LHC: Revealing the existence of the $B - L$ symmetry*, Phys. Rev. D **80** (2009) 073015, arXiv:0907.4186 [hep-ph].

[66] P. Fileviez Pérez, T. Han, G. Huang, T. Li, and K. Wang, *Neutrino Masses and the CERN LHC: Testing the type II seesaw mechanism*, Phys. Rev. D **78** (2008) 015018, arXiv:0805.3536 [hep-ph].

[67] ATLAS Collaboration, G. Aad *et al.*, *Search for doubly-charged Higgs bosons in like-sign dilepton final states at $\sqrt{s} = 7$ TeV with the ATLAS detector*, Eur. Phys. J. C **72** (2012) 2244, arXiv:1210.5070 [hep-ex].

[68] A. Melfo, M. Nemevšek, F. Nesti, G. Senjanović, and Y. Zhang, *Type II neutrino seesaw mechanism at the LHC: The roadmap*, Phys. Rev. D **85** (2012) 055018, arXiv:1108.4416 [hep-ph].

[69] J. A. Aguilar-Saavedra, P. M. Boavida, and F. R. Joaquim, *Flavoured searches for type-III seesaw at the LHC*, arXiv:1308.3226 [hep-ph].

[70] P. Fileviez Pérez, *Type III seesaw and left-right symmetry*, JHEP **03** (2009) 142, arXiv:0809.1202 [hep-ph].

[71] E. Ma, *Verifiable radiative seesaw mechanism of neutrino mass and dark matter*, Phys. Rev. D **73** (2006) 077301, arXiv:hep-ph/0601225.

[72] P. Fileviez Pérez and M. B. Wise, *On the origin of neutrino masses*, Phys. Rev. D **80** (2009) 053006, arXiv:0906.2950 [hep-ph].

[73] P. Fileviez Pérez, T. Han, S. Spinner, and M. K. Trenkel, *Lepton number violation from colored states at the LHC*, JHEP **01** (2011) 046, arXiv:1010.5802 [hep-ph].

[74] A. Zee, *A theory of lepton number violation and neutrino Majorana masses*, Phys. Lett. B **93** (1980) 389, Erratum ibid. B **95** (1980) 461.

[75] L. Wolfenstein, *A theoretical pattern for neutrino oscillations*, Nucl. Phys. B **175** (1980) 93.

[76] X.-G. He, *Is the Zee model neutrino mass matrix ruled out?*, Eur. Phys. J. C **34** (2004) 371, arXiv:hep-ph/0307172.

[77] A. Zee, *Qantum numbers of Majorana neutrino masses*, Nucl. Phys. B **264** (1986) 99.

[78] K. S. Babu, *Model of "calculable" Majorana neutrino masses*, Phys. Lett. B **203** (1988) 132.

[79] G. D'Ambrosio, G. F. Giudice, G. Isidori, and A. Strumia, *Minimal flavour violation: an effective field theory approach*, Nucl. Phys. B **645** (2002) 155, arXiv:hep-ph/0207036.

[80] CMS Collaboration, S. Chatrchyan *et al.*, *Search for narrow resonances and quantum black holes in inclusive and b-tagged dijet mass spectra from pp collisions at* $\sqrt{s} = 7$ *TeV*, JHEP **01** (2013) 013, arXiv:1210.2387 [hep-ex].

[81] ATLAS Collaboration, G. Aad *et al.*, *ATLAS search for new phenomena in dijet mass and angular distributions using pp collisions at* $\sqrt{s} = 7$ *TeV*, JHEP **01** (2013) 029, arXiv:1210.1718 [hep-ex].

[82] M. I. Gresham and M. B. Wise, *Color octet scalar production at the CERN LHC*, Phys. Rev. D **76** (2007) 075003, arXiv:0706.0909 [hep-ph].

[83] M. Gerbush, T. J. Khoo, D. J. Phalen, A. Pierce, and D. Tucker-Smith, *Color-octet scalars at the CERN LHC*, Phys. Rev. D **77** (2008) 095003, arXiv:0710.3133 [hep-ph].

[84] A. V. Manohar and M. B. Wise, *Flavor changing neutral currents, an extended scalar sector, and the Higgs production rate at the CERN Large Hadron Collider*, Phys. Rev. D **74** (2006) 035009, arXiv:hep-ph/0606172.

[85] K. L. McDonald, *Light neutrinos from a mini-seesaw mechanism in warped space*, Phys. Lett. B **696** (2011) 266, arXiv:1010.2659 [hep-ph].

[86] C. F. v. Weizsäcker, *Zur Theorie der Kernmassen*, ZS. f. Phys. **96** (1935) 431.

[87] H. A. Bethe and R. F. Bacher, *Nuclear physics A. Stationary states of nuclei*, Rev. Mod. Phys. **8** (1936) 82.

[88] A. S. Barabash, *Precise half-life values for two-neutrino double-β decay*, Phys. Rev. C **81** (2010) 035501, arXiv:1003.1005 [nucl-ex].

[89] H. V. Klapdor-Kleingrothaus, I. V. Krivosheina, A. Dietz, and O. Chkvorets, *Search for neutrinoless double beta decay with enriched* ^{76}*Ge in Gran Sasso 1990–2003*, Phys. Lett. B **586** (2004) 198, arXiv:hep-ph/0404088.

[90] H. V. Klapdor-Kleingrothaus and I. V. Krivosheina, *The evidence for the observation of* $0\nu\beta\beta$ *decay: The identification of* $0\nu\beta\beta$ *events from the full spectra*, Mod. Phys. Lett. A **21** (2006) 1547.

[91] B. Schwingenheuer, *Status and prospects of searches for neutrinoless double beta decay*, Ann. Phys. (Berlin) **525** (2013) 269, arXiv:1210.7432 [hep-ex].

[92] H. V. Klapdor-Kleingrothaus, A. Dietz, L. Baudis, G. Heusser, I. V. Krivosheina, S. Kolb, B. Majorovits, H. Paes, H. Strecker, V. Alexeev, A. Balysh, A. Bakalyarov, S. T. Belyaev, V. I. Lebedev, and S. Zhukov, *Latest results from the Heidelberg–Moscow double beta decay experiment*, Eur. Phys. J. A **12** (2001) 147, arXiv:hep-ph/0103062.

[93] IGEX Collaboration, C. E. Aalseth *et al.*, *The IGEX ^{76}Ge neutrinoless double-beta decay experiment: Prospects for next generation experiments*, Phys. Rev. D **65** (2002) 092007, arXiv:hep-ex/0202026.

[94] C. E. Aalseth, F. T. Avignone, R. L. Brodzinski, S. Cebrian, E. Garcia, D. Gonzales, W. K. Hensley, I. G. Irastorza, I. V. Kirpichnikov, A. A. Klimenko, H. S. Miley, A. Morales, J. Morales, A. Ortiz de Solorzano, S. B. Osetrov, V. S. Pogosov, J. Puimedon, J. H. Reeves, M. L. Sarsa, A. A. Smolnikov, A. S. Starostin, A. G. Tamanyan, A. A. Vasenko, S. I. Vasiliev, and J. A. Villar, *The IGEX experiment revisited: A response to the critique of Klapdor-Kleingrothaus, Dietz and Krivosheina*, Phys. Rev. D **70** (2004) 078302, arXiv:nucl-ex/0404036.

[95] E. Majorana, *Teoria simmetrica dell'elettrone e del positrone*, Nuovo Cim. **14** (1937) 171.

[96] G. Racah, *Sulla simmetria tra particelle e antiparticelle*, Nuovo Cim. **14** (1937) 322.

[97] W. H. Furry, *On transition probabilities in double beta-disintegration*, Phys. Rev. **56** (1939) 1184.

[98] M. Doi, T. Kotani, and E. Takasugi, *Double beta decay and Majorana neutrino*, Prog. Theor. Phys. Suppl. **83** (1985) 1.

[99] H. Primakoff and S. P. Rosen, *Double beta decay*, Rep. Prog. Phys. **22** (1959) 121.

[100] W. C. Haxton and G. J. Stephenson Jr., *Double beta decay*, Prog. Part. Nucl. Phys. **12** (1984) 409.

[101] T. Tomoda, *Double beta decay*, Rep. Prog. Phys. **54** (1991) 53.

[102] J. Suhonen and O. Civitarese, *Weak-interaction and nuclear-structure aspects of nuclear double beta decay*, Phys. Rep. **300** (1998) 123.

[103] J. Kotila and F. Iachello, *Phase space factors for double-β decay*, Phys. Rev. C **85** (2012) 034316, arXiv:1209.5722 [nucl-th].

[104] S. Stoica and M. Mirea, *New calculations for phase space factors involved in double beta decay*, arXiv:1307.0290 [nucl-th].

[105] G. Audi, A. H. Wapstra, and C. Thibault, *The* AME*2003 atomic mass evaluation (II). Tables, graphs and references*, Nucl. Phys. A **729** (2003) 337.

[106] A. A. Kwiatkowski, T. Brunner, J. D. Holt, A. Chaudhuri, U. Chowdhury, M. Eibach, J. Engel, A. T. Gallant, A. Grossheim, M. Horoi, A. Lennarz, T. D. Macdonald, M. R. Pearson, B. E. Schultz, M. C. Simon, R. A. Senkov, V. V. Simon, K. Zuber, and J. Dilling, *New determination of double-β-decay properties in ^{48}Ca: high-precision $Q_{\beta\beta}$-value measurement and improved nuclear matrix element calculations*, arXiv:1308.3815 [nucl-ex].

[107] B. J. Mount, M. Redshaw, and E. G. Myers, *Double-β-decay Q values of ^{74}Se and ^{76}Ge*, Phys. Rev. C **81** (2010) 032501.

[108] D. L. Lincoln, J. D. Holt, G. Bollen, M. Brodeur, S. Bustabad, J. Engel, S. J. Novario, M. Redshaw, R. Ringle, and S. Schwarz, *First direct double-β decay Q-value measurement of ^{82}Se in support of understanding the nature of the neutrino*, Phys. Rev. Lett. **110** (2013) 012501, arXiv:1211.5659 [nucl-ex].

[109] S. Rahaman, V.-V. Elomaa, T. Eronen, J. Hakala, A. Jokinen, J. Julin, A. Kankainen, A. Saastamoinen, J. Suhonen, C. Weber, and J. Äystö, *Q values of the ^{76}Ge and ^{100}Mo double-beta decays*, Phys. Lett. B **662** (2008) 111, arXiv:0712.3337 [nucl-ex].

[110] D. Fink, J. Barea, D. Beck, K. Blaum, C. Böhm, C. Borgmann, M. Breitenfeldt, F. Herfurth, A. Herlert, J. Kotila, M. Kowalska, S. Kreim, D. Lunney, S. Naimi, M. Rosenbusch, S. Schwarz, L. Schweikhard, F. Šimkovic, J. Stanja, and K. Zuber, *Q value and half-lives for the double-β-decay nuclide ^{110}Pd*, Phys. Rev. Lett. **108** (2012) 062502, arXiv:1112.5786 [nucl-ex].

[111] S. Rahaman, V.-V. Elomaa, T. Eronen, J. Hakala, A. Jokinen, A. Kankainen, J. Rissanen, J. Suhonen, C. Weber, and J. Äystö, *Double-beta decay Q values of ^{116}Cd and ^{130}Te*, Phys. Lett. B **703** (2011) 412.

[112] M. Redshaw, E. Wingfield, J. McDaniel, and E. G. Myers, *Mass and double-beta-decay Q value of ^{136}Xe*, Phys. Rev. Lett. **98** (2007) 053003.

[113] P. M. McCowan and R. C. Barber, *Q value for the double-β decay of ^{136}Xe*, Phys. Rev. C **82** (2010) 024603.

[114] V. S. Kolhinen, T. Eronen, D. Gorelov, J. Hakala, A. Jokinen, A. Kankainen, I. D. Moore, J. Rissanen, A. Saastamoinen, J. Suhonen, and J. Äystö, *Double-β decay Q value of ^{150}Nd*, Phys. Rev. C **82** (2010) 022501.

[115] J. Barea, J. Kotila, and F. Iachello, *Nuclear matrix elements for double-β decay*, Phys. Rev. C **87** (2013) 014315, arXiv:1301.4203 [nucl-th].

[116] J. Barea and F. Iachello, *Neutrinoless double-β decay in the microscopic interacting boson model*, Phys. Rev. C **79** (2009) 044301.

[117] J. Schechter and J. W. F. Valle, *Neutrinoless double-β decay in $SU(2) \times U(1)$ theories*, Phys. Rev. D **25** (1982) 2951.

[118] P.-H. Gu, *Significant neutrinoless double beta decay with quasi-Dirac neutrinos*, Phys. Rev. D **85** (2012) 093016, arXiv:1101.5106 [hep-ph].

[119] H. Päs, M. Hirsch, H. V. Klapdor-Kleingrothaus, and S. G. Kovalenko, *Towards a superformula for neutrinoless double beta decay*, Phys. Lett. B **453** (1999) 194.

[120] H. Päs, M. Hirsch, H. V. Klapdor-Kleingrothaus, and S. G. Kovalenko, *A superformula for neutrinoless double beta decay II: the short range part*, Phys. Lett. B **498** (2001) 35, arXiv:hep-ph/0008182.

[121] F. Bonnet, M. Hirsch, T. Ota, and W. Winter, *Systematic decomposition of the neutrinoless double beta decay operator*, JHEP **03** (2013) 055, arXiv:1212.3045 [hep-ph].

[122] A. Halprin, P. Minkowski, H. Primakoff, and S. P. Rosen, *Double-beta decay and a massive Majorana neutrino*, Phys. Rev. D **13** (1976) 2567.

[123] R. N. Mohapatra and J. D. Vergados, *New contribution to neutrinoless double beta decay in gauge models*, Phys. Rev. Lett. **47** (1981) 1713.

[124] M. Hirsch, H. V. Klapdor-Kleingrothaus, and O. Panella, *Double beta decay in left-right symmetric models*, Phys. Lett. B **374** (1996) 7, arXiv:hep-ph/9602306.

[125] R. N. Mohapatra, *New contributions to neutrinoless double-beta decay in supersymmetric theories*, Phys. Rev. D **34** (1986) 3457.

[126] M. Hirsch, H. V. Klapdor-Kleingrothaus, and S. G. Kovalenko, *Supersymmetry and neutrinoless double β decay*, Phys. Rev. D **53** (1996) 1329, arXiv:hep-ph/9502385.

[127] W. Rodejohann, *Neutrino-less double beta decay and particle physics*, Int. J. Mod. Phys. E **20** (2011) 1833, arXiv:1106.1334 [hep-ph].

[128] J. Barry and W. Rodejohann, *Lepton number and flavour violation in TeV-scale left-right symmetric theories with large left-right mixing*, JHEP **09** (2013) 153, arXiv:1303.6324 [hep-ph].

[129] V. Tello, M. Nemevšek, F. Nesti, G. Senjanović, and F. Vissani, *Left-right symmetry: From the LHC to neutrinoless double beta decay*, Phys. Rev. Lett. **106** (2011) 151801, arXiv:1011.3522 [hep-ph].

[130] J. F. Nieves, *Dirac and pseudo-Dirac neutrinos and neutrinoless double beta decay*, Phys. Lett. B **147** (1984) 375.

[131] E. Takasugi, *Can the neutrinoless double beta decay take place in the case of Dirac neutrinos?*, Phys. Lett. B **149** (1984) 372.

[132] M. Hirsch, S. Kovalenko, and I. Schmidt, *Extended black box theorem for lepton number and flavor violating processes*, Phys. Lett. B **642** (2006) 106, arXiv:hep-ph/0608207.

[133] MEG Collaboration, J. Adam *et al.*, *New constraint on the existence of the $\mu^+ \to e^+\gamma$ decay*, Phys. Rev. Lett. **110** (2013) 201801, arXiv:1303.0754 [hep-ex].

[134] J. A. Casas and A. Ibarra, *Oscillating neutrinos and $\mu \to e, \gamma$*, Nucl. Phys. B **618** (2001) 171, arXiv:hep-ph/0103065.

[135] Y. Liao and J.-Y. Liu, *Radiative and flavor-violating transitions of leptons from interactions with color-octet particles*, Phys. Rev. D **81** (2010) 013004, arXiv:0911.3711 [hep-ph].

[136] MEG Collaboration, J. Adam *et al.*, *New limit on the lepton-flavor-violating decay $\mu^+ \to e^+\gamma$*, Phys. Rev. Lett. **107** (2011) 171801, arXiv:1107.5547 [hep-ex].

[137] BABAR Collaboration, B. Aubert *et al.*, *Searches for lepton flavor violation in the decays $\tau^{\pm} \to e^{\pm}\gamma$ and $\tau^{\pm} \to \mu^{\pm}\gamma$*, Phys. Rev. Lett. **104** (2010) 021802, arXiv:0908.2381 [hep-ex].

[138] P. F. Harrison, D. H. Perkins, and W. G. Scott, *A redetermination of the neutrino mass-squared difference in tri-maximal mixing with terrestrial matter effects*, Phys. Lett. B **458** (1999) 79, arXiv:hep-ph/9904297.

[139] P. F. Harrison, D. H. Perkins, and W. G. Scott, *Tri-bimaximal mixing and the neutrino oscillation data*, Phys. Lett. B **530** (2002) 167, arXiv:hep-ph/0202074.

[140] F. Iachello and J. Barea, *Advances in the theory of $0\nu\beta\beta$ decay*, Nucl. Phys. B (Proc. Suppl.) **217** (2011) 5.

[141] T. Tomoda, $0^+ \to 2^+$ *$0\nu\beta\beta$ decay triggered directly by the Majorana neutrino mass*, Phys. Lett. B **474** (2000) 245, arXiv:hep-ph/9909330.

[142] M. F. Kidd, J. H. Esterline, W. Tornow, A. S. Barabash, and V. I. Umatov, *New results for double-beta decay of ^{100}Mo to excited final states of ^{100}Ru using the TUNL-ITEP apparatus*, Nucl. Phys. A **821** (2009) 251, arXiv:0902.4418 [nucl-ex].

[143] A. S. Barabash, P. Hubert, A. Nachab, and V. I. Umatov, *Investigation of $\beta\beta$ decay in ^{150}Nd and ^{148}Nd to the excited states of daughter nuclei*, Phys. Rev. C **79** (2009) 045501, arXiv:0904.1924 [nucl-ex].

[144] R. B. Firestone, V. S. Shirley, C. M. Baglin, S. Y. F. Chu, and J. Zipkin, *Table of isotopes, 8th edition*. John Wiley & Sons, Inc., New York, 1996, 1998, 1999.

[145] S. Umehara, T. Kishimoto, I. Ogawa, R. Hazama, H. Miyawaki, S. Yoshida, K. Matsuoka, K. Kishimoto, A. Katsuki, H. Sakai, D. Yokoyama, K. Mukaida, S. Tomii, Y. Tatewaki, T. Kobayashi, and A. Yanagisawa, *Neutrino-less double-β decay of ^{48}Ca studied by CaF_2(Eu) scintillators*, Phys. Rev. C **78** (2008) 058501, arXiv:0810.4746 [nucl-ex].

[146] Majorana Collaboration, R. Gaitskell *et al.*, *The Majorana zero-neutrino double-beta decay experiment*, arXiv:nucl-ex/0311013.

[147] K. Zuber, *Long term prospects for double beta decay*, arXiv:1002.4313 [nucl-ex].

[148] GERDA Collaboration, S. Schönert *et al.*, *The GERmanium Detector Array (GERDA) for the search of neutrinoless $\beta\beta$ decays of ^{76}Ge at LNGS*, Nucl. Phys. B (Proc. Suppl.) **145** (2005) 242.

[149] L. Alvarez-Gaumé and E. Witten, *Gravitational anomalies*, Nucl. Phys. B **234** (1984) 269.

[150] A. Pais, *Remark on baryon conservation*, Phys. Rev. D **8** (1973) 1844.

[151] S. Rajpoot, *Gauge symmetries of electroweak interactions*, Int. J. Theor. Phys. **27** (1988) 689.

[152] X.-G. He and S. Rajpoot, *Anomaly-free left-right-symmetric models with gauged baryon and lepton numbers*, Phys. Rev. D **41** (1990) 1636.

[153] R. Foot, G. C. Joshi, and H. Lew, *Gauged baryon and lepton numbers*, Phys. Rev. D **40** (1989) 2487.

[154] C. D. Carone and H. Murayama, *Realistic models with a light $U(1)$ gauge boson coupled to baryon number*, Phys. Rev. D **52** (1995) 484, arXiv:hep-ph/9501220.

[155] H. Georgi and S. L. Glashow, *Decays of a leptophobic gauge boson*, Phys. Lett. B **387** (1996) 341, arXiv:hep-ph/9607202.

[156] CMS Collaboration, S. Chatrchyan *et al.*, *Combined search for the quarks of a sequential fourth generation*, Phys. Rev. D **86** (2012) 112003, arXiv:1209.1062 [hep-ex].

[157] G. D. Kribs, T. Plehn, M. Spannowsky, and T. M. P. Tait, *Four generations and Higgs physics*, Phys. Rev. D **76** (2007) 075016, arXiv:0706.3718 [hep-ph].

[158] G. Bélanger, B. Dumont, U. Ellwanger, J. F. Gunion, and S. Kraml, *Global fit to Higgs signal strengths and couplings and implications for extended Higgs sectors*, arXiv:1306.2941 [hep-ph].

[159] M. S. Chanowitz, M. A. Furman, and I. Hinchliffe, *Weak interactions of ultra heavy fermions (II)*, Nucl. Phys. B **153** (1979) 402.

[160] M. S. Chanowitz, *Electroweak constraints on the fourth generation at two loop order*, Phys. Rev. D **88** (2013) 015012, arXiv:1212.3209 [hep-ph].

[161] K. Ishiwata and M. B. Wise, *Higgs properties and fourth generation leptons*, Phys. Rev. D **84** (2011) 055025, arXiv:1107.1490 [hep-ph].

[162] A. Joglekar, P. Schwaller, and C. E. Wagner, *Dark matter and enhanced $h \to \gamma\gamma$ rate from vector-like leptons*, JHEP **12** (2012) 064, arXiv:1207.4235 [hep-ph].

[163] P. Schwaller, T. M. P. Tait, and R. Vega-Morales, *Dark matter and vectorlike leptons from gauged lepton number*, Phys. Rev. D **88** (2013) 035001, arXiv:1305.1108 [hep-ph].

[164] W.-Y. Keung and G. Senjanović, *Majorana neutrinos and the production of the right-handed charged gauge boson*, Phys. Rev. Lett. **50** (1983) 1427.

[165] M. Nemevšek, F. Nesti, G. Senjanović, and Y. Zhang, *Limits on the left-right symmetry scale and heavy neutrinos from early LHC data*, Phys. Rev. D **83** (2011) 115014, arXiv:1103.1627 [hep-ph].

[166] T. Han, I. Lewis, R. Ruiz, and Z.-g. Si, *Lepton number violation and W' chiral couplings at the LHC*, Phys. Rev. D **87** (2013) 035011, arXiv:1211.6447 [hep-ph].

[167] M. Nemevšek, G. Senjanović, and V. Tello, *Connecting Dirac and Majorana neutrino mass matrices in the minimal left-right symmetric model*, Phys. Rev. Lett. **110** (2013) 151802, arXiv:1211.2837 [hep-ph].

[168] S. M. Barr, B. Bednarz, and C. Benesh, *Anomaly constraints and new $U(1)$ gauge bosons*, Phys. Rev. D **34** (1986) 235.

[169] E. Ma, *New $U(1)$ gauge symmetry of quarks and leptons*, Mod. Phys. Lett. A **17** (2002) 535, arXiv:hep-ph/0112232.

[170] P. Fileviez Pérez and S. Spinner, *Spontaneous R-parity breaking and left-right symmetry*, Phys. Lett. B **673** (2009) 251, arXiv:0811.3424 [hep-ph].

[171] D. K. Ghosh, G. Senjanović, and Y. Zhang, *Naturally light sterile neutrinos from theory of R-parity*, Phys. Lett. B **698** (2011) 420, arXiv:1010.3968 [hep-ph].

[172] J. Kopp, P. A. N. Machado, M. Maltoni, and T. Schwetz, *Sterile neutrino oscillations: the global picture*, JHEP **05** (2013) 050, arXiv:1303.3011 [hep-ph].

[173] A. Solaguren-Beascoa and M. C. Gonzalez-Garcia, *Dark radiation confronting LHC in Z' models*, Phys. Lett. B **719** (2013) 121, arXiv:1210.6350 [hep-ph].

[174] L. A. Anchordoqui, H. Goldberg, and G. Steigman, *Right-handed neutrinos as the dark radiation: Status and forecasts for the LHC*, Phys. Lett. B **718** (2013) 1162, arXiv:1211.0186 [hep-ph].

[175] P. Fileviez Pérez and S. Spinner, *Supersymmetry at the LHC and the theory of R-parity*, arXiv:1308.0524 [hep-ph].

[176] F. Deppisch and H. Päs, *Pinning down the mechanism of neutrinoless double β decay with measurements in different nuclei*, Phys. Rev. Lett. **98** (2007) 232501, arXiv:hep-ph/0612165.

[177] A. Ali, A. V. Borisov, and D. V. Zhuridov, *Probing new physics in the neutrinoless double beta decay using electron angular correlation*, Phys. Rev. D **76** (2007) 093009, arXiv:0706.4165 [hep-ph].

[178] Daya Bay Collaboration, F. P. An *et al.*, *Observation of electron-antineutrino disappearance at Daya Bay*, Phys. Rev. Lett. **108** (2012) 171803, arXiv:1203.1669 [hep-ex].

[179] RENO Collaboration, J. K. Ahn *et al.*, *Observation of reactor electron antineutrinos disappearance in the RENO experiment*, Phys. Rev. Lett. **108** (2012) 191802, arXiv:1204.0626 [hep-ex].

[180] Double Chooz Collaboration, Y. Abe *et al.*, *Indication of reactor $\bar{\nu}_e$ disappearance in the Double Chooz experiment*, Phys. Rev. Lett. **108** (2012) 131801, arXiv:1112.6353 [hep-ex].

Acknowledgments

Starting a PhD project is like setting foot on a long and winding road, not being completely sure where it will eventually lead. During the years of travel, I met many people that pointed me in the right direction, helped to remove obstacles, provided useful advice or (not less important) their friendship and love. Without their support, it would have been impossible to go all the way and this thesis would not exist.

First of all, I want to express my gratitude to my doctoral advisor Prof. Manfred Lindner, who accepted me as a PhD student and provided a perfect environment for this project. Thank you for triggering discussions, for providing helpful physics input, and for giving me the opportunity to participate in many conferences, workshops, and summer schools during the past years.

I am grateful that Prof. Joerg Jaeckel kindly accepted the duty of being the second referee of this thesis, and I thank Prof. Klaus Blaum and Prof. Klaus Pfeilsticker for kindly agreeing to be members of the examination committee.

I would like to thank Prof. Morimitsu Tanimoto from Niigata University and Prof. Jisuke Kubo from Kanazawa University, both in Japan, for their invitation to take part in the Japan Society for the Promotion of Science (JSPS) program "Young Researcher Overseas Visits Program for Vitalizing Brain Circulation." I had a wonderful time and learned a lot during my visits at Kanazawa University in February–March and October2012.

During the time of my PhD, I worked on different projects with many collaborators. I enjoyed all the discussions we had, and most of the physics I learned over the years is thanks to them: Mayumi Aoki, Sandhya Choubey, Pavel Fileviez Pérez, Damien P. George, Pascal Humbert, Jisuke Kubo, Manfred Lindner, Kristian L. McDonald, Alexander Merle, Manimala Mitra, Dominik Neuenfeld, Werner Rodejohann, Hiroshi Takano, and Kai Zuber.

A special thanks goes to Pavel Fileviez Pérez, who so generously shared his time, his ideas, and his physical insights with me. I enjoyed all our projects a lot, and I learned so much from you.

It would not have been so much fun to work on this thesis without our nice division, and I would like to thank all the division members for providing this wonderful atmosphere. A special thanks goes to Daniel Schmidt for being a very pleasant office mate during these years and for always being open to a quick black board discussion.

I am indebted to James Barry, Pavel Fileviez Pérez, Julian Heeck, and Werner Rodejohann for carefully reading the manuscript and giving valuable suggestions.

I would not be where I am today without my family. I am deeply grateful for the love, encouragement, and continual support of my parents Ingrid and Rudolf Dürr, thereby leaving me all the freedom I needed to pursue my interests. Ich danke meinen Großeltern Oma Anneliese und Opa Richard für all ihre Liebe und ihre großzügige Unterstützung, die so vieles möglich gemacht hat. Oma Luise und Opa Walter sind in meinen Gedanken bei uns.

I thank Paul Niemeyer for his friendship. My time in Heidelberg would not have been the same without you.

Last but not least, a warm thank you goes to Veronika Hogger.

I acknowledge support by the International Max Planck Research School for Precision Tests of Fundamental Symmetries (IMPRS-PTFS) of the Max Planck Society and by the Heidelberg Graduate School of Fundamental Physics (HGSFP).